Scaled equation of state parameters for gases in the critical region

Cite as: Journal of Physical and Chemical Reference Data **5**, 1 (1976); https://doi.org/10.1063/1.555529
Published Online: 15 October 2009

J. M. H. Levalt Sengers, W. L. Greer, and J. V. Sengers

Scaled Equation of State Parameters for Gases in the Critical Region

J. M. H. Levelt Sengers

Institute for Basic Standards, National Bureau of Standards, Washington, D.C. 20234

W. L. Greer*

Institute for Molecular Physics, University of Maryland, College Park, Md. 20742

and

J. V. Sengers

Institute for Molecular Physics, University of Maryland, College Park, Md. 20742

and

Institute for Basic Standards, National Bureau of Standards, Washington, D.C. 20234

The anomalous thermodynamic behavior of fluids near the critical point can be described in terms of scaling laws. In this paper we consider two critical region equations of state, to be referred to as the NBS equation and the Linear Model parametric equation, that satisfy the scaling laws. A complete formulation of the thermodynamic properties in terms of the two equations is given. The statistical methods used for fitting these equations to experimental data are described. Each of the equations is fitted to experimental equation of state data for six fluids, namely He^3, He^4, Xe, CO_2, O_2, and H_2O. An evaluation of the recorded experimental material is included. We find that the two equations represent the experimental data in the range $|T-T_c|/T_c < 0.03$ and $|\rho-\rho_c|/\rho_c < 0.25$ equally well and that the exponents and amplitudes of the power laws deduced from the two equations agree closely. The optimum critical exponents appear to vary little from substance to substance. Moreover, a restricted version of the Linear Model with only two freely adjustable constants, in addition to the critical point parameters and the critical exponents, fits the data well in most cases, in agreement with expectations based on universality of critical behavior. The principle of universality is discussed and applied to predict critical region parameters for nine additional fluids, including several for which only limited experimental information is available. These additional fluids are Ar, Kr, N_2, H_2, CH_4, C_2H_4, SF_6, NH_3, and D_2O. We thus conclude with a single universal equation for the critical region of all fifteen fluids considered in this paper.

Key words: Air constituents; critical region parameters; ethylene; heavy noble gases; helium; Linea. Model; methane; NBS equation; scaling laws; statistical analysis; steam; universality.

Contents

*Present address: Department of Chemistry, George Mason University, Fairfax, Va. 22030

List of Tables

List of Tables—Continued

1. Introduction

The purpose of this paper is to present an accurate characterization of the anomalous thermodynamic behavior in the critical region of a number of gases. The need for a new characterization has been felt acutely in the last 10 years, during which it became common knowledge that the methods for data correlation used until then had been inherently in error in the critical region. We are referring here to the engineering calculations that make use of so-called "classical" equations of state, i.e. equations which are analytical at the critical point and which can be considered as improved versions of van der Waals' equation of state. Analytical equations yield a critical isotherm that is asymptotically of the third or of the fifth degree, a quadratic or a quartic coexistence curve, a finite constant volume specific heat C_v in the one-phase region and an analytic vapor pressure curve. On the other hand, real fluids have a critical isotherm that is somewhat flatter than a fourth-degree curve but not as flat as a fifth-degree curve, a coexistence curve that is almost cubic, a weakly divergent specific heat C_v and a nonanalytic vapor pressure curve.

In recent years, new theories of critical phenomena have produced a form for the equation of state in the vicinity of the critical point which incorporates the observed nonanalytic character of the thermodynamic behavior and which also leads to a reduction of the number of independent variables. The critical behavior is associated with long range fluctuations in the system and the physical properties depend primarily on a single variable, namely the correlation length. Therefore, the function which characterizes the anomalous thermodynamic behavior near the critical point is a function of one variable, which is a combination of the two original independent variables, density and temperature. This reduction of the number of independent variables in the critical region from two to one is known as scaling. Furthermore, since the correlation length is much larger than the range of the intermolecular interaction, the behavior of the system becomes highly insensitive to details of the molecular interaction and, thus, is expected to have a universal character. The range of validity of such a scaled universal description is determined by the requirement that the correlation length be much larger than the range of the interaction. This defines a region around the critical point which we will call the critical region. In practice, this region is located within approximately 25 percent of the critical density and about 3 percent of the critical temperature.

The literature on critical phenomena is rapidly increasing. For a survey of the development of the subject concerning one-component fluids the reader is referred to some other papers of one of the authors [L1, L2, L3].[1]

This paper is organized as follows:

We first formulate in section 2 a description of the thermodynamic behavior of fluids in terms of the scaling laws. We then describe in section 3 two scaled equations of state that have been used successfully. The first equation is an equation formulated by Vicentini-Missoni, Levelt Sengers and Green [V1] to which we shall refer, for the sake of convenience, as the NBS equation. The second equation is the Linear Model parametric equation proposed by Schofield, Litster and Ho [S1, S2]. Since the Linear Model is the most versatile of the two equations, we give a list of the expressions for the

[1] Symbols in brackets indicate literature references.

various thermodynamic properties in terms of the Linear Model in section 3.3.

A method for fitting the NBS equation to experimental equation of state data was formulated earlier [V1]. For the purpose of this paper it was also necessary to develop a method of statistical analysis for fitting the Linear Model to the experimental data. This method is described in section 4.

We then proceed in section 5 to fit the NBS equation and the Linear Model to the equation of state data of Habgood and Schneider for xenon [H1], the data of Roach for helium[4] [R1], the data of Wallace and Meyer for helium[3] [W1], the data of Michels et al. for carbon dioxide [M1], the data of Rivkin et al. for steam [R2, R3, R4] and the data of Weber for oxygen [W2]. In each case, a detailed discussion is given of the experimental accuracy, the choice of critical parameters and the analysis of the coexistence curve. The optimum fit for each of the two scaled equations is presented and the results compared. Deviations between the experimental and calculated data are plotted and compared with estimates of the experimental error. For the Linear Model fits, we also present a complete error analysis of the six adjustable parameters.

From the results obtained, we can derive the coefficients and exponents of the power laws that describe the anomalous behavior of a number of thermodynamic properties on approaching the critical point. The values of these coefficients and exponents are included in the tables of critical region parameters presented in section 5. We also make a comparison with other independent sources of experimental information, when available, such as the data of Kierstead for helium[4] [K1, K2] and the data of Estler, Wilcox and Hocken [E1] and those of Thoen and Garland [T1] for xenon.

We conclude this paper with a discussion of the question of universality in section 6. The principle of universality requires the critical exponents to have the same value for all fluids: furthermore, it implies that, in addition to the critical temperature, density and pressure, only two other parameters can be freely chosen in the scaled equation of state. Hence, the validity of this principle would imply great economy in the description of the thermodynamic behavior of fluids in the critical region. The material gathered in this paper permits a test of the principle of universality. We conclude that universality holds at least within the accuracy of the data available for six fluids. We then use this for developing a description of the critical region for nine additional fluids. We thus conclude with a list of critical region parameters for 15 different fluids in terms of a universal equation of state.

2. Thermodynamic Description in Terms of Scaling Laws

2.1. Choice of Variables

If volume and temperature are chosen as the independent variables, then the characteristic thermodynamic potential is the Helmholtz free energy per mole; in this description pressure P and volume V are conjugate variables and the equation of state $P(V, T)$ is obtained by differentiation of the Helmholtz free energy with respect to V. On the other hand, if density and temperature are chosen as the independent variables, then the characteristic thermodynamic potential is the Helmholtz free energy per *unit volume*; in that description chemical potential μ and density ρ are conjugate variables and the corresponding equation of state $\mu(\rho, T)$ is obtained by differentiation of the Helmholtz free energy density with respect to ρ.

The choice of variables in which the scaling laws are formulated is dictated by considerations of symmetry which have been amply discussed elsewhere [L3, V1]. Be it sufficient here to remind the reader that the coexistence curve, when plotted as a function of density, shows considerably more symmetry than when plotted as a function of volume, as illustrated in figure 1. An equally striking difference in symmetry features is noted above the critical temperature, when a $\mu(\rho)$-isotherm is compared with a $P(V)$-isotherm, as illustrated in figure 2: the $\mu(\rho)$-isotherms are antisymmetric with respect to the point ρ_c, $\mu(\rho_c)$, in contrast to $P(V)$-isotherms. These symmetry properties are perfectly satisfied in the lattice gas model; for a real fluid they are only satisfied asymptotically when the critical point is approached. The scaling laws in the form we use them do assume these symmetry properties. The scaling laws are only valid asymptotically and, therefore, the range of experimental validity has to be tested in each individual case.

In view of these symmetry features we adopt density ρ and temperature T as the independent variables. The extensive thermodynamic functions, such as Helmholtz free energy, A, entropy, S, and heat capacity at constant volume, C_v, are taken per *unit volume*. The equation of state to be considered will be the chemical potential, μ, as a function of ρ and T. The basic thermodynamic formulae are

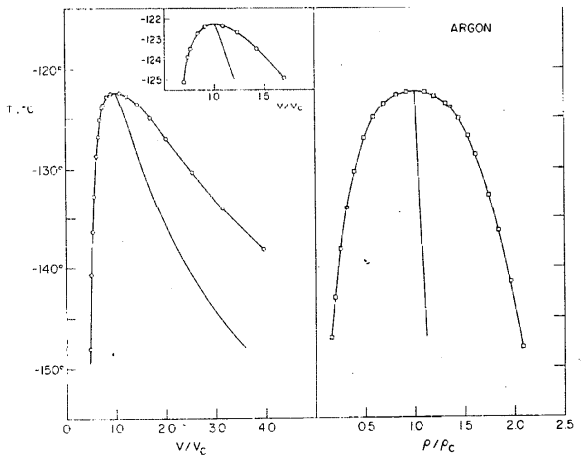

FIGURE 1. The coexistence curve of argon in terms of volume and temperature and in terms of density and temperature.

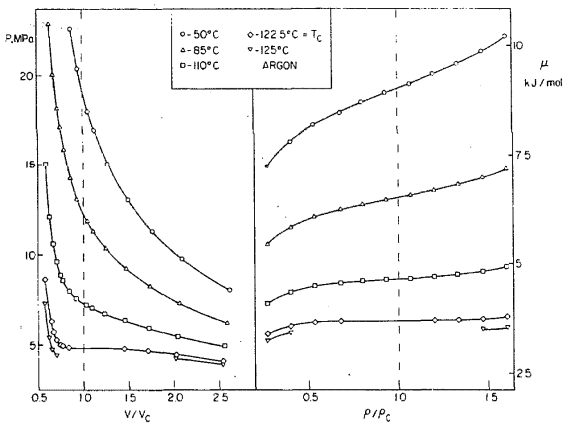

FIGURE 2. $P(V)$-isotherms and $\mu(\rho)$-isotherms of argon in the critical region. In contrast to the $P(V)$-isotherms, the $\mu(\rho)$-isotherms are nearly antisymmetric with respect to ρ_c.

$$dA = \mu d\rho - SdT, \tag{1.1a}$$

$$S = -(\partial A/\partial T)_\rho, \tag{1.1b}$$

$$C_v = -T(\partial^2 A/\partial T^2)_\rho, \tag{1.1c}$$

$$\mu = (\partial A/\partial \rho)_T, \tag{1.1d}$$

while the pressure follows from a Legendre transformation

$$-P = A - \mu\rho. \tag{1.1e}$$

The "generalized compressibility" $(\partial\rho/\partial\mu)_T$ will play an important role; it is related to the isothermal compressibility $K_T \equiv -V^{-1}(\partial V/\partial P)_T$ by the relation

$$(\partial\rho/\partial\mu)_T = \rho^2 K_T. \tag{1.1f}$$

All properties are made dimensionless by expressing them in units of appropriate combinations of critical parameters. We thus define

$$\rho^* = \rho/\rho_c, \qquad T^* = T/T_c, \qquad A^* = A/P_c,$$

$$\mu^* = \mu\rho_c/P_c, \qquad \Delta\mu^* = (\Delta\mu)\rho_c/P_c, \qquad P^* = P/P_c,$$

$$S^* = ST_c/P_c, \qquad C_v^* = C_v T_c/P_c, \qquad K_T^* = K_T P_c. \tag{1.2}$$

The critical density and temperature in reduced units will be occasionally indicated by $\rho_c^*(=1)$ and $T_c^*(=1)$. In addition we introduce quantities defined with respect to their values at the critical point

$$\Delta T^* = T^* - 1 = (T - T_c)/T_c,$$

$$\Delta\rho^* = \rho^* - 1 = (\rho - \rho_c)/\rho_c. \tag{1.3}$$

The chemical potential difference $\Delta\mu$ plays an important role in scaling. It is defined as

$$\Delta\mu = \mu(\rho, T) - \mu(\rho_c, T), \tag{1.4}$$

where $\mu(\rho_c, T)$ is the chemical potential on the critical isochore at temperature T. If for real fluids the $\mu(\rho)$-isotherms are truly antisymmetric near T_c, then $\mu(\rho_c, T)$ would have to be a regular function of temperature, as it is in the lattice gas. In the scaled equations to be used in this paper, regularity of $\mu(\rho_c, T)$ is assumed. For a further discussion we refer the reader to other publications [G1, K2, L4, V1, W3].

2.2. Power Laws

It is assumed that the critical anomalies can be described by power laws when the critical point is approached along a specific path such as the critical isochore, the critical isotherm or the coexistence boundary. The power laws needed for the purpose of this paper are defined as follows

Coexistence Curve

$$\Delta\rho^* = \pm B\,|\,\Delta T^*\,|^\beta \tag{2.1}$$

Critical Isotherm

$$\Delta\mu^* = D(\Delta\rho^*)\,|\,\Delta\rho^*\,|^{\delta-1} \qquad (\Delta T^* = 0) \tag{2.2}$$

Compressibility

$$\rho^{*2}K_T^* = \Gamma(\Delta T^*)^{-\gamma} \qquad (\rho^* = 1,\ \Delta T^* > 0) \tag{2.3a}$$

$$\rho^{*2}K_T^* = \Gamma'\,|\,\Delta T^*\,|^{-\gamma'} \qquad (\text{coexistence curve}, \Delta T^* < 0) \tag{2.3b}$$

Specific Heat

$$\frac{C_v^*}{T^*} = \frac{A^+}{\alpha}\{(\Delta T^*)^{-\alpha} - 1\} \qquad (\rho^* = 1,\ \Delta T^* > 0) \tag{2.4a}$$

$$\frac{C_v^*}{T^*} = \frac{A_I^-}{\alpha'}\{|\,\Delta T^*\,|^{-\alpha'} - 1\} \qquad (\text{along coexistence curve}, \Delta T^* < 0) \tag{2.4b}$$

$$\frac{C_v^*}{T^*} = \frac{A_{II}^-}{\alpha''}\{|\,\Delta T^*\,|^{-\alpha''} - 1\} \qquad (\rho^* = 1, \Delta T^* < 0, \text{2-phase region}) \tag{2.4c}$$

The paths along which these power laws are defined are indicated schematically in figure 3.

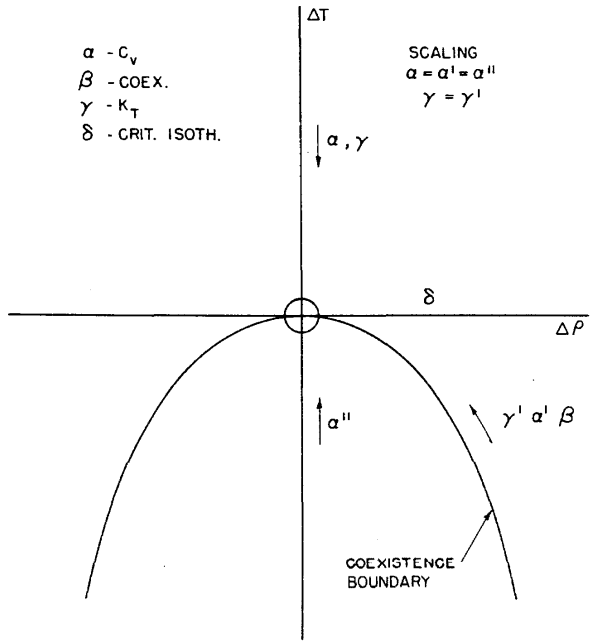

FIGURE 3. Special paths in the $\Delta\rho-\Delta T$ plane and power law exponents defined along them.

The scaling laws to be introduced in the subsequent section impose a number of conditions upon the critical exponents in the power laws. First, the exponents associated with the behavior of C_v and of K_T when the critical temperature is approached from below, are taken to be identical with the exponents that describe the behavior of these same properties of C_v and K_T, when the critical temperature is approached from above:

$$\alpha=\alpha'=\alpha'', \qquad \gamma=\gamma'. \tag{2.5}$$

Furthermore, the critical exponents α, β, γ, δ are assumed to satisfy the equalities

$$2-\alpha=\beta(\delta+1), \tag{2.6a}$$

$$\gamma=\beta(\delta-1), \tag{2.6b}$$

so that only two exponents can be chosen independently. In this paper we shall use the exponent β of the coexistence curve and the exponent δ of the critical isotherm as the two critical exponents to be selected.

2.3. Scaling Law for Equation of State and Compressibility

The scaling laws are a phenomenological consequence of the physical intuition that the anomalous critical behavior depends on one length only, namely the correlation length which measures the size of the critical fluctuations [K3]. Hence, when appropriately reduced, the anomalous part of the thermodynamic functions must become a function of one, rather than two independent variables. This assumption can be formulated mathematically by the hypothesis that the anomalous part of the thermodynamic potentials is a generalized homogeneous function of its variables [H2, L2, W3].

It is somewhat easier to visualize the scaling laws as a straightforward generalization of a Taylor series expansion of the classical equation near the critical point, first considered by van der Waals in 1893 [L1, V2]. If we expand the reduced chemical potential of a classical equation in powers of $\Delta\rho^*$ and ΔT^* around the critical point, we obtain

$$\mu^*(\Delta\rho^*, \Delta T^*)=\mu^*(\rho_c, T_c)+\mu_{01}(\Delta T^*)+\ldots$$
$$+\mu_{11}(\Delta\rho^*)(\Delta T^*)+\ldots$$
$$+\mu_{21}(\Delta\rho^*)^2(\Delta T^*)+\ldots$$
$$+\mu_{30}(\Delta\rho^*)^3+\ldots \tag{2.7}$$

The coefficients μ_{10} and μ_{20} of the terms proportional to $\Delta\rho^*$ and $(\Delta\rho^*)^2$ in the expansion vanish as a consequence of the definition of the critical point as a point of marginal stability. The first two terms on the right hand side in (2.7) are asymptotically equal to the chemical potential $\mu^*(\rho_c, T)$ on the critical isochore. Thus, remembering the definition (1.4) of $\Delta\mu^*$, we have in first approximation for a classical equation

$$\Delta\mu^*=\mu_{30}(\Delta\rho^*)^3\left[1+\frac{\mu_{11}}{\mu_{30}}\frac{\Delta T^*}{(\Delta\rho^*)^2}\right]. \tag{2.8}$$

The critical isotherm is obtained from (2.8) by setting $\Delta T^*=0$; since $\Delta\mu^*=0$ at the coexistence curve, its form is obtained by setting the term in square brackets equal to zero for $\Delta T^*<0$. Thus, in the classical theory the critical isotherm has the asymptotic form $\Delta\mu^*=D(\Delta\rho^*)^\delta$ with $D=\mu_{30}$ and $\delta=3$, and the coexistence curve has the asymptotic form $\Delta\rho^*=\pm B|\Delta T^*|^\beta$ with $B=(\mu_{11}/\mu_{30})^{1/2}$ and $\beta=1/2$. If we now define the variable x as

$$x\equiv\Delta T^*/|\Delta\rho^*|^{1/\beta}, \tag{2.9}$$

so that, at coexistence, $x=-x_0$ with

$$x_0=B^{-1/\beta}, \tag{2.10}$$

we may then rewrite the classical equation (2.8) as

$$\Delta\mu^*=\Delta\rho^*|\Delta\rho^*|^{\delta-1}[D(1+x/x_0)]. \tag{2.11}$$

For real fluids β is not equal to 1/2 and δ is not equal to 3. However, permitting arbitrary values for the exponents β and δ and allowing for a more general dependence upon the variable x, we may generalize the classical equation (2.11) to

$$\Delta\mu^*=\Delta\rho^*|\Delta\rho^*|^{\delta-1}h(x), \tag{2.12}$$

which is, in Griffiths' formulation, the scaling law for the chemical potential originally proposed by Widom [G1, W3]. One can readily demonstrate that all the power laws introduced in section 2.2, together with the exponent equalities (2.5) and (2.6), are indeed implied by the scaled form (2.12). Notice that $\Delta\mu^*$ is indeed a function of only one variable x, when scaled by the antisymmetric quantity $\Delta\rho^*|\Delta\rho^*|^{\delta-1}$.

The scaled equation for the compressibility $\rho^{*2}K_T^* = (\partial\rho^*/\partial\mu^*)_T$ follows immediately from (2.12)

$$\rho^{*2}K_T^* = |\Delta\rho^*|^{1-\delta}\left[\delta h(x) - \frac{x}{\beta}\frac{dh(x)}{dx}\right]^{-1}. \tag{2.13}$$

Thus, the compressibility is a function of the variable x only, when scaled by the symmetric quantity $|\Delta\rho^*|^{1-\delta}$.

The scaling variable $x = \Delta T^*/|\Delta\rho^*|^{1/\beta}$ assumes the value $-x_0$ at the phase boundary, the value 0 on the critical isotherm and the value $+\infty$ on the critical isochore. Since the chemical potential is a constant along any isotherm in the two-phase region, $\Delta\mu^* = 0$ at coexistence and, thus, $h(-x_0) = 0$. The function $h(x)$ becomes infinite at the critical isochore. In addition to the boundary conditions $h(-x_0) = 0$ and $h(\infty) = \infty$, the function $h(x)$ is restricted by several conditions, formulated by Griffiths [G1]. These conditions arise first of all from the requirements of thermodynamic stability. Thus, for the compressibility to be positive, it is necessary that

$$\beta\delta h(x) \geq x\frac{dh(x)}{dx}, \tag{2.14}$$

as follows from (2.13). Additional conditions are imposed on $h(x)$ by the assumption that $\mu(\rho, T)$ is an analytic function throughout the one-phase region with the exception of the critical point and perhaps the phase boundary. Thus, in this theory the existence of higher-order phase transitions on special curves such as the critical isotherm or critical isochore is excluded. The analyticity of $\mu(\rho, T)$ in the one-phase region, combined with the assumed analyticity of $\mu(\rho_c, T)$ mentioned earlier, implies analyticity for the function $\Delta\mu^*(\Delta\rho^*, \Delta T^*)$ inside the one-phase region. The relation (2.12) then implies that $h(x)$ has to be analytic in x in the range $-x_0 < x < \infty$; it can, therefore, be expanded in a power series in x at every point in this range. Specifically, an expansion

$$h(x) = \sum_{n=0}^{\infty} h_n x^n, \tag{2.15}$$

should be valid for small values of x (near the critical isotherm). Analyticity at large x (at the critical isochore) implies that, around $x = \infty$, $h(x)$ can be expanded as follows:

$$h(x) = \sum_{n=1}^{\infty} \eta_n x^{\beta(\delta+1-2n)}. \tag{2.16}$$

Notice that the leading term of this expansion is $\eta_1 x^\gamma$ with $\gamma = \beta(\delta-1)$.

2.4. Scaling Law for the Helmholtz Free Energy

The basic scaling law (2.12) introduced in the preceding section represents the equation of state $\mu(\rho, T)$. However, an equation of state does not yield a complete description of the thermodynamic behavior of the system. It thus becomes necessary to inquire about the scaled form of the corresponding thermodynamic potential which is the Helmholtz free energy per unit volume. Since $\mu^* = (\partial A^*/\partial\rho^*)_T$ we have, in terms of the difference variables $\Delta\rho^*$, $\Delta\mu^*$:

$$\left(\frac{\partial A^*}{\partial\Delta\rho^*}\right)_T = \mu^*(\rho_c, T) + \Delta\mu^*. \tag{2.17}$$

We, therefore, postulate that A^* assumes the form

$$A^* = A_0^*(T^*) + \rho^*\mu^*(\rho_c^*, T^*) + A_{sc}^*(\Delta\rho^*, \Delta T^*). \tag{2.18}$$

The integration constant $A_0^*(T^*)$ is an undetermined function of temperature. From the antisymmetry of $\Delta\mu^*$ and the relations (2.12) and (2.17), it follows that the scaled part A_{sc}^* is symmetric in $\Delta\rho^*$ and, therefore, has the form

$$A_{sc}^* = |\Delta\rho^*|^{\delta+1}a(x). \tag{2.19}$$

The new scaling function $a(x)$ for the free energy is related to the original scaling function $h(x)$ for the equation of state by

$$\beta h(x) = -xa'(x) + \beta(\delta+1)a(x), \tag{2.20}$$

where the prime denotes differentiation with respect to x.

Because of the analytic properties of $h(x)$, $a(x)$ is also analytic in the range $-x_0 < x < \infty$. The general solution of the differential equation (2.20) is

$$a(x) = \frac{x}{x_1}\left|\frac{x}{x_1}\right|^{1-\alpha} a(x_1) - \beta x\,|x|^{1-\alpha}\int_{x_1}^{x} dy\,|y|^{\alpha-3}h(y), \tag{2.21}$$

with $\alpha = 2-\beta(\delta+1)$ and x_1 a value of x in the range $0 < x < \infty$. The first term on the right hand side is manifestly nonanalytic at $x=0$. Since $a(x)$ has to be analytic, the nonanalyticity of the first term on the right hand side in (2.21) has to be cancelled by the value of the lower limit of the integral. That is, once $h(x)$ is known, $a(x)$ is uniquely determined through analyticity. In those cases where $h(x)$ is of a sufficiently simple functional form for the integral in (2.20) to be evaluated explicitly (as in the Linear Model version of the parametric equation of state, to be discussed subsequently), $a(x)$ has a unique, explicit functional form. The function $a(x)$ can be expanded in powers of x everywhere in the

range $-x_0 \leq x \leq \infty$. Specifically, we have, for small x

$$a(x) = \sum_{n=0}^{\infty} a_n x^n, \tag{2.22}$$

where the coefficients a_n are related to the coefficients h_n in the expression (2.15) by

$$a_n = \frac{\beta h_n}{2-\alpha-n}. \tag{2.23}$$

Using this expansion (2.22), Griffiths [G1] obtains for values of x within the radius of convergence $|x| = x_0$ of the power series expansion (2.15) of $h(y)$

$$a(x) = \frac{\beta h_0}{2-\alpha} + \frac{\beta h_1 x}{1-\alpha} - \beta x |x|^{1-\alpha} \int_0^x dy\, |y|^{\alpha-3}[h(y) - h_1 y - h_0]. \tag{2.24}$$

On the other hand, the general solution (2.21) may be written as

$$a(x) = Cx^{2-\alpha} + \beta x^{2-\alpha} \int_{\infty}^{x} dy\, y^{\alpha-3} h(y), \tag{2.25}$$

for all $x > 0$. The constant C is defined as

$$C = \lim_{x_1 \to \infty} \frac{a(x_1)}{x_1^{2-\alpha}}.$$

In the region of overlap, the general solution (2.25) has to equal the solution (2.24). Therefore, we find[2] for the constant C

$$C = -\beta \int_0^{\infty} dy\, y^{\alpha-3}[h(y) - h_1 y - h_0]. \tag{2.26}$$

In summary, the equations (2.24) and (2.25), together with the expression (2.26) for the constant C, allow us to calculate the scaling function $a(x)$ for the free energy from the scaling function $h(x)$ for the equation of state.

2.5. Scaled Expressions for the Thermodynamic Functions in Terms of h(x) and a(x)

Chemical Potential

One-phase $$\Delta\mu^* = \Delta\rho^* |\Delta\rho^*|^{\delta-1} h(x) \tag{2.27a}$$

Two-phase $$\Delta\mu^* = 0 \tag{2.27b}$$

Compressibility

$$\rho^{*2} K_T^* = |\Delta\rho^*|^{1-\delta}[\delta h(x) - \beta^{-1} x h'(x)]^{-1} \tag{2.28}$$

Helmholtz Free Energy

One-phase
$$A^* = A_0^*(T^*) + \rho^* \mu^*(\rho_c^*, T^*) + |\Delta\rho^*|^{\delta+1} a(x) \tag{2.29a}$$

Two-phase
$$A^* = A_0^*(T^*) + \rho^* \mu^*(\rho_c^*, T^*) + x_0^{\alpha-2} a(-x_0) |\Delta T^*|^{2-\alpha} \tag{2.29b}$$

Pressure

One-phase
$$P^* = -A_0^*(T^*) + \Delta\rho^* |\Delta\rho^*|^{\delta-1} h(x) + |\Delta\rho^*|^{\delta+1}\{h(x) - a(x)\} \tag{2.30a}$$

Two-phase (vapor pressure)
$$P_{\text{vap}}^* = -A_0^*(T^*) - x_0^{\alpha-2} a(-x_0) |\Delta T^*|^{2-\alpha} \tag{2.30b}$$

Entropy

One-phase $$S^* = A_0^{*\prime}(T^*) + \rho^* \mu^{*\prime}(\rho_c^*, T^*) + |\Delta\rho^*|^{(1-\alpha)/\beta} a'(x)| \tag{2.31a}$$

Two-phase $$-S^* = A_0^{*\prime}(T^*) + \rho^* \mu^{*\prime}(\rho_c^*, T^*) - (2-\alpha) x_0^{\alpha-2} a(-x_0) |\Delta T^*|^{1-\alpha} \tag{2.31b}$$

Heat Capacity

One-phase $$-C_v^*/T^* = A_0^{*\prime\prime}(T^*) + \rho^* \mu^{*\prime\prime}(\rho_c^*, T^*) + |\Delta\rho^*|^{-\alpha/\beta} a''(x) \tag{2.32a}$$

One-phase, at phase boundary $$-C_v^*/T^* = A_0^{*\prime\prime}(T^*) + \rho^* \mu^{*\prime\prime}(\rho_c^*, T^*) + x_0^{\alpha} a''(-x_0) |\Delta T^*|^{-\alpha} \tag{2.32b}$$

Two-phase $$-C_v^*/T^* = A_0^{*\prime\prime}(T^*) + \rho^* \mu^{*\prime\prime}(\rho_c^*, T^*) + (2-\alpha)(1-\alpha) x_0^{\alpha-2} a(-x_0) |\Delta T^*|^{-\alpha} \tag{2.32c}$$

Jump across phase boundary

$$\Delta(-C_v^*/T^*) = \beta x_0^{\alpha-1} h'(-x_0) |\Delta T^*|^{-\alpha} \tag{2.32d}$$

In these expressions primes denote differentiation with respect to the relevant variable; for $A_0^*(T^*)$ and $\mu^*(\rho_c^*, T^*)$ this variable is the temperature T^*, for the functions $h(x)$ and $a(x)$ this variable is x. In the two-phase region the density ρ^* is to be interpreted as the average density of the system.

3. Scaled Equations of State

3.1. NBS Equation

The scaled expressions presented in section 2.5 are not useful for data correlation unless one specifies an explicit form for the function $h(x)$ or $a(x)$. However,

[2] Contrary to equation (28) in ref. [G1], this expression for C contains the true $h(y)$, not its series expansion around $y = 0$.

the choices are severely restricted by the conditions formulated by Griffiths as discussed in section 2.3. A closed form for $h(x)$ that fulfills most, but not all, of these conditions was proposed by Vicentini-Missoni, Levelt Sengers and Green [V1]. We shall refer to this equation as the NBS equation; it is defined as

$$h(x)=E_1\left(\frac{x+x_0}{x_0}\right)\left[1+E_2\left(\frac{x+x_0}{x_0}\right)^{2\beta}\right]^{(\gamma-1)/2\beta} \tag{3.1}$$

This equation contains the critical parameters ρ_c, T_c (through the definition of x), two critical exponents, β, γ, and three constants, x_0, E_1 and E_2. As we shall see, the exponents β and γ and the parameter E_2 vary only slightly from substance to substance and are probably universal as discussed in chapter 6. The constants x_0 and E_1 on the other hand, vary considerably from substance to substance.

The coefficients of the power laws defined in section 2.2 are related to the constants in the NBS equation by

$$B=x_0^{-\beta}, \tag{3.2}$$

$$D=E_1(1+E_2)^{(\gamma-1)/2\beta}, \tag{3.3}$$

$$\Gamma=x_0^{\gamma}E_1^{-1}E_2^{(1-\gamma)/2\beta}, \tag{3.4a}$$

$$\Gamma'=\beta x_0^{\gamma}E_1^{-1}, \tag{3.4b}$$

$$\Gamma/\Gamma'=\beta^{-1}E_2^{(1-\gamma)/2\beta}. \tag{3.4c}$$

No simple explicit formulae can be given for the specific heat coefficients A^+, A_I^-, A_{II}^- in terms of the constants of the NBS equation.

The NBS equation has two singularities, one at $x=-x_0$ (coexistence curve) and the other at $x=\infty$ (critical isochore). The function is analytic in the range $-x_0<x<\infty$. However, the expansion for large values of x has, in addition to the terms x^{γ}, $x^{\gamma-2\beta}$ as required by (2.16), also spurious terms, the leading one being proportional to $x^{\gamma-1}$. As a consequence, only the first and the second density derivatives of the chemical potential at $x=\infty$ exist. This may, however, be sufficient for most practical purposes.

From the NBS equation one can readily calculate the compressibility as a function of $\Delta\rho^*$ and ΔT^* using (2.28). However, the equation has the disadvantage that the corresponding free energy function $a(x)$ cannot be derived in closed form, but must be obtained by numerical integration. Techniques for doing this have been discussed by Vicentini-Missoni et al. [L5, V1] and by Schmidt [S3].

3.2. Linear Model Parametric Equation

We have seen that the requirement of analyticity of thermodynamic behavior in the one-phase region except at the critical point, led to a number of conditions on the function $h(x)$. These conditions cannot be met readily by a single expression in closed form. Furthermore, even if one were able to find a closed form expression for the function $h(x)$, it still could probably not be integrated analytically to yield a closed form expression for the function $a(x)$. Finally, the fact that both x and $h(x)$ become infinite on the critical isochore leads to complications in the presentation of data.

The problems with analyticity can be overcome rigorously by using parametric scaled equations introduced by Schofield [S1] and Josephson [J1]. This formulation entails a transformation from the physical variables, $\Delta\rho^*$ and ΔT^*, into two parametric variables, r and θ. The variable r is meant in some sense, to describe a "distance from the critical point" and the variable θ a "location on a contour of constant r." The idea of this approach is to incorporate all anomalies represented by the power laws in the r-dependence, while keeping the θ-dependence strictly analytic. In this way, nonanalyticities are confined to $r=0$, the critical point, and no irregularities will appear anywhere else in the one-phase region.

The manner in which the thermodynamic variables are expressed in terms of r and θ is not unique [F1]. The constraints that the power laws and the scaling laws are preserved are met by the following choice

$$\Delta T^*=rT(\theta), \tag{3.5a}$$

$$\Delta\rho^*=r^{\beta}M(\theta), \tag{3.5b}$$

$$\Delta\mu^*=r^{\beta\delta}H(\theta). \tag{3.5c}$$

On constructing the ratios $\Delta\mu^*/(\Delta\rho^*)|\Delta\rho^*|^{\delta-1}$ and $x=\Delta T^*/|\Delta\rho^*|^{1/\beta}$, one sees immediately that both ratios depend on θ alone, so that the scaling law (2.12) is implied by the parametric representation (3.5).

Choices compatible with the observed lowest-order symmetry are those for which $M(\theta)$ and $H(\theta)$ are antisymmetric functions and $T(\theta)$ is a symmetric function of θ. The parameter θ can be chosen to span the range -1 to $+1$, such that it equals zero on the critical isochore and ±1 on the coexistence boundary, as indicated schematically in figure 4. For the functions $T(\theta)$, $M(\theta)$ and $H(\theta)$, the simplest choices compatible with these requirements are

$$T(\theta)=1-b^2\theta^2, \tag{3.6a}$$

$$M(\theta)=k\theta, \tag{3.6b}$$

$$H(\theta)=a(\theta)\theta(1-\theta^2),\ a(\theta)\text{ symmetric in }\theta, \tag{3.6c}$$

where k and b ($b>1$) are adjustable constants. In this representation θ assumes the value $\pm1/b$ on the critical isotherm.

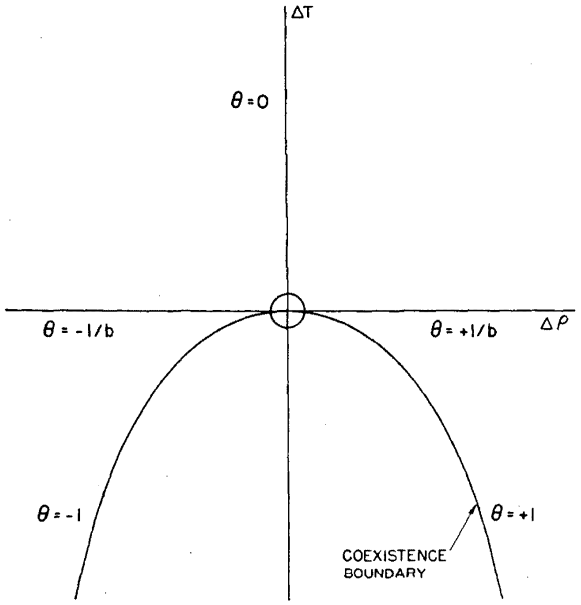

FIGURE 4. Schematic representation of the variable θ in the parametric equation of state.

In this formulation $a(\theta)$ is still an unknown function of θ. When $a(\theta)=a$ is assumed to be a constant independent of θ, then (3.6) represents the Linear Model parametric equations introduced by Schofield [S1]. The name refers to the linear dependence of the function $M(\theta)$ on θ. If a is taken to be a constant, then the linearity of $M(\theta)$ is a consequence that can be investigated experimentally [H3]. However, in order to verify the validity of the Linear Model with the methods of statistical analysis, we have found it more convenient to start from the linear equation (3.6b) for $M(\theta)$ and to check whether the experimental values of $a(\theta)$ are indeed independent of θ.

The constant b^2 is constrained by thermodynamic stability to a value in the range [H4]

$$1 < b^2 < (1-2\beta)^{-1}. \tag{3.7}$$

The constant k is related to the constant x_0, introduced earlier in (2.10), by

$$k=[(b^2-1)/x_0]^{\beta}. \tag{3.8}$$

In addition to the critical parameters ρ_c and T_c, the Linear Model has thus two adjustable exponents, β, δ, and three adjustable constants, b^2, k and a, which is the same number of adjustable parameters as in the NBS equation. Again there are indications that one of these adjustable constants is redundant. Schofield, Litster and Ho have, therefore, suggested that b^2 not be considered independent, but that it may be calculated from [S2]

$$b^2_{\mathrm{SLH}}=\frac{\delta-3}{(\delta-1)(1-2\beta)}. \tag{3.9}$$

We shall refer to the Linear Model subject to condition (3.9) as the restricted Linear Model. While some authors automatically include equation (3.9) in the definition of the Linear Model, we leave b^2 as as independent adjustable parameter, subject only to the constraint imposed by (3.8). As the data analyses to be discussed reveal. the value of b^2 from equation (3.9) is actually the best choice in most cases.

The coefficients of the power laws defined in section 2.2 are related to the constants in the Linear Model equations by

$$B=k(b^2-1)^{-\beta}=x_0^{-\beta}, \tag{3.10}$$

$$D=ak^{-\delta}b^{\delta-3}(b^2-1), \tag{3.11}$$

$$\Gamma=k/a, \tag{3.12a}$$

$$\Gamma'=(b^2-1)^{\gamma-1}\{1-b^2(1-2\beta)\}k/2a, \tag{3.12b}$$

$$\Gamma/\Gamma'=2(b^2-1)^{1-\gamma}\{1-b^2(1-2\beta)\}^{-1}, \tag{3.12c}$$

$$A^+=-(2-\alpha)(1-\alpha)\alpha f_0, \tag{3.13a}$$

$$A_{\mathrm{II}}^-=-\alpha\beta(b^2-1)^{\alpha}\{1-b^2(1-2\beta)\}^{-3}[\{(1-\alpha)\cdot[1-b^2(1-2\beta)]-2\beta b^2(1-2\beta)\}\{(\delta+1)f_0+(\delta-1)f_2+(\delta-3)f_4\}-2\beta\{1-b^2(1-2\beta)\}\cdot\{(\delta-1)f_2+2(\delta-3)f_4\}], \tag{3.13b}$$

$$A_{\mathrm{III}}^-=-(2-\alpha)(1-\alpha)\alpha(f_0+f_2+f_4)(b^2-1)^{\alpha-2}. \tag{3.13c}$$

In (3.13) we have introduced the symbols f_0, f_2, f_4 defined as [H4]

$$f_0=-\frac{ak\{\delta-3-b^2\alpha(\delta-1)\}}{2b^4(1-\alpha)\alpha(\delta+1)}, \tag{3.14a}$$

$$f_2=+\frac{ak\{\beta(\delta-3)-b^2\alpha(1-2\beta)\}}{2b^2(1-\alpha)\alpha}, \tag{3.14b}$$

$$f_4=-\frac{ak(1-2\beta)}{2\alpha}. \tag{3.14c}$$

We note that, in contrast to the NBS equation, the coefficients A^+, A_{I}^-, A_{II}^- of the specific heat anomalies can all be expressed explicitly in closed form.

3.3. Thermodynamic Properties in Terms of the Linear Model

In calculating thermodynamic functions from the equation of state, it is necessary to perform an integration of the equation of state that often cannot be performed in closed form. It is here that a major advantage of the Linear Model is apparent. The simplicity of the function $M(\theta)$ permits integration in closed form so that the free energy and other thermodynamic properties can be obtained in closed parametric form.

In this section we present a summary of all relevant thermodynamic functions in terms of the Linear Model.

With some minor differences we use the notation of Hohenberg and Barmatz who first presented a list of these formulas [H4].

Variables

$$\Delta T^* = r(1-b^2\theta^2)$$

$$\Delta\rho^* = r^\beta k\theta \qquad (3.15)$$

$$-1 \leq \theta \leq 1$$

Chemical Potential

One-phase $$\Delta\mu^* = r^{\beta\delta} a\theta(1-\theta^2) \qquad (3.16a)$$

Two-phase $$\Delta\mu^* = 0 \qquad (3.16b)$$

Compressibility

$$\rho^{*2}K_T^* = r^{-\gamma}\frac{k}{a}\frac{1-b^2\theta^2(1-2\beta)}{1-3\theta^2+b^2\theta^2\{2\beta\delta(1-\theta^2)+3\theta^2-1\}} \qquad (3.17)$$

Helmholtz Free Energy

One-phase $$A^* = A_0^*(T^*) + \rho^*\mu^*(\rho_c^*, T^*) + r^{2-\alpha}(f_0 + f_2\theta^2 + f_4\theta^4) \qquad (3.18a)$$

Two-phase $$A^* = A_0^*(T^*) + \rho^*\mu^*(\rho_c^*, T^*) + r^{2-\alpha}(f_0 + f_2 + f_4) \qquad (3.18b)$$

Pressure

One-phase $$P^* = -A_0^*(T^*) + r^{\beta\delta}a\theta(1-\theta^2) + r^{\delta-\alpha}\{ak\theta^2(1-\theta^2) - f_0 - f_2\theta^2 - f_4\theta^4\} \qquad (3.19a)$$

Two-phase (vapor pressure)

$$P_{vap}^* = -A_0^*(T^*) - r^{2-\alpha}(f_0 + f_2 + f_4) \qquad (3.19b)$$

Entropy

One-phase $$-S^* = A_0^{*\prime}(T^*) + \rho^*\mu^{*\prime}(\rho_c^*, T^*) + r^{1-\alpha}\frac{\beta a_2}{1-b^2\theta^2(1-2\beta)} \qquad (3.20a)$$

Two-phase $$-S^* = A_0^{*\prime}(T^*) + \rho^*\mu^{*\prime}(\rho_c^*, T^*) + r^{1-\alpha}\frac{(2-\alpha)(f_0+f_2+f_4)}{1-b^2} \qquad (3.20b)$$

Heat Capacity

One-phase $$-C_v^*/T^* = A_0^{*\prime\prime}(T^*) + \rho^*\mu^{*\prime\prime}(\rho_c^*, T^*) + r^{-\alpha}\frac{\beta(a_1a_2-a_3)}{\{1-b^2\theta^2(1-2\beta)\}^3} \qquad (3.21a)$$

Two-phase $$-C_v^*/T^* = A_0^{*\prime\prime}(T^*) + \rho^*\mu^{*\prime\prime}(\rho_c^*, T^*) + r^{-\alpha}\frac{(2-\alpha)(1-\alpha)(f_0+f_2+f_4)}{(1-b^2)^2} \qquad (3.21b)$$

where

$$a_1 = (1-\alpha)\{1-b^2\theta^2(1-2\beta)\} - 2\beta b^2\theta^2(1-2\beta)$$

$$a_2 = (\delta+1)f_0 + (\delta-1)f_2\theta^2 + (\delta-3)f_4\theta^4 \qquad (3.22)$$

$$a_3 = 2\beta\theta^2\{1-b^2\theta^2(1-2\beta)\}\{(\delta-1)f_2 + 2(\delta-3)f_4\theta^2\}$$

while the quantities f_0, f_2, f_4 are defined by (3.14).

4. Method of Statistical Analysis

4.1. Introduction

The purpose of the statistical data analysis presented in this paper is to answer the following two questions: (1) do the proposed scaled equations of state represent the experimental data to within their random error, and (2) how do the random experimental errors affect the accuracy of the parameters determined in the fit? The techniques of linear least squares can only be used to answer these questions under very restrictive conditions. Thus, only the dependent variable is supposed to be subject to error, and the functional form has to be linear in the parameters that are to be determined. The cases we study here violate both conditions and there are, therefore, no rigorous statistical tools available for our purpose.

Statistical techniques for fitting the NBS equation to experimental equation of state data were developed earlier [V1]. For the purpose of this paper it was also necessary to develop a statistical method for fitting the Linear Model to the experimental data. This task is not trivial; the model is not only nonlinear in several of the adjustable parameters, but also transformations have to be made from the physical to the parametric variables.

The approach we have taken is, to apply the methods of linear least-squares statistics under the assumption that the function can be linearized in the parameters in at least a small range of parameter values near the optimum set. We will first summarize some results of linear least-squares statistics that we have used, and then proceed to show how these results can be adapted to the more general nonlinear problems encountered in our work. In describing the method of statistical analysis we shall follow Natrella and Scheffé in using a matrix formulation wherever practical [L6, N1, S4].

4.2. Linear Least-Squares Analysis

The general problem of linear least-squares is to fit a set of n observations Y_i, subject to random error, to a linear combination of a set of k functions $X_1, \ldots X_k$ of the independent variables which are free of error and whose values are indicated by $X_{1i}, \ldots, X_{ki}$ $(i=1 \ldots n)$. It is convenient to consider the observable Y as an n-dimensional column vector denoted by $\mathbf{Y}$. The set of function values $X_{1i}, \ldots, X_{ki}$ $(i=1 \ldots n)$ can then

be represented by a matrix X of n rows and k columns. The expectation value $\boldsymbol{E}(\boldsymbol{Y})$ of $\boldsymbol{Y}$ is assumed to be a vector of the form

$$\boldsymbol{E}(\boldsymbol{Y}) = X\boldsymbol{\beta}. \tag{4.1}$$

Here $\boldsymbol{\beta}$ is a k-dimensional column vector representing the k adjustable parameters multiplying the functions $X_1 \ldots X_k$.

The variances and covariances of the observable $\boldsymbol{Y}$ are conveniently described by

$$\mathrm{Var}\,\boldsymbol{Y} = \sigma_y^2 B, \tag{4.2}$$

where B is the $n \times n$ variance-covariance matrix of the experimental data.

If the independent variables are free of error, then the fundamental theorem of least squares says that unbiased, most probably estimates for the parameters $\boldsymbol{\beta}$ are obtained by minimizing the sum-of-squares SS, given by

$$\mathrm{SS} \equiv (\boldsymbol{Y} - X\boldsymbol{\beta})^{\mathrm{T}} B^{-1} (\boldsymbol{Y} - X\boldsymbol{\beta}), \tag{4.3}$$

with respect to the β's. The superscript T denotes a transpose. The optimized set $\hat{\boldsymbol{\beta}}$ is calculated from the so-called normal equations

$$X^{\mathrm{T}} B^{-1} X\hat{\boldsymbol{\beta}} = X^{\mathrm{T}} B^{-1} \boldsymbol{Y}. \tag{4.4}$$

The variance-covariance matrix of the coefficients $\boldsymbol{\beta}$ is the inverse of the matrix of normal equations. We have

$$\mathrm{Var}\,\hat{\boldsymbol{\beta}} = (X^{\mathrm{T}} B^{-1} X)^{-1} \sigma_y^2. \tag{4.5}$$

The variance σ_y^2, if not known a priori from repeated measurements, can be estimated from the observed deviations from the fitted function, $\boldsymbol{Y} - X\hat{\boldsymbol{\beta}}$, as

$$\sigma_{y,\mathrm{est.}}^2 = \frac{1}{n-k} [\boldsymbol{Y} - X\hat{\boldsymbol{\beta}}]^{\mathrm{T}} B^{-1} [\boldsymbol{Y} - X\hat{\boldsymbol{\beta}}]. \tag{4.6}$$

In the case that the experimental data are uncorrelated, the matrix B in equation (4.2) is diagonal, and we have, for each experimental point Y_i,

$$\sigma_{y_i}^2 = \sigma_y^2 B_{ii}. \tag{4.7}$$

The inverse of the $n \times n$ diagonal matrix with elements B_{ii} is another $n \times n$ diagonal matrix called the weight matrix. If we call its elements w_i, then the expression (4.6) for the variance of the fit, σ_y^2, goes over into the more familiar form

$$\sigma_y^2 = \frac{1}{n-k} \sum w_i S_i^2, \tag{4.8}$$

with $S_i = Y_i - (X\boldsymbol{\beta})_i = Y_{i,\mathrm{exp}} - Y_{i,\mathrm{calc}}$. The absolute value of σ_y^2 will depend on the values chosen for the elements of the matrix B, through (4.2) or (4.7). Thus, if the diagonal elements of B are chosen to be equal to $B_{ii} = \sigma_{yi}^2$, or those of the weight matrix to $w_{ii} = 1/\sigma_{yi}^2$, then we have assigned *absolute weights*. The value of σ_y^2 may be estimated according to (4.6) or (4.8). The variance σ_y^2, when absolute weights are given, is called the reduced variance χ^2; it is generally estimated from (4.6). If this estimate is based on a large number of experimental points, χ^2 will be quite close to unity. In fact, χ^2 is distributed as chi-square, and, if the number of degrees of freedom is appreciable, as is true in most of our applications, χ^2 will exceed the value unity by 0.1 or more by chance in no more than 30 percent of the cases [B1, N1].

Thus, if in a particular fit using absolute weights a value of the reduced variance is obtained that greatly exceeds unity, closer scrutiny of the procedures may reveal one or more of the following problems.

(1) The experimental variances $\sigma_{y_i}^2$ have been underestimated so that weights have been assigned that are too large. In most cases, the information needed for independent determination of the $\sigma_{y_i}^2$, namely repeated measurements at each point, is simply not available and the variances $\sigma_{y_i}^2$ have to be estimated using our insight into the experimental method used, or information about it provided by the experimenter. Thus, an inordinately large (or, for that matter, small) value of χ^2 may reveal that our understanding of the experimental accuracy is incomplete.

(2) The model function used is wrong. The functional form used may be incorrect, or one or more fixed parameters have been assigned wrong values. In either case, the experimental function values will depart from the calculated ones in a systematic way, while at least some of the deviations will grossly exceed the estimated standard deviation σ_{y_i}. If the functional form has been chosen incorrectly, the model function has to be rejected. If, however, only some parameters have been chosen incorrectly, the possibility exists of improving the fit and decreasing the value of χ^2 by modifying the parameters in the fit. In fact, minimization of χ^2 by stepwise variation of parameters in the fitting function is a technique we have extensively used in this paper.

(3) One or more experimental points are in error. In order to determine whether this is the case, the individual deviations between experimental and predicted values are inspected. Here the assignment of absolute weights is a very useful tool. Each deviation is compared with the estimated standard deviation at the same point, $\sigma_{y_i} = (1/w_i)^{1/2}$. For the numbers of data points handled here, deviations larger than three times the standard deviation are unlikely to occur by chance, and points at which such deviations occur have to be rejected unless factors listed under (1) or (2) are present.

Summarizing, our procedure will be to make an absolute weight assignment on the basis of our insight into the experimental procedure, and then to minimize χ^2 by variation of adjustable parameters in the model function. The adequacy of the model function and the absence of erroneous data can be tested using the properties of the reduced variance χ^2 and the distribution of individual errors σ_y.

4.3. Nonlinear Least-Squares Analysis

The data analysis in the present paper will fall almost invariably outside the reach of linear least-squares fitting procedures. The reasons are one or more of the following.

(1) The model functions used are nonlinear in one or more of the parameters.

(2) Independent as well as dependent variables are subject to error.

The methods of linear least-squares, as sketched in the previous section, will, however, still be approximately valid if the functional form used can be expanded to linear order for parameter values near the optimum ones. This assumption is basic to the work that follows.

In matrix formulation we have, instead of the linear relation $\boldsymbol{E}(\boldsymbol{Y})=X\boldsymbol{\beta}$, the more general form

$$\boldsymbol{E}(\boldsymbol{Y})=\boldsymbol{Y}(X,\boldsymbol{\beta}). \tag{4.9}$$

Expanding the functional form $\boldsymbol{Y}(X,\boldsymbol{\beta})$ in the vicinity of the parameter set $\boldsymbol{\beta}^\circ$, we obtain

$$\boldsymbol{E}(\boldsymbol{Y})=\boldsymbol{Y}(X,\boldsymbol{\beta}^\circ)+Y_\beta(\boldsymbol{\beta}-\boldsymbol{\beta}^\circ). \tag{4.10}$$

Here Y_β is the $n\times k$ matrix of derivatives $\partial Y_i/\partial\beta_j$, $i=1\ldots n$, $j=1\ldots k$. Note that the relation (4.10) is linear in the parameter adjustments $\boldsymbol{\beta}-\boldsymbol{\beta}^\circ$, the derivatives Y_β replacing the functions X in (4.1). In the linear case, we minimized the weighted sum of squares of the differences $\boldsymbol{Y}-\boldsymbol{E}(\boldsymbol{Y})$ with respect to $\boldsymbol{\beta}$; now, we minimize $\boldsymbol{Y}-\boldsymbol{E}(\boldsymbol{Y})-\boldsymbol{Y}(X,\boldsymbol{\beta}^\circ)$ with respect to the β's. Note that $\boldsymbol{Y}-\boldsymbol{Y}(X,\boldsymbol{\beta}^\circ)$ are the experimental residuals $\Delta\boldsymbol{Y}^\circ=\boldsymbol{Y}_{\text{exp}}-\boldsymbol{Y}^\circ_{\text{calc}}$, calculated with respect to the parameter set $\boldsymbol{\beta}^\circ$. Consequently, we have reduced the nonlinear problem of fitting $\boldsymbol{Y}$ to $\boldsymbol{Y}(X,\boldsymbol{\beta})$ to a linear least-squares problem, namely that of fitting the "zero-order" residuals $\Delta\boldsymbol{Y}^\circ$ to the derivatives Y_β. In practice, these derivatives are obtained analytically or numerically from the function $\boldsymbol{Y}(X,\boldsymbol{\beta}^\circ)$ at the parameter values $\boldsymbol{\beta}^\circ$.

The calculation of the adjustments $\hat{\boldsymbol{\beta}}-\boldsymbol{\beta}^\circ$ proceeds parallel to the calculations of the $\boldsymbol{\beta}$'s sketched in the previous section. In particular, the variances and covariances of the parameter adjustments $\hat{\boldsymbol{\beta}}-\boldsymbol{\beta}^\circ$, and, therefore those of the $\hat{\boldsymbol{\beta}}$'s themselves, are calculated from the equivalent of (4.5):

$$\text{Var}\,(\hat{\boldsymbol{\beta}}-\boldsymbol{\beta}^\circ)=\text{Var}\,\hat{\boldsymbol{\beta}}=(Y_\beta^{\mathrm{T}}B^{-1}Y_\beta)^{-1}\sigma_y^2. \tag{4.11}$$

The procedure we have generally followed in this paper is to calculate the "best" parameter set $\boldsymbol{\beta}^\circ$ from a combined stepwise variation/least-squares fit to the data, in which some parameters were kept fixed in those cases where they were well-known. After the value of χ^2 could no longer be lowered by further parameter changes considered reasonable in the physical context, the linearization procedure was used for the sole purpose of obtaining the variance-covariance matrix (4.11) for all parameters involved. This way, the errors and correlations of all parameters including those occurring nonlinearly could be estimated.

4.4 Nonlinear Least-Squares and Propagation of Error

Having outlined the procedures for statistical treatment of parameters occurring nonlinearly, we now turn to the second obstacle to usage of linear least-squares, namely, the fact that independent as well as dependent variables are subject to error. Thus, we want to make adjustments not only in the dependent, but also in the independent variables. A sum of squares has to be minimized while weighted so as to reflect not only the accuracy of the different variables, but also the "steepness" of the functional dependence on each of these variables. A slight generalization of the linearization procedure outlined in the previous section will be necessary.

Since all variables are subject to error, there is no point in distinguishing between dependent and independent variables. So we lump all variables together and denote the collection by $\boldsymbol{Z}$, an m-dimensional vector of observables.

Then the functional relationship between the expectation values of the Z's which includes the adjustable parameters $\beta_1\ldots\beta_k$, can be written as a set of condition equations

$$\begin{aligned} &F_1\{E(Z_1)\ \ldots\ E(Z_m);\ \beta_1\ \ldots\ \beta_k\}=0,\\ &\vdots\\ &F_n\{E(Z_1)\ \ldots\ E(Z_m);\ \beta_1\ \ldots\ \beta_k\}=0. \end{aligned} \tag{4.12}$$

Thus the n condition equations $\boldsymbol{F}(\boldsymbol{Z},\boldsymbol{\beta})=0$ replace the n linear equations $\boldsymbol{E}(\boldsymbol{Y})-X\boldsymbol{\beta}=0$, given in (4.1). While in the linear problem the sum $\Sigma w_i\{Y_i-E(Y_i)\}^2$ was minimized with respect to the β's with $\boldsymbol{E}(\boldsymbol{Y})-X\boldsymbol{\beta}=0$, we will now want to minimize $\Sigma w_i\{Z_i-E(Z_i)\}^2$ with respect to the β's, while fulfilling the conditions (4.12). To this end, we again linearize the equations (4.12), by expanding around a set of parameter values $\boldsymbol{\beta}^\circ$ and a set of Z values for which we take the experimentally measured set.

We then obtain

$$\boldsymbol{F}^\circ=F_Z^{\mathrm{T}}\{\boldsymbol{Z}-\boldsymbol{E}(\boldsymbol{Z})\}+F_\beta(\boldsymbol{\beta}_j-\boldsymbol{\beta}_j^\circ). \tag{4.13}$$

Here $\boldsymbol{F}^\circ=\boldsymbol{F}\{\boldsymbol{Z},\boldsymbol{\beta}^\circ\}$ and F_Z is the $m\times n$ matrix of derivatives $\partial F_j/\partial Z_i$, $i=1\ldots m$, $j=1\ldots n$, and F_β is the $n\times k$ matrix of derivatives $-\partial F_j/\partial\beta_l$, $j=1\ldots n$, $l=1\ldots k$. We can write (4.13) more compactly as

$$\boldsymbol{F}^\circ-F_\beta\Delta\boldsymbol{\beta}=F_Z^{\mathrm{T}}\Delta\boldsymbol{Z}, \tag{4.14}$$

where

$$\Delta\boldsymbol{\beta}=\boldsymbol{\beta}-\boldsymbol{\beta}^\circ. \tag{4.15}$$

Now suppose we minimize the weighted sum of squares SS:

$$\text{SS}=(\boldsymbol{F}^\circ-F_\beta\Delta\boldsymbol{\beta})^{\mathrm{T}}L^{-1}(\boldsymbol{F}^\circ-F_\beta\Delta\boldsymbol{\beta}), \tag{4.16}$$

with respect to $\Delta\boldsymbol{\beta}$. Here the $n\times n$ matrix L is defined by

$$L = F_Z^{\mathrm{T}} F_Z. \tag{4.17}$$

Using (4.14), it is easily seen that

$$(\boldsymbol{F}^{\circ} - F_\beta \Delta\boldsymbol{\beta})^{\mathrm{T}} L^{-1} (\boldsymbol{F}^{\circ} - F_\beta \Delta\boldsymbol{\beta}) = [F_Z^{\mathrm{T}} \Delta\boldsymbol{Z}]^{\mathrm{T}} [F_Z^{\mathrm{T}} F_Z]^{-1} [F_Z^{\mathrm{T}} \Delta\boldsymbol{Z}] = (\Delta\boldsymbol{Z})^{\mathrm{T}} (\Delta\boldsymbol{Z}). \tag{4.18}$$

Thus the sum of squares of $\boldsymbol{F}^{\circ} - F_\beta \Delta\boldsymbol{\beta}$, weighted by the matrix L, equals the unweighted sum of squares of the adjustments $\Delta\boldsymbol{Z}$. Therefore, by solving the linear least-squares problem (4.16) we achieve a minimization of the sum of squares of the ΔZ.

By analogy with (4.3) and (4.4), the solution of minimization of (4.16) is

$$F_\beta^{\mathrm{T}} L^{-1} F_\beta \Delta\boldsymbol{\beta} = F_\beta^{\mathrm{T}} L^{-1} \boldsymbol{F}^{\circ}, \tag{4.19}$$

while

$$\mathrm{Var}\ \Delta\boldsymbol{\beta} = (F_\beta^{\mathrm{T}} L^{-1} F_\beta)^{-1} \sigma_Z^2. \tag{4.20}$$

Then, the adjustments of the experimental Z values follow from

$$\Delta\boldsymbol{Z} = F_Z L^{-1} (\boldsymbol{F}^{\circ} - F_\beta \Delta\boldsymbol{\beta}). \tag{4.21}$$

So far, the $\Delta\boldsymbol{Z}$ have been treated as being of equal weight. The extension to correlated data of unequal variance is entirely straightforward. The variance of $\boldsymbol{Z}$ is now given by

$$\mathrm{Var}\ \boldsymbol{Z} = \sigma_Z^2 A, \tag{4.22}$$

where A is an $m\times m$ matrix. The L matrix in (4.17) is generalized to

$$L' = F_Z^{\mathrm{T}} A F_Z. \tag{4.23}$$

The adjustments of the β's are calculated from

$$F_\beta^{\mathrm{T}} L'^{-1} F_\beta \Delta\boldsymbol{\beta} = F_\beta^{\mathrm{T}} L'^{-1} \boldsymbol{F}^{\circ}. \tag{4.24}$$

Comparing (4.24) with (4.4) we see that the new matrix L'^{-1} plays the role of the former weight matrix B^{-1}.

The variance-covariance matrix of the adjustments $\Delta\boldsymbol{\beta}$ is given by

$$\mathrm{Var}\ \Delta\boldsymbol{\beta} = (F_\beta^{\mathrm{T}} L'^{-1} F_\beta)^{-1} \sigma_Z^2, \tag{4.25}$$

while the adjustments of the Z follow from

$$\Delta\boldsymbol{Z} = A F_Z L'^{-1} (\boldsymbol{F}^{\circ} - F_\beta \Delta\boldsymbol{\beta}). \tag{4.26}$$

The results (4.22) through (4.26) are sufficiently general to be applicable to a variety of nonlinear least-squares problems. One such problem, of particular interest to us here, is that of the case in which all variables are subject to error. For simplicity, we will assume that the dependent variable $\boldsymbol{Y}$, an n-dimensional vector, can be explicitly expressed as a function of independent variables X_1, X_2, such that

$$\boldsymbol{E(Y)} = \boldsymbol{Y}(E(X_1), E(X_2), \ldots; \beta_1 \ldots \beta_k). \tag{4.27}$$

We will assume that the errors in dependent and independent variables are uncorrelated but of unequal variance. Thus

$$\mathrm{Var}\ \boldsymbol{Z} = \sigma_Z^2 A, \tag{4.28}$$

where A is an $m\times m$ diagonal matrix. The first n elements $A_{ii}^{(0)}$, $i=1 \ldots n$, refer to the variances of the Y_i, the next n elements $A_{ii}^{(1)}$, $i=1 \ldots n$, to the variances of the first independent variable X_1, etc. The condition equations (4.12) are now replaced by (4.27) expressing the expectation values of the n-dimensional vector $\boldsymbol{Y}$ as a function of the expectation values of the independent variables X_1, X_2, and the adjustable parameters $\boldsymbol{\beta}$. Therefore, the matrix of derivatives, F_Z, now consists of a vertical stack of $n\times n$ square diagonal matrices: the first one, involving the derivatives $\partial F/\partial Y_1$ to $\partial F/\partial Y_n$, being a unit matrix, the second one having diagonal elements $\partial F/\partial X_{1i}$, $i=1 \ldots n$, etc. It follows that the matrix L' in (4.23) is diagonal, of size $n\times n$, with elements of the form

$$L'_{ii} = A_{ii}^{(0)} + A_{ii}^{(1)} (\partial Y_i/\partial X_{1i})^2 + A_{ii}^{(2)} (\partial Y_i/\partial X_{2i})^2 + \ldots \tag{4.29}$$

(Strictly speaking, (4.29) is oversimplified, since instead of Y and X, their expectation values should have been used.)

Thus the fact that all variables are subject to error is, in this linear approximation, accounted for by modifying the absolute weight of the individual points $Y_i(X_{1i}, X_{2i} \ldots)$ to a new weight w_i such that

$$w_i^{-1} = A_{ii}^{(0)} + A_{ii}^{(1)} (\partial Y_i/\partial X_{1i})^2 + A_{ii}^{(2)} (\partial Y_i/\partial X_{2i})^2 + \ldots \tag{4.30}$$

The use of these modified weights is the equivalent of the procedure of "propagation of error".

In the present work, propagation of error has been used extensively. However, for the sake of completion we mention that the calculation of $\Delta\boldsymbol{\beta}$, the variance-covariance matrix and of $\Delta\boldsymbol{Y}$ and $\Delta\boldsymbol{X}$ proceeds straightforwardly according to (4.24), (4.25) and (4.26). It may be pointed out that the adjustments are partitioned between the independent and dependent variables in the following way

$$\Delta Y_i = \frac{A_{ii}^{(0)}}{A_{ii}^{(0)} + A_{ii}^{(1)} \left(\frac{\partial Y_i}{\partial X_{1i}}\right)^2 + A_{ii}^{(2)} \left(\frac{\partial Y_i}{\partial X_{2i}}\right)^2 + \ldots} (\boldsymbol{F}^{\circ} - F_\beta \Delta\boldsymbol{\beta})_i, \tag{4.31}$$

$$\Delta X_{1i} = \frac{A_{ii}^{(1)}}{A_{ii}^{(0)} + A_{ii}^{(1)} \left(\frac{\partial Y_i}{\partial X_{1i}}\right)^2 + A_{ii}^{(2)} \left(\frac{\partial Y_i}{\partial X_{2i}}\right)^2 + \ldots} \left(\frac{\partial Y_i}{\partial X_{1i}}\right) (\boldsymbol{F}^{\circ} - F_\beta \Delta\boldsymbol{\beta})_i.$$

4.5. Fitting the Linear Model

The Linear Model, as formulated in section 3.2, contains seven parameters, namely, ρ_c, T_c, β, δ, a, b^2 and k or x_0. The values of these parameters are determined by the following procedures. First, the critical density ρ_c is determined either as the point of antisymmetry of the $\Delta\mu$-isotherms or from the diameter of the coexistence curve [L7, V1]; it is verified whether both procedures yield the same value for ρ_c within the precision of the analysis. The coefficient x_0 and the exponent β are determined from power law fits to coexistence curve data in accordance with [L7].

$$(\rho^*_{\text{liquid}}-\rho^*_{\text{gas}})/2=x_0^{-\beta}|\Delta T^*|^{\beta}, \tag{4.32}$$

starting with a best estimate for T_c. The parameters T_c, δ, b^2 and a are then determined from an analysis of experimental $\Delta\mu^*$ data as a function of density and temperature. It is checked whether the optimum value obtained for T_c is consistent with the value used in (4.32). The critical pressure P_c appears only as a normalization factor in the calculation of $\Delta\mu^*$ and is, therefore, not important in the analysis; it is simply taken as the experimental pressure corresponding to the density and temperature attributed to the critical point.

The problem is thus reduced to that of finding the optimum values of T_c, δ, b^2 and a from the experimental $\Delta\mu^*$ as a function of density and temperature, assuming that ρ_c, β and x_0 are known. We proceed as follows. For a given choice of T_c, δ and b^2 we construct, for each T, ρ pair, the quantity

$$x=\frac{\Delta T^*}{|\Delta\rho^*|^{1/\beta}}=\frac{1-b^2\theta^2}{k^{1/\beta}|\theta|^{1/\beta}}, \tag{4.33}$$

with k determined through equation (3.8). Equation (4.33) is solved by standard numerical methods to yield a value of the parameter θ for each experimental $(\Delta T^*, \Delta\rho^*)$ point. As a next step the quantity $a(\theta)$ is calculated as

$$a(\theta)=\frac{k^{\delta}|\theta|^{\delta-1}}{1-\theta^2}\,h(x)=\frac{k^{\delta}|\theta|^{\delta-1}}{1-\theta^2}\,\frac{|\Delta\mu^*|}{|\Delta\rho^*|^{\delta}}. \tag{4.34}$$

Hence, each experimental value of $\Delta\mu^*$ as a function of $\Delta\rho^*$ and ΔT^* is converted into an "experimental" value of $a(\theta)$ as a function of θ. For the Linear Model to be valid, $a(\theta)$ must be independent of θ to within the precision of the experiments. The weighted average $\bar{a}$ of the experimental $a(\theta)$ values is determined together with the reduced variance χ^2. The procedure is then repeated for other choices of T_c, δ and b^2, until a minimum value of χ^2 is returned from the fit.

An absolute weight assignment to the experimental $a(\theta)$ is obtained as follows. First, an estimate is made of the experimental error in chemical potential, density and temperature. Let σ_{T^*}, σ_{ρ^*} and σ_{μ^*} be the estimated standard deviations of the reduced temperature T^*, the reduced density ρ^*, and the reduced chemical potential μ^*, respectively. Using the law of propagation of errors (4.30), we write

$$\sigma_a^2=\left(\frac{\partial a}{\partial T^*}\right)^2_{\rho^*,\mu^*}\sigma^2_{T^*}+\left(\frac{\partial a}{\partial \rho^*}\right)^2_{T^*,\mu^*}\sigma^2_{\rho^*}+\left(\frac{\partial a}{\partial \mu^*}\right)^2_{T^*,\rho^*}\sigma^2_{\mu^*}. \tag{4.35}$$

Because of the intervening transformation to parametric variables, the calculation of the variance of a is a little complicated. We first calculate the variance of θ using (4.33) and the experimental errors σ_{T^*} and σ_{ρ^*} and then calculate the variance in a (θ) due to the direct error in $\Delta\rho^*$ and $\Delta\mu^*$ and the propagated errors in θ from $\Delta\rho^*$ and ΔT^*. We thus obtain

$$\sigma_a^2=a^2(\theta)\left[\left(\frac{\sigma_{T^*}}{\Delta T^*}\right)^2\beta^2q^2(\theta)+\left(\frac{\sigma_{\rho^*}}{\Delta\rho^*}\right)^2\{\delta-q(\theta)\}^2+\left(\frac{\sigma_{\mu^*}}{\Delta\mu^*}\right)^2\right], \tag{4.36}$$

with

$$q(\theta)=\frac{\{(\delta-1)(1-\theta^2)+2\theta^2\}(1-b^2\theta^2)}{\{1-b^2\theta^2(1-2\beta)\}(1-\theta^2)}. \tag{4.36a}$$

To each experimental value $a_i=a(\theta_i)$ we thus assign the weight $w_{ai}=1/\sigma^2_{a_i}$ with $\sigma^2_{a_i}$ given by (4.36). The variance s^2 of the average of $a(\theta)$, $\bar{a}$, over all N data points is

$$s^2=\left[\frac{\sum(a_i/\sigma_{a_i})^2}{\sum(1/\sigma_{a_i})^2}-\bar{a}^2\right]\frac{N}{N-1}, \tag{4.37}$$

and the reduced variance χ^2 equals

$$\chi^2=\frac{s^2}{N}\sum\frac{1}{\sigma^2_{a_i}}. \tag{4.38}$$

Assuming that the experimental errors have been properly estimated, the Linear Model provides a valid representation of the data, if χ^2 is of order unity as discussed in section 4.2.

4.6. Error Estimation for the Parameters in the Linear Model

Suppose that a minimum is found on the χ^2 surface after stepwise variation of T_c, δ, b^2, keeping ρ_c, β and x_0 fixed. The location of the minimum determines all parameters in the Linear Model, namely a in addition to the six just mentioned. The question now arises as to

what kind of variability would have existed in these seven parameters, had they all been varied simultaneously. The results of section 4.3 will be used to answer this question. As was shown in (4.10), the functional form for the quantity a, given by (4.34) in combination with (4.33), should be expanded in the vicinity of the "best" parameter set. The matrix Y_β of derivatives of the functional form with respect to all derivatives, occurring in (4.10), is then used to form the matrix of normal equations, the inverse of which, cf. (4.11), forms the variance-covariance matrix of the parameters.

For the Linear Model, the matrix of derivatives Y_β can be calculated analytically. Again, the transformation to parametric variables presents some complications, but these are not insurmountable. Thus, as a first step, the derivatives of θ with respect to the adjustable parameters T_c, ρ_c, x_0, b are calculated from (4.33). Then, the derivatives of a with respect to all parameters are calculated from (4.34) realizing that there is, in addition to the direct dependence on ρ_c, x_0, b^2, β, also an implicit dependence on these parameters through θ. The resulting derivatives of a with respect to the six adjustable parameters T_c, ρ_c, β, x_0, δ, b^2 are presented in the Appendix and can be evaluated in a straightforward manner.

Since a is an adjustable parameter itself, the matrix Y_β contains a column of unity, in addition to the derivatives of a with respect to the six other parameters. One problem was encountered in constructing the matrix Y_β. It turned out that the derivative $(\partial a/\partial b)_\beta$ is constant for the choice $b^2 = b^2_{\mathrm{SLH}}$, defined in (3.9). As a consequence, two columns of the matrix Y_β are proportional to each other. If b^2 is close to b^2_{SLH}, the adjustments of a and b will be nearly dependent. Thus, the adjustments of a and b cannot be separated in the cases we have studied. The practical course we have taken is, to ascribe the contribution arising from the unit column in Y_β to errors in b^2 and to quote as error in a the experimental standard deviations defined by (4.37).

In the fits to the Linear Model, we have performed the error calculation as outlined above, and we present for each gas, in addition to the standard deviation of each individual parameter, the variance-covariance matrix of the six parameters with diagonal elements normalized to unity.

4.7. Fitting the NBS Equation

The NBS equation

$$\Delta\mu^* = (\Delta\rho^*)|\Delta\rho^*|^{\delta-1}E_1\left(\frac{x+x_0}{x_0}\right)\left[1+E_2\left(\frac{x+x_0}{x_0}\right)^{2\beta}\right]^{(\gamma-1)/2\beta}, \tag{4.39}$$

was fitted to experimental $\Delta\mu^*(\Delta\rho^*, \Delta T^*)$ data by the same procedure used earlier in reference [V1]. The parameters ρ_c, x_0 and β are again determined from an analysis of coexistence curve date and from symmetry conditions and have the same values as used in fitting the Linear Model. Then for a given choice of T_c and γ, an experimental quantity $G(x)$ is constructed as

$$[G(x)]_{\mathrm{exp}} = \left[\frac{|\Delta\mu^*|}{|\Delta\rho^*|^\delta}\left(\frac{x_0}{x+x_0}\right)\right]^{2\beta/(\gamma-1)}, \tag{4.40}$$

with $x = \Delta T^*/|\Delta\rho^*|^{1/\beta}$.

According to the NBS equation (4.39), the quantity $G(x)$ is a linear function of the experimental variable $\{(x+x_0)/(x_0\}^{2\beta}$

$$[G(x)]_{\mathrm{calc}} = E_1^{2\beta/(\gamma-1)}\left[1+E_2\left(\frac{x+x_0}{x_0}\right)^{2\beta}\right]. \tag{4.41}$$

Thus, a weighted linear least-square fit of equation (4.41) to the experimental values of $G(x)$ yields, for each choice of δ (or γ) and T_c, an intercept $E_1^{2\beta/(\gamma-1)}$ and slope $E_2E_1^{2\beta/(\gamma-1)}$, from which values of E_1 and E_2 are extracted; in addition a value is obtained for the reduced variance χ^2 of each fit. The parameters δ and T_c are then varied in fine steps, until a minimum value is obtained for χ^2.

The absolute weight assignment to the experimental values of $G(x)$ is obtained by calculating the variance of $G(x)$ from the estimated standard deviations σ_{T^*}, σ_{ρ^*} and σ_{μ^*} using the law of propagation of errors (4.30):

$$\sigma_G^2 = \left(\frac{\partial G}{\partial T^*}\right)^2_{\rho^*,\mu^*}\sigma^2_{T^*} + \left(\frac{\partial G}{\partial \rho^*}\right)^2_{T^*,\mu^*}\sigma^2_{\rho^*} + \left(\frac{\partial G}{\partial \mu^*}\right)^2_{T^*,\rho^*}\sigma^2_{\mu^*}, \tag{4.42}$$

which, using (4.33), reduces to

$$\sigma_G^2 = G^2(x)\left(\frac{2\beta}{\gamma-1}\right)^2\left[\left(\frac{\sigma_{T^*}}{\Delta T^*}\right)^2\left(\frac{x}{x+x_0}\right)^2 + \left(\frac{\sigma_{\rho^*}}{\Delta\rho^*}\right)^2\left\{\delta - \frac{x}{\beta(x+x_0)}\right\}^2 + \left(\frac{\sigma_{\mu^*}}{\Delta\mu^*}\right)^2\right]. \tag{4.43}$$

The absolute weight assigned to each experimental G value is the inverse of σ_G^2, given by (4.43).

For the NBS equation we did not conduct a detailed error analysis of all parameters, as was done for the Linear Model. First, the necessary derivatives were hard to obtain analytically. Secondly, in view of the fact that it is integrable and that it satisfies all the conditions of analyticity, the Linear Model seems the more fundamental approach. Since the NBS equation and the Linear Model have the same number of adjustable parameters and appear to fit the data equally well, we expect that the error estimates for the critical exponents in the two equations will be the same.

5. Data Evaluation and Results of Analysis

5.1. Introduction

The NBS equation and the Linear Model were fitted to chemical potential data as a function of density and

temperature. Most of the available experimental data are pressure data as a function of density at selected temperatures. Values for the chemical potential difference $\Delta\mu$ were obtained by integrating $P(\rho)$ data along isotherms

$$\Delta\mu = \int_{P(\rho_c,T)}^{P(\rho,T)} \rho^{-1} dP, \tag{5.1}$$

using the Gibbs-Duhem relation $(\partial P/\partial\mu)_T = \rho$.

Tables of $\Delta\mu$ as a function of density and temperature for Xe, He^4 and CO_2 were presented earlier in reference [V1]. We found it desirable to repeat the calculations for CO_2 and we present a somewhat revised table of $\Delta\mu$ values. We have also made a few corrections in the table of $\Delta\mu$ values previously reported for He^4. For He^3 we have used the $\Delta\mu$ values tabulated by Wallace and Meyer [W4]. For steam a computer program for numerical integration was written in view of the large amount of experimental data. However, the *PV* data of steam are rather widely spaced in density which reduces the accuracy of the values deduced for $\Delta\mu$. Weber's data [W2] for O_2, being density profile data, did not require numerical integration.

In order to fit the NBS equation it is necessary that the pressure data be converted into chemical potential data. In this paper we want to make an intercomparison between the NBS equation and the Linear Model and to present sets of consistent parameters so that the two scaled equations of states can be used interchangeably. Therefore, for the purpose of this paper the two scaled equations of state are fitted to the same set of input data, i.e. *chemical potential* data. However, as a consequence of its integrability, it is in principle possible to fit the Linear Model directly to the experimental *pressure* data. A method for doing this has been developed in collaboration with Murphy [M2, M3].

For each gas we give a detailed discussion of the accuracy of the experimental data, the choice of critical parameters, the results of an analysis of the coexistence curve and optimum values for the parameters in the two scaled equations. For both equations of state we present a plot of deviations of the experimental $\Delta\mu$ values from the fitted curve. In order to show the quality of the fit we consider normalized deviations $(\Delta\mu^*_{\text{exp}} - \Delta\mu^*_{\text{calc}})/\sigma_{\Delta\mu^*}$, where $\sigma_{\Delta\mu^*}$ is the total estimated uncertainty in $\Delta\mu^*$ due to the uncertainties σ_{T^*}, σ_{ρ^*} and σ_{μ^*} in temperature, density and chemical potential

$$\sigma^2_{\Delta\mu^*} = \sigma^2_{T^*}\left(\frac{\partial\Delta\mu^*}{\partial T^*}\right)^2_{\rho^*} + \sigma^2_{\rho^*}\left(\frac{\partial\Delta\mu^*}{\partial\rho^*}\right)^2_{T^*} + \sigma^2_{\mu^*}. \tag{5.2}$$

Since the density is usually several orders more precisely known than the small increments in pressure along the near-critical isotherms, the estimated error, σ_{μ^*} in the chemical potential μ^* was taken to be twice the estimated error σ_{P^*} in the pressure.

For the Linear Model we also present a plot of normalized deviations $(a-\bar{a})/\sigma_a$ of the experimental $a(\theta)$ values from the average value $\bar{a}$, where σ_a was defined in (4.36); these plots show directly to what extent the Linear Model approximation to the parametric representation is justified.

It turns out that the NBS equation and the Linear Model represent the experimental data equally well. If the two equations are equivalent, then one way of interrelating the parameters in the two equations explicitly, is to require that both equations yield the same coefficients D and Γ in the power laws (2.2) and (2.3) with the result [C1]:

$$E_2^{-1} = \left[\frac{b^{(\delta-3)/(\gamma-1)}}{b^2-1}\right]^{2\beta} - 1, \tag{5.3}$$

$$E_1 = \frac{a(b^2-1)^\gamma}{k^\delta E_2^{(\gamma-1)/2\beta}}. \tag{5.4}$$

These relations are approximately satisfied by the parameters of the best fits.

The NBS equation is a convenient equation, when one needs only to calculate the chemical potential or the compressibility as a function of density and temperature. Closed form expressions for the singular contributions to the other thermodynamic functions can only be given in terms of the Linear Model parameters. Use of the Linear Model requires that equation (4.33) be inverted to determine the value of the parametric variable θ as a function of $\Delta\rho^*$ and ΔT^*.

In the tables of equation of state parameters we also present the corresponding values of the coefficients and exponents of all power laws defined in section 2.2. The coefficients A^+, A_{I}^- and A_{II}^- for the specific heat anomaly are given for the Linear Model only. Calculation of the specific heat from the NBS equation is tedious; we made some checks which indicated that the NBS equation yields the same values for the coefficients A^+, A_{I}^- and A_{II}^- to within about one percent. However, these coefficients do vary strongly with changes in the values assumed for the critical exponents β and δ.

The equations presented in this paper yield an accurate description of the chemical potential and the compressibility. The coefficients for the specific heat C_v are given for the sake of completeness and consistency. An analysis of experimental C_v data in terms of a scaled equation of state has been attempted by a few authors, but with limited success [B2, H5, M4]. In analyzing C_v data one encounters the following complications. The exponent α of the specific heat anomaly is small and very sensitive to small changes in the values of the exponents β and δ. Since the anomaly is weak, the background terms $A_0^{*\prime\prime}(T^*)$ and $\rho^*\mu^{*\prime\prime}(\rho_c^*, T^*)$ in (3.21) play a crucial role in the analysis; these background terms cannot be deduced from the equations of state presented here. Moreover, C_v being a second derivative, one cannot exclude the possibility that extended scaling terms need to be included if one wants to describe the C_v data in the density and temperature

range under consideration [C2]. A systematic analysis of the C_v data in terms of scaled equations of state requires, therefore, further research which is outside the scope of this paper.

In all tables in this paper the thermodynamic variables are expressed in SI-units. That is, the pressure is expressed in MPa (megapascals), the density in kg/m^3 and the temperature in kelvins or degrees C. However, in the discussion we occasionally also refer to pressure in terms of bars (= 0.1 MPa), atmospheres (= 0.101325 MPa) or Torrs (= 0.101325/760 MPa).

5.2. Xenon

5.2.a. Data Sources for Xenon

The critical constants and vapor pressure of xenon were first measured by Patterson, Cripps and Whytlaw-Gray in 1912 [P1]. An accurate determination of the entire vapor pressure curve was made by Michels and Wassenaar in Amsterdam in 1950 [M5]. Within their combined errors the Amsterdam values agreed with the old data. An extensive set of *PVT* data for xenon, covering temperatures from 16.65 °C to 100 °C and pressures up to 400 atmospheres, were reported by Beattie, Barriault and Brierley in 1951 [B3]. However, these data are not suitable for a scaled analysis, because they include only one isotherm in the critical region proper.

The equation of state and coexistence curve of xenon in the critical region were determined in great detail, with high accuracy, and with full appreciation of gravity effects, by Schneider and coworkers at the National Research Council in Canada in the 1950's [H1, W5].

In the coexistence curve experiment Weinberger and Schneider [W5] used glass cells, approximately 1 cm in diameter and 10 cm long, that could be held in horizontal or vertical position, thus enabling them to assess the effects of gravity. The gas densities were measured by weight to 0.2 percent accuracy. The temperature stability was better than 1 mK. However, the data span only a narrow temperature range and, therefore, in spite of the high quality of the measurements, they are not suitable for an accurate determination of the coexistence curve parameters B and β.

The equation of state work, conducted by Habgood and Schneider on xenon [H1], is a prime example of careful and accurate critical region experimentation. A horizontal glass vessel of 1 cm i.d. was connected to a filling system that included a weighing bomb, and to a pressure measuring system in a mercury U tube placed inside the thermostat. The gas height was thus limited to a maximum of 16 mm, noxious volumes were avoided completely and the pressure was measured at a well-determined level near the center of the bomb. The temperature was controlled to ±1 mK, the density was again measured to ±0.2 percent by a weighing technique, while the pressure was measured with a reproducibility better than ±0.001 atm. Two sets of data were obtained, one for the $P-T$ relation along a number of isochores, the other for the $P-V$ relation along a set of isotherms. The existence of some small discrepancies between the two data sets was noticed earlier, the isochoric data appearing to be more consistent and more precise [V1]. The isochoric data form the basis for the analysis presented here.

New coexistence curve data were recently reported by Cornfeld and Carr [C3], who revived the method of twin cells first used by Young in 1891 [Y1]. The data cover a range of 80 degrees below T_c and are of good quality. However, there are no data points closer than 1.8 °C from T_c, a limitation which is inherent in Young's method.

Two sources of density versus height profiles for xenon in the immediate vicinity of the critical point have recently become available. The first source is the work of Wilcox, Estler and Hocken [E1], in which the refractive index gradient was studied by a laser beam interference technique. The vicinity of the critical point, $|\Delta T^*| < 10^{-4}$, was mapped out in this experiment and the coexistence curve was studied over the range $10^{-5} < |\Delta T^*| < 5 \times 10^{-2}$. The second source is an experiment reported by Thoen and Garland, who combined sound velocity and sound absorption measurements with a determination of the dielectric constant as a function of height [T1]. We shall compare the results of both profile experiments with the results of our analysis of Schneider's *PVT* data in section 5.2.f.

In addition to this equation of state work, direct measurements of the specific heat C_v of xenon have also been reported. The data were obtained by Edwards, Lipa and Buckingham [E2] at the critical density as a function of temperature. The measurements were conducted with an adiabatic calorimeter in a "ramping" mode, the rate of temperature increase at constant heat input being inversely proportional to C_v. The height of the cell was 1 cm and gravity effects are expected to be important for reduced temperatures smaller than 2×10^{-4} (i.e. $|T - T_c| < 0.006$ °C). From the data range not affected by gravity, Buckingham and coworkers deduced a value 1/8 for the exponent α.

5.2.b. The Coexistence Curve of Xenon

The coexistence curve measurements of Weinberger and Schneider [W5] span a range of temperatures from 15 °C to the critical temperature 16.59 °C. The data obtained with the vertical bomb are affected by gravity in almost the entire experimental temperature range. Hohenberg and Barmatz [H4] have shown that the experimentally observed relationship between the temperature of meniscus disappearance and the filling density in the field of gravity can be described on the basis of the Linear Model with $\beta = 0.351$. For the data obtained with the horizontal bomb, gravity effects are expected to become appreciable at temperatures within 0.3 °C of the critical temperature. The gravity effects to be expected in these data were recently calculated

by one of us using the NBS equation and they are presented in table 1 [L2].

TABLE 1. Expected gravity effect on the coexistence curve of xenon in horizontal bomb, 1.2 cm high ($\bar{\rho}$ = average filling density; ρ = true interface density)

$T_c - T$, °C	$\lvert(\bar{\rho}-\rho)/\rho_c\rvert$	$T_c - T$, °C	$\lvert(\bar{\rho}-\rho)/\rho_c\rvert$
0.001	0.0397	0.095	0.0033
0.006	0.0257	0.254	0.0011
0.020	0.0138	0.496	0.0005
0.045	0.0073		

It would have been possible to fit the data to the power law (2.1) after applying the gravity corrections. However, the wisdom of such a procedure is questionable. Since a stirrer was used in the experiment, we do not know whether the full profile was actually developed as pointed out by Hohenberg and Barmatz [H4]. In determining the coexistence curve parameters we have, therefore, only considered the 8 data points available below 16.476 °C. Using absolute weights as described in reference [L7], we find $\beta = 0.358 \pm 0.002$ for a choice of $T_c = 289.744$ K and $\beta = 0.350 \pm 0.002$ for a choice of $T_c = 289.736$ K, the higher value of T_c corresponding to the lowest standard deviation of the power law fit. However, in this experiment T_c was directly observed to be (289.740 ± 0.001) K; the corresponding value of β is 0.354 ± 0.002. Since gravity effects flatten the coexistence curve, the true value of β may be slightly higher. For the noble gases argon and krypton Pings and coworkers recently found $\beta = 0.357$ [G2, W6].

In table 2 we present a list of values recently reported for the exponent β of xenon.

The coexistence curve data of Cornfeld and Carr [C3] span a large range in temperature. Since they do not include measurements within 1 °C of the critical temperature, gravity corrections do not need to be considered. The data yield a value $\beta = 0.362 \pm 0.005$ which is rather insensitive to the choice of T_c and the temperature range of the fit. However, on the basis of data taken previously with another method, Carr and coworkers have suggested that β would become smaller for temperature ranges closer to the critical temperature [S5].

From the interferometric experiments performed by Wilcox, Estler and Hocken [E1] the exponent β was obtained in two distinctly different ways. On the one hand, the coexistence curve was determined in the range $10^{-5} < |\Delta T^*| < 5 \times 10^{-2}$ and it was found that the exponent β decreased when the range of the power law fit was shrunk. While β was somewhat larger than 0.35 when the data were fitted in the range $10^{-3} < |\Delta T^*| < 5 \times 10^{-2}$, the value of that exponent appeared to become as low as 0.337 in the range $10^{-5} < |\Delta T^*| < 10^{-3}$. On the other hand, a scaled fit to all profile data in the even narrower temperature range $-10^{-4} < \Delta T^* < +10^{-4}$ returned the value $\beta = 0.357$, compatible with the "large range" values deduced from the coexistence curve data.

Thoen and Garland [T1] report $\beta = 0.357 \pm 0.002$ for data in the range $|\Delta T^*| < 10^{-2}$.

We conclude that the true value of the exponent β for a substance as extensively and carefully studied as xenon is still not entirely clear. A satisfactory resolution of these discrepancies may depend on our insight into the nature of the order parameter and the corrections to scaling.

For the purpose of analyzing the *PVT* data of Schneider and coworkers we have used the value $\beta = 0.350$ which in hindsight, may be somewhat low. With this choice for β the data of Weinberger and Schneider yield the value 0.186 for the coefficient x_0.

5.2.c. The Equation of State Data and Critical Parameters for Xenon

The values of the critical parameters for xenon are rather well established. A survey of the values reported

TABLE 2. Values reported for the critical exponent β of xenon

Experimenters	Ref.	Data analyzed by	Ref.	Method of analysis	Range of ΔT^*	Value of β
Cornfeld and Carr	[C3]	J. M. H. Levelt Sengers.	[L3]	power law	$0.1 > \lvert\Delta T^*\rvert > 0.005$	0.362 ± 0.004
				power law	$0.06 > \lvert\Delta T^*\rvert > 0.005$	0.362 ± 0.005
Wilcox, Estler, Hocken	[E1]	same authors	[E1]	power law	$0.001 > \lvert\Delta T^*\rvert > 0.00001$	0.337 ± 0.003
				power law	$0.05 > \lvert\Delta T^*\rvert > 0.00001$	0.344 ± 0.003
				power law	$0.05 > \lvert\Delta T^*\rvert > 0.001$	0.353 ± 0.001
				power law	$0.05 > \lvert\Delta T^*\rvert > 0.01$	0.357 ± 0.001
				compressibility model.	$-0.0001 < \Delta T^* < 0.0001$	0.3520 ± 0.0006
				Wilcox's scaled equation.	$-0.0001 < \Delta T^* < 0.0001$	0.3583 ± 0.0002
Thoen and Garland	[T1]	same authors	[T1]	power law	$-0.01 < \Delta T^* < 0.001$	0.357 ± 0.002
Weinberger and Schneider	[W5]	present authors		power law	$0.06 > \lvert\Delta T^*\rvert > 0.004$	0.354 ± 0.002

TABLE 3. Critical parameters reported for xenon

Authors	T_c, K	P_c, atm	ρ_c, kg/m³	Ref
Patterson et al	289.75	58.22	1155	[P1]
Weinberger, Schneider	289.740 ± 0.001		1105	[W5]
Whiteway, Mason	289.74 ± 0.01		1110	[W7]
Habgood, Schneider	289.740 ± 0.003	57.636 ± 0.005	1099	[H1]
Cornfeld, Carr	289.74		1113	[C3]
Thoen, Garland	289.793			[T1]
Buckingham et al	289.694 ± 0.002	(from fit to C_v)		[E2]
	289.73	(from max. relax. time)		

TABLE 4. Reduced equation of state data for xenon

T, K	$\Delta\rho^{*}$ [a]	$10^4 \cdot \Delta\mu^{*}$ [a, b]	$\frac{x+x_0}{x_0}$ [a, c]
289.940	−0.1347	−8.26 ± 0.35	2.140
289.940	−0.1319	−7.43 ± 0.35	2.210
289.940	−0.0916	−3.74 ± 0.35	4.434
289.940	−0.0499	−0.94 ± 0.35	2.046 × 10
289.940	+0.0301	+0.53 ± 0.35	8.351 × 10
289.940	+0.0614	+1.48 ± 0.35	1.175 × 10
289.940	+0.1456	+9.51 ± 0.35	1.912
290.140	−0.1347	−13.04 ± 0.35	3.281
290.140	−0.1319	−11.79 ± 0.35	3.420
290.140	−0.0916	−6.07 ± 0.35	7.869
290.140	−0.0499	−1.87 ± 0.35	3.993 × 10
290.140	+0.0301	+1.45 ± 0.35	1.660 × 10²
290.140	+0.0614	+3.56 ± 0.35	2.249 × 10
290.140	+0.1456	+15.46 ± 0.36	2.824
290.340	−0.1347	−17.70 ± 0.36	4.421
290.340	−0.1319	−16.10 ± 0.36	4.630
290.340	−0.0916	−8.57 ± 0.35	1.130 × 10
290.340	−0.0499	−2.68 ± 0.35	5.939 × 10
290.340	+0.0614	+5.80 ± 0.35	3.324 × 10
290.340	+0.1456	+20.59 ± 0.36	3.736
290.740	−0.1319	−26.83 ± 0.36	7.051
290.740	−0.0916	−15.77 ± 0.36	1.817 × 10
290.740	−0.0499	−7.07 ± 0.35	9.831 × 10
290.740	0.0387	−5.66 ± 0.35	2.024 × 10²
290.740	−0.0251	−3.52 ± 0.35	6.957 × 10²
290.740	−0.0095	−1.41 ± 0.35	1.117 × 10⁴
290.740	+0.0614	+9.49 ± 0.35	5.473 × 10
290.740	+0.1456	+31.49 ± 0.36	5.561
291.140	−0.1319	−37.69 ± 0.37	9.471
291.140	−0.0916	−23.05 ± 0.36	2.504 × 10
291.140	−0.0499	−10.80 ± 0.36	1.372 × 10²
291.140	−0.0387	−8.24 ± 0.36	2.830 × 10²
291.140	−0.0279	−5.37 ± 0.36	7.190 × 10²
291.140	−0.0251	−5.28 ± 0.36	9.735 × 10²
291.140	−0.0095	−2.18 ± 0.36	1.564 × 10⁴
291.140	+0.0614	+14.12 ± 0.36	7.622 × 10
291.140	+0.1456	+43.12 ± 0.37	7.385
291.540	−0.1319	−48.55 ± 0.37	1.189 × 10
291.540	−0.0916	−29.60 ± 0.37	3.191 × 10
291.540	−0.0499	−14.44 ± 0.36	1.762 × 10²
291.540	−0.0387	−11.48 ± 0.36	3.635 × 10²
291.540	−0.0095	−2.73 ± 0.36	2.011 × 10⁴
291.540	+0.0301	+8.99 ± 0.36	7.436 × 10²
291.540	+0.0614	+19.28 ± 0.36	9.771 × 10

[a] $\rho_c = 1110$ kg/m³.
[b] $P_c/\rho_c = 0.05192$ atm · m³/kg = 0.005261 MPa · m³/kg.
[c] $T_c = 289.740$ K, $\beta = 0.350$, $x_0 = 0.186$.

for the critical parameters in the literature is presented in table 3. By direct observation Weinberger and Schneider [W5] found $T_c = (289.740 \pm 0.001)$ K; this value was confirmed by Habgood and Schneider [H1] to within ±0.003 K. Therefore, in fitting the xenon data the critical temperature was not treated as an adjustable parameter, but fixed at the value $T_c = 289.740$ K.

Using the law of rectilinear diameter Weinberger and Schneider deduced for the critical density $\rho_c = 1105$ kg/m³. Habgood and Schneider feel that a slightly higher value of ρ_c would be consistent with their data. Whiteway and Mason [W7] have reported $\rho_c = 1110$ kg/m³, while Cornfeld and Carr have obtained $\rho_c = 1113$ kg/m³. We have found that a value $\rho_c = 1110$ kg/m³ gives good antisymmetry of the supercritical chemical potential isotherms.

The critical pressure follows from the data of Habgood and Schneider, once the value of T_c is chosen: $P_c = 57.636$ atm = 5.8400 MPa at $T_c = 289.740$ K.

The PVT data of Habgood and Schneider [H1] along isochores were combined to form isotherms and then converted into chemical potential data by numerical integration as discussed in section 5.1. The reduced chemical potential data $\Delta\mu^{*}$ are tabulated in table 4 as a function of temperature T and density $\Delta\rho^{*}$. For the convenience of the user we have also listed the values of $(x+x_0)/x_0$ for the individual data points. The value used for reducing the chemical potential data is $\mu_c = P_c/\rho_c = 0.05192$ atm m³/kg.

5.2.d. Analysis of the Xenon Data in Terms of the NBS Equation

The fit of the NBS equation to the xenon data was carried out by fixing $\rho_c = 1110$ kg/m³, $x_0 = 0.186$ and $\beta = 0.350$, varying δ and T_c over a two-dimensional grid and adjusting E_1 and E_2 at each point on the grid by the method of least squares as described in section 4.7. For the absolute weight assignment the experimental errors were estimated as

$$\sigma_{T^{*}} = 0.34 \times 10^{-5} \ (0.001\ ^{\circ}\mathrm{C}),$$

$$\sigma_{\rho^{*}} = 2 \times 10^{-4},\ \sigma_{\mu^{*}} = 0.35 \times 10^{-4}. \qquad (5.5)$$

At each point on the grid we calculated the value of the reduced variance χ^2; part of the χ^2 surface is shown in table 5. The fit is insensitive to the choices of δ and T_c. At $T_c = 289.740$ K the best fit corresponds to $\delta = 4.53$, but χ^2 is almost independent of T_c and increases only

TABLE 5. The values of χ^2 as a function of δ and T_c for Xe. NBS equation with $\beta=0.35$, $x_0=0.186$

	$\delta=4.47$	4.50	4.53	4.56
$T_c=289.739$ K	2.27	2.08	1.99	1.99
289.740 K	2.25	2.08	1.99	2.01
289.741 K	2.25	2.08	1.99	2.01

slowly with variations in δ. The reason for this behavior is likely to be found in the very narrow temperature range spanned by the data, so that the parameters are ill-determined even though the quality of the data is excellent.

We have also made some fits using the parameters $x_0=0.1743$ and $\beta=0.362$ deduced from Cornfeld and Carr's coexistence curve data. This choice led to a slightly improved fit, with minimum χ^2 values near 1.84.

5.2.e. Analysis of the Xenon Data in Terms of the Linear Model

The fit of the Linear Model to the xenon data was carried out by again fixing ρ_c, x_0 and β, varying δ, T_c and b^2 on a three-dimensional grid and calculating the average value $\bar{a}$ of $a(\theta)$ at each point on the grid as described in section 4.5. The assignment of absolute errors was again based on the estimated errors in ΔT^*, $\Delta\rho^*$ and $\Delta\mu^*$ given in (5.5). The quality of the fit was insensitive to the choice of T_c and b^2. We, therefore, preferred the experimental value 289.740 K for T_c and made the choice $b^2=b^2_{SLH}$, defined in (3.9) for the restricted Linear Model. For this choice of b^2, we show part of the χ^2 surface in table 6. The minimum value of χ^2 is obtained for $\delta=4.46$, slightly lower than the optimum value $\delta=4.53$ for the NBS equation. However, in view of the shallowness of the χ^2 surface, this difference is not significant.

For the Linear Model fit we calculated the variance-covariance matrix for simultaneous variation of all parameters, as described in section 4.6. This matrix is shown in table 7 with the diagonal elements normalized to unity. We also display the variance-covariance matrix when all parameters except T_c are considered variable.

5.2.f. Critical Region Parameters for Xenon

The parameters for the best restricted Linear Model fit to the xenon data with $T_c=289.740$ K and $\delta=4.46$ are presented in table 8. We also list the corresponding values of the coefficients and exponents of the power laws defined in section 2.2.

TABLE 6. The values of χ^2 as a function of δ for Xe. Linear Model with $\beta=0.35$, $x_0=0.186$, $b^2=b^2_{SLH}$, $T_c=289.740$ K.

δ	χ^2	δ	χ^2
4.40	1.56	4.46	1.46
4.42	1.51	4.48	1.46
4.44	1.48	4.50	1.49

TABLE 7. Correlation matrix of parameters. Linear Model fit for xenon

	T_c	ρ_c	x_0	β	δ	b
T_c	1					
ρ_c	−0.005	1				
x_0	−0.44	+0.34	1			
β	+0.53	−0.39	−0.99	1		
δ	−0.71	+0.27	+0.94	−0.97	1	
b	+0.02	+0.34	+0.87	−0.82	+0.66	1
		ρ_c	x_0	β	δ	b
ρ_c		1				
x_0		+0.37	1			
β		−0.36	−0.998	1		
δ		+0.37	+0.99	−0.99	1	
b		+0.34	+0.98	−0.99	+0.96	1

The errors quoted for ρ_c, x_0, β, δ and b^2 are those corresponding to one standard deviation in the five-parameter linearized error calculation with T_c kept constant. The error quoted for a is the standard deviation of the mean of $a(\theta)$ as obtained in the Linear Model fit.

As explained in sections 3.2 and 4.6, in our analysis the test of the validity of the Linear Model approximation of the parametric equation of state is formulated as

TABLE 8. Critical region parameters for Xe from data of Schneider et al. for the best restricted Linear Model and for the equivalent and the optimum NBS equation

Linear Model		Equivalent NBS equation		Optimum NBS equation	
P_c	5.8400 MPa	P_c	5.8400 MPa	P_c	5.8400 MPa
ρ_c	(1110±0.3) kg/m³	ρ_c	1110 kg/m³	ρ_c	1110 kg/m³
T_c	289.740 K	T_c	289.740 K	T_c	289.740 K
x_0	0.186±0.10	x_0	0.186	x_0	0.186
β	0.350±0.04	β	0.350	β	0.350
δ	4.46±0.3	δ	4.46	δ	4.53
a	17.682±0.5	E_1	2.4798	E_1	2.7276
b^2_{SLH}	1.4066±0.04	E_2	0.32184	E_2	0.35069
χ	1.21	χ	1.53	χ	1.41

TABLE 8. Critical region parameters for Xe from data of Schneider et al. for the best restricted Linear Model and for the equivalent and the optimum NBS equation—Continued

Linear Model		Equivalent NBS equation		Optimum NBS equation	
α	0.089	α	0.089	α	0.065
γ	1.211	γ	1.211	γ	1.236
B	1.802	B	1.802	B	1.802
D	2.721	D	2.697	D	3.018
Γ	0.07436	Γ	0.07402	Γ	0.06528
Γ'	0.01777	Γ'	0.01841	Γ'	0.01606
Γ/Γ'	4.18	Γ/Γ'	4.02	Γ/Γ'	4.06
A^+	2.11				
$A_{\bar{1}}$	0.0727				
$A_{\bar{11}}$	3.94				

the test of whether the individual experimental values of the quantity $a(\theta)$ are constant to within their experimental accuracy. For this purpose we present in figure 5 a plot of the normalized deviations of $a(\theta)$ from the average value $\bar{a}$, with σ_a defined in (4.36), as a function of $(x+x_0)/x_0$. In order to show the accuracy to which the Linear Model describes the original experimental $\Delta\mu^*$ data, we present in figure 6 a plot of the normalized deviations $(\Delta\mu^*_{\text{exp}}-\Delta\mu^*_{\text{calc}})/\sigma_{\Delta\mu^*}$ with $\sigma_{\Delta\mu^*}$ defined in (5.2).

In table 8 we also present the parameters for the equivalent NBS equation, that is the NBS equation with the same value $\delta=4.46$ as in the Linear Model fit, as well as for the optimum NBS equation with $\delta=4.53$. A plot of the normalized deviations $(\Delta\mu^*_{\text{exp}}-\Delta\mu^*_{\text{calc}})/\sigma_{\Delta\mu^*}$ for the optimum NBS equation is presented in figure 7.

5.2.g. Comparison with Results of Other Authors

As mentioned in section 5.2.a. two other sets of thermodynamic measurements for xenon are available from which critical region parameters have been derived. One set consists of the laser interferometry measurements of density profiles obtained by Estler, Wilcox and Hocken. The data were obtained in the narrow temperature band $-10^{-4}<\Delta T<10^{-4}$ around critical, approaching T_c as close as 10^{-7}. The data and their analysis can be found in Estler's Ph.D. thesis [E1].

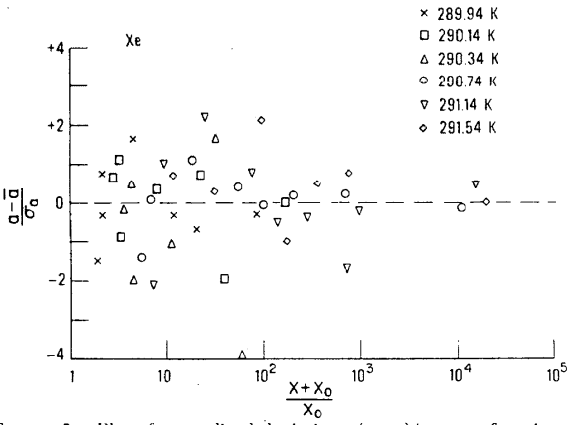

FIGURE 5. Plot of normalized deviations $(a-\bar{a})/\sigma_a$ as a function of $(x+x_0)/x_0$ for the optimum Linear Model fit to the xenon data.

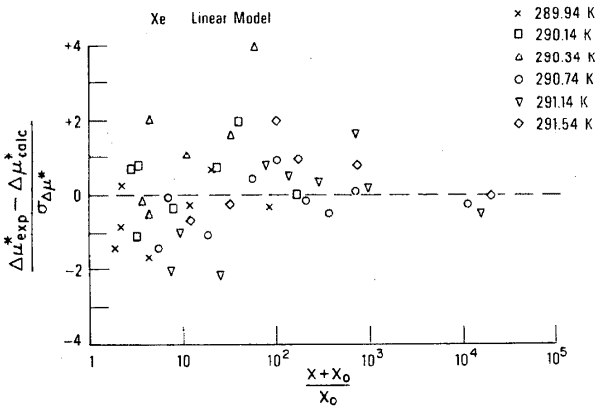

FIGURE 6. Plot of normalized deviations $(\Delta\mu^*_{\text{exp}}-\Delta\mu^*_{\text{calc}})/\sigma_{\Delta\mu^*}$ as a function of $(x+x_0)/x_0$ for xenon when the data are represented by the Linear Model.

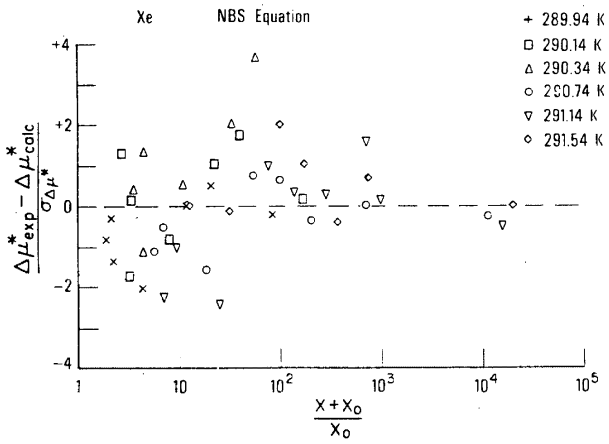

FIGURE 7. Plot of normalized deviations $(\Delta\mu^*_{\text{exp}}-\Delta\mu^*_{\text{calc}})/\sigma_{\Delta\mu^*}$ as a function of $(x+x_0)/x_0$ for xenon, when the data are represented by the optimum NBS Equation.

Estler et al. did not analyze their data in terms of the scaled equations used in this paper, but instead analyzed the data in terms of a more general scaled parametric equation proposed by Wilcox [W8] and also in terms of a "compressibility model" scaled parametric equation proposed by Ho and Litster [H6]. The values thus obtained by Estler et al. for the coefficients and exponents in the various power laws are listed in table

9. Of the two scaled equations used by Estler et al., the compressibility model has the same number of adjustable parameters, namely five, as the restricted Linear Model used in our analysis. With the exception of the value of the coefficient D for the critical isotherm, the critical region parameters determined by Estler et al. from their density profiles are in good agreement with the values deduced by us from the PVT data of Schneider et al. Although the value of D is extremely sensitive to the choice of δ, the δ values preferred by Estler do not differ enough from our choice to warrant the large difference in D and the deduction of its value from the density profile data should be reconsidered.

TABLE 9. Critical region power law parameters for Xe reported by other authors

	Estler et al.[a] [E1]	Estler et al.[b] [E1]	Thoen and Garland[c] [T1]
α	0.054 ±0.001	0.093 ±0.002	0.079
β	0.3583±0.0002	0.3520±0.0006	0.357
γ	1.2296±0.0005	1.203 ±0.002	1.207
δ	4.432 ±0.001	4.418 ±0.002	4.38
B	1.823	1.687	1.843
D	1.837	1.767	2.852
Γ	0.0663	0.0922	0.0676
Γ'	0.0182	0.0222	0.0168
Γ/Γ'	3.654	4.145	4.030

[a] Analysis in terms of Wilcox's parametric equation.
[b] Analysis in terms of compressibility model parametric equation.
[c] Analysis in terms of restricted Linear Model.

The second set of thermodynamic data for the critical region of xenon is that of Thoen and Garland who measured density versus height profiles simultaneously from the velocity and adsorption of sound [T1]. The coexistence curve was measured to yield values for B and β. Compressibility data on the critical isochore reported by Smith, Giglio and Benedek [S6] were used to fix the value of the coefficient Γ in the power law for the compressibility. The other parameters in the restricted Linear Model were then varied to fit the zero-frequency speed of sound. The values thus obtained for the coefficients and the exponents in the power laws are presented in the last column of table 9. The Linear Model parameters obtained by Thoen and Garland are in quite close agreement with our choice.

The values reported in the literature for the exponent β of the coexistence curve were discussed in section 5.2.b. A survey of the values reported for the exponent γ of xenon is presented in table 10. The original high value, 1.26, assigned by Vicentini-Missoni et al. must be attributed to a choice of T_c at a value lower than observed experimentally. All other values recently reported appear to be in reasonable agreement and a value near 1.21 seems to emerge as highly probable.

5.2.h. Discussion

Xenon is the first gas for which highly accurate density profile data can be compared with good PVT data. Such a comparison is of crucial importance. Good agreement between the two sets of data would imply that the asymptotic range of the validity of the scaling laws in fluids is large, so that valid conclusions regarding the asymptotic behavior of the equation of state near the critical point can be drawn from an analysis of PVT data taken in the fairly large range of 25 percent in $\Delta\rho^*$ and several percent in ΔT^*. This statement can also be reversed. Accurate data, such as the density profile data, obtained in the limited range $|\Delta T^*| < 10^{-4}$ could then be used to predict the equation of state in a range covering several percent in ΔT^*. Until recently, it was much harder to obtain these density profile data than to obtain conventional equation of state data. The main limitation was not the accuracy of the method (refractive index or capacitance measurement) but the failure to meet the extreme demands of temperature control. This situation, however, has been reversed since highly stable thermostats were developed by Wilcox and coworkers [E1]. With temperature stability of the order of 10 μK, the measurement of a complete isotherm by laser interference tech-

TABLE 10. Values reported for the critical exponent γ of xenon

Experimenters	Ref.	Data analyzed by	Ref.	Method of analysis	Range of ΔT^*	Value of γ
Habgood and Schneider	[H1]	Vicentini-Missoni et al.	[V1]	NBS equation	$0.0006 < \Delta T < 0.006$	1.26 ±0.06
Habgood and Schneider	[H1]	present authors		Linear Model	$0.0006 < \Delta T < 0.006$	1.21 ±0.03
Smith, Giglio, Benedek	[S6]	Smith, Giglio, Benedek	[S6]	power law	$0.0001 < \Delta T < 0.03$	1.21 ±0.03
Wilcox, Estler, Hocken	[E1]	Wilcox, Estler, Hocken	[E1]	power law	$0.0001 < \Delta T < 0.1$	1.260 ±0.002
				power law	$0.00001 < \Delta T < 0.001$	1.232 ±0.006
				compressibility model	$-0.0001 < \Delta T < 0.0001$	1.2296±0.0005
				Wilcox's scaled equation	$-0.0001 < \Delta T < 0.0001$	1.203 ±0.002

niques takes no more than a day of almost fully automatic data generation.

Regarding the agreement of the optical and *PVT* data, however, the situation is not quite as hopeful as table 9 suggests. For one thing, those exponents β, that are obtained by direct count of the number of fringes disappearing at the interface [E1, B8], have a tendency to vary with the range and to become quite low, about 0.33, in the range $\Delta T^* < 10^{-4}$. Moreover, recent determinations of density profiles in a number of fluids [H7] do not confirm the Stoneybrook result but lead to lower values for β. In contrast, preempting the results of our analysis of the density profile data of oxygen (table 32), the exponents obtained for this gas in the gravity-affected region $\Delta T^* < 10^{-4}$ agree very well with the results we have obtained for other fluids in larger ranges around critical, which suggests that the range of validity of the asymptotic laws is large.

Since the agreement of the results of profile studies and those of *PVT* data has not been proven beyond all reasonable doubt, the question about the range of validity of the scaling laws in fluids must be considered unresolved.

5.3. Helium 4

5.3.a. Introductory Comments

The discovery of helium in 1868 occurred at about the same time that Andrews discovered the existence of a gas-liquid critical point in carbon dioxide. Shortly thereafter van der Waals formulated his equation of state and the law of corresponding states. Although a respectable number of "permanent" gases had been liquified before the turn of the century, helium was not among those. The question whether helium would have a critical point as well, caused lively debate and much speculation. An experimental attempt to answer this question had to wait until the invention of the Dewar vessel in 1892. Then, physicists at the University of Leiden started moving deliberately towards the liquefaction of helium. From the behavior of the isotherms at low temperatures, determined in the first years of this century, Kamerlingh Onnes estimated a critical temperature of 5 K or 6 K on the basis of corresponding states [K4]. Moreover, his determination of the Joule-Thomson inversion temperature led him to the conclusion that liquefaction of helium would be feasible by a Joule-Thomson process using hydrogen at reduced pressures as a cooling agent. The liquefaction of helium was achieved by Kamerlingh Onnes in 1908 and rough estimates of the critical temperature and density were obtained [K5].

The first accurate determination of the critical parameters was reported in 1911, namely $T_c = 5.25$ K and $P_c = 1718$ Torr [K6]. At the same time superconductivity was discovered and the research at Leiden began to take a distinctly new direction. As a result, the liquefaction of helium and the early determination of its critical parameters marked not only a high point in the 40-year-old research on the equation of state of gases, but also the onset of a decline of interest in such studies. Kamerlingh Onnes' critical parameters of helium were enshrined in Keesom's classical book on the subject [K7]. They were incorporated in the 1958 helium vapor pressure scale which still forms the basis for thermometry at low temperatures. Only in the late fifties did a renewed interest in critical phenomena lead to new experimental studies of the critical region of helium. Since then, a wealth of material has been gathered which forms the basis for the correlation presented here.

In the course of this century many attempts have been made to correlate the properties of helium, a survey of which falls outside the scope of this article. The most recent correlation was conducted by McCarty for this journal [M6] and we refer to his article for general references to the literature. It was McCarty's goal to fit data for a number of thermodynamic properties of helium over a large range of temperatures and densities. Due to the nature of the equations used by him, McCarty had to exclude the critical region from his correlation. Thus the present section on the critical region properties of helium may be considered a complement to McCarty's correlation.

5.3.b. On the Temperature Scale in the Critical Region of He^4

The critical region of He^4 presents a unique experimental complication, since the internationally accepted temperature scale [B4, V3] in this region is based on the vapor pressure-temperature relation of He^4 itself. The use of the so-called T_{58} scale has two major disadvantages for studying the critical region of He^4. First of all, the scale extends only up to the critical point and is not defined above T_c. Secondly, the scale is based on an analytic representation of the vapor pressure relation, which, according to present-day insights, must fail at the critical point. In addition to these fundamental difficulties, there is evidence that the T_{58} scale deviates from the thermodynamic scale by as much as 10 mK near 5 K [C4]. Furthermore, the slope near T_c is too low, perhaps by as much as 5 percent. Finally, the scale is based on a vapor pressure relation that terminates at a pressure that is supercritical [K2, M4]. The procedure adopted by most experimenters is to use a secondary thermometer, usually a carbon or germanium resistor, which is calibrated with respect to the He^4 vapor pressure at temperatures not too close to the critical temperature. An analytical representation of the resistance as a function of temperature is then used to extrapolate to the critical temperature and upwards. Kierstead [K1, K2] had his germanium thermometers calibrated with respect to the NBS provisional scale based on acoustic thermometry [P2].

This arbitrariness in the thermometric procedures makes it difficult to compare experiments from different laboratories. It will also contribute to the uncertainty of reported critical exponents; however, the effect of

smooth deviations from the thermodynamic scale is expected to be small for the larger exponents, because the large changes in the anomalous property occur over small temperature intervals.

5.3.c. Data Sources for He^4

The revival of experimentation in the critical region of He^4 in the sixties had a precursor in the highly accurate redetermination of the coexistence curve by Edwards and coworkers [E3, E4, E5]. Edwards measured the refractive indices of the coexisting phases using a Jamin interferometer. The cell was immersed in a bath of liquid helium, the vapor pressure of the bath being an indication of the temperature. The main experimental questions in this work are, whether the vapor pressure of the bath did indeed indicate the temperature of the cell, and whether the absolute fringe count for the liquid phase had been achieved. In the initial interpretation of the data some difficulties were encountered which must be attributed to the fact that the critical temperature was assumed to have the value determined by Kamerlingh Onnes. When it was realized by Moldover and Little [M7] that T_c is much lower than Kamerlingh Onnes' value, all data of Edwards fell right into place. In the most recent analysis of his data Edwards [E6] reports $T_c = 5.18988$ K and $\beta = 0.3598$, in substantial agreement with later work. The value of the exponent β is quite close to that found for other fluids.

The work of Moldover and Little on the specific heat C_v of He^4 [M7, M8] established the existence of a weak divergence very much like that found by Voronel and coworkers for heavier gases [B5, V4]. The specific heat was measured in an adiabatic calorimeter along five isochores including the critical. The critical temperature was established as (5.189 ± 0.001) K on the T_{58} scale, and the critical density as $\rho_c = (69.58 \pm 0.07)$ kg/m^3 [M4]. The actual temperature measurements were performed with carbon resistors, calibrated repeatedly with respect to the vapor pressure of helium. A careful assessment was made of the possible errors introduced by the nonanalyticity of T_{58} and by the extrapolation above T_c.

The first set of measurements of the equation of state of He^4 in the critical region is that of Roach and Douglass [R1, R5]. In these experiments, a capacitor was immersed in the cell with fluid He^4 under investigation. The capacitance was measured as a function of pressure and temperature. A germanium thermometer was clamped directly to the capacitor assembly, and calibrated along the coexistence curve of He^4 before each run. A three-constant resistance-temperature relation was used for inter- and extrapolation. The pressure deformation of the capacitor was obtained somewhat indirectly, namely, through intercomparison with Edwards' refractive index data on the liquid side of the coexistence curve. In calculating densities from the dielectric constant measurements the Clausius-Mosotti function $(\epsilon - 1)/(\epsilon + 2)$ was assumed to be a linear function of the density ρ. This assumption leads to some questions concerning the accuracy of the value 69.0 kg/m^3 reported for the critical density ρ_c; in reduced units, however, the reported densities should be quite precise. Roach reports $T_c = 5.1888$ K and $\beta = 0.354$ from his own analysis of the coexistence curve. The pressure was measured on a quartz Bourdon gauge with a reproducibility close to ± 0.1 Torr $= \pm 0.6 \times 10^{-4}$ P_c, but the absolute accuracy of the pressure is at most 1 part in 10^4 of the critical pressure. The effect of gravity introduces a problem in this experiment. The problem is not in the spacing of the capacitance plates which was only 0.0025 cm, but is associated with the fact that the pressure was not measured at the level of the capacitance. A long vertical capillary connected the Bourdon gage with the top of the sample cell, which itself was several cm high. Consequently, the measured pressures differ by an inestimable amount from the pressures at the location where the dielectric constant is measured.

Roach's data, provided prior to publication, were first scaled by Vicentini-Missoni, Levelt Sengers and Green [V1]. In this paper we present a refined analysis of the published data [R1] (which differ from the prepublication data in a few details), using both the NBS equation and the Linear Model.

Roach's work was followed by new precise data published by Kierstead [K1, K2]. Kierstead measured the values of pressure increments along isochores using a differential quartz Bourdon gage of low range, with 10^{-3} Torr resolution. A reference pressure, known to 0.1 Torr but stabilized to 10^{-3} Torr, was used. The values of $(dP/dT)_V$, so obtained, have an estimated precision of 0.1 percent, while the density of each isochore was determined to 1 part in 5000 by gas expansion into known volumes. Hydrostatic heads were kept quite small in this experiment; the sample cell was only 1 mm high and the filling tube was brought out horizontally and was heated to temperatures far above T_c at a short distance from the cell. The total gas head was estimated to be only 0.035 Torr. Temperatures were measured on two germanium thermometers calibrated on the NBS acoustical scale. The resolution of the temperature was 0.3 μK, but the long-term stability of the thermometers was not better than 0.5 mK.

In his first paper [K2], Kierstead reported three isochores within 1 percent of the critical density. From these data he concluded that $P_c = (1706.12 \pm 0.10)$ Torr, $\rho_c = (69.64 \pm 0.07)$ kg/m^3 and $T_c = (5.1983 \pm 0.0021)$ K on the NBS provisional scale. Calculating the temperature on the T_{58} scale from his observed critical pressure, he obtained $T_c = (5.18992 \pm 0.00010)$ K. In his second paper [K1], Kierstead reported work on 29 isochores within 20 percent of the critical density. This work did not result in a new absolute value for T_c, because of a shift in calibration of the germanium thermometers. The critical density was found to be $\rho_c = (69.580 \pm 0.014)$ kg/m^3, in good agreement with the

previous determination. The value of ρ_c, reported by Kierstead, is in excellent agreement with other volumetric determinations of this quantity, namely $\rho_c = (69.58 \pm 0.07)$ kg/m^3 as determined by Moldover [M4] and $\rho_c = (69.76 \pm 0.20)$ kg/m^3 as determined by El Hadi and Durieux [E7]. On the other hand, the more indirect determinations of ρ_c from refractive index or dielectric constant measurements yield somewhat lower values, namely $\rho_c = (69.323 \pm 0.069)$ kg/m^3 as found by Edwards [E6] and $\rho_c = 69.0$ kg/m^3 as found by Roach [R1]. We feel that Kierstead's values for this quantity is most reliable.

In his second paper, Kierstead also presented an analysis of his data in terms of the Linear Model equation of state, covering a range of ± 3 percent in reduced temperature and ± 20 percent in reduced density. However, the deviation plots revealed some systematic deviations as a function of density indicating that the antisymmetry of $\mu(\rho)$, as assumed in the Linear Model, was not satisfied to within the precision of the data. He then proceeded to describe his data within their error in terms of a more general parametric equation. The critical region parameters deduced from Kierstead's data will be further discussed in section 5.3.h.

5.3.d. The Coexistence Curve of He^4

A survey of the values reported in the literature for the critical parameters and the coexistence curve parameters of He^4 is presented in table 11.

We have made several attempts at analyzing Roach's coexistence curve data, but with less than total success. Since gas and liquid densities were not measured in conditions of coexistence, it is necessary to represent the data as

$$|\rho - \bar{\rho}|/\rho_c = |\rho - \rho_c + C\Delta T^*|/\rho_c = B|\Delta T^*|^\beta, \qquad (5.6)$$

where $\bar{\rho} = \rho_c - C\Delta T^*$ is the equation of the diameter of the coexistence curve [L7].

Since, in calculating the densities from the observed dielectric constant, the Clausius-Mosotti function was assumed to be a linear function of ρ, one must allow for the possibility that the slope of the diameter, C, may be different from the slope deduced from other direct determinations of coexisting densities. Consequently, in fitting equation (5.6) to the data we needed to treat ρ_c, T_c, B, β and C as adjustable parameters.

We have determined the parameters B and β by the method of least squares, while the parameters ρ_c, T_c and C were varied on a grid. The four data points closest to the critical point were excluded from the analysis because of errors due to gravity. The inclusion of other points in the fit resulted in values for the critical temperature and density which were not sharply defined. This results from the scatter of the data near the critical point being more than one would estimate on the basis of the experimental accuracy, which leads to large values of and shallow minima for the reduced variance χ^2. If the power law fit is restricted to data points with $|\Delta T^*| > 0.01$, then χ^2 exhibits a more pronounced dependence on the choice for T_c and ρ_c. The optimum value for T_c is then found to lie in the range 5.188 K to 5.189 K and for ρ_c in the range 68.96 kg/m^3 to 69.02 kg/m^3. Values for the exponent β in the range 0.349 to 0.359 are compatible with Roach's data, as long as T_c is chosen accordingly. Values for the reduced slope in the vicinity of $\rho/\rho_c = 0.12$ implied by the measurements of Edwards [E4] and El Hadi [E7] are also in accord with the data of Roach.

Since the value of the exponent β is not sharply defined from the data of Roach, we have decided to lean heavily on Kierstead's finding that $\beta = 0.355$. We have, therefore, selected a power law fit to Roach's coexistence curve that yielded $\beta = 0.35556$, occurring at $T_c = 5.188$ K. The corresponding value of the coefficient B is 1.426 which implies $x_0 = 0.3687$. It is with these choices of β and x_0 that we have analyzed Roach's data in terms of the NBS equation and the Linear Model.

5.3.e. The Equation of State Data for He^4

The chemical potential data, calculated from the PVT data of Roach by the procedure described in section 5.1, are presented in table 12. The data are the same as those listed in reference [V1] except for some minor adjustments in the reduction factors. The chemical potential data $\mu(\rho)$ exhibit antisymmetry in the range $\Delta\rho^* = \pm 25$ percent with respect to the density $\rho_c = 69.3$ kg/m^3. Although the absolute values of Roach's densities are

TABLE 11. Values reported for the critical and coexistence curve parameters of He^4

Authors	P_c, Torr	T_c, K	ρ_c, kg/m^3	β	B
Kamerlingh Onnes [B4]	1718	5.1994			
Mathias et al. [M9]			69.3		
Roach [R1]	1705.0	5.1888	69.0	0.354 ±0.010	1.47
Edwards [E6]	1705.84±0.86	5.1897 ±0.0007			
		5.18988±0.00008	69.323±0.069	0.3598±0.0060	1.417±0.024
Moldover [M4]		5.1891 ±0.0007	69.58 ±0.07		
El Hadi et al. [E7]			69.76 ±0.2		
Kierstead I [K2]	1706.12±0.10	5.18992±0.00010	69.64 ±0.07	0.3554±0.003	1.395
Kierstead II [K1]			69.58 ±0.02		

in doubt because of the conversion from measured dielectric constants, the shift of 0.5 percent, between the critical density $\rho_c = 69.0$ kg/m³ from the coexistence curve and the value $\rho_c = 69.3$ kg/m³ from the point of antisymmetry of the isotherms, is a matter of internal consistency and, therefore, reason for worry. It is perhaps related to a lack of complete antisymmetry of the $\mu(\rho)$ isotherms noticed by Kierstead [K1].

In table 12 we have listed $\Delta\mu^*$ as a function of $\Delta\rho^*$ and T. The experimental densities were reduced by the factor $\rho_c = 69.3$ kg/m³ and the experimental chemical potential values by the factor $\mu_c = P_c/\rho_c = 24.60$ Torr m³/kg.

TABLE 12. Reduced equation of state data for He^4

T, K	$\Delta\rho^{*\,a}$	$10^4 \cdot \Delta\mu^{*\,a,b}$	$\frac{x+x_0}{x_0}^{a,c}$
5.1097	+0.3343	+27.0±1.5	0.1026
5.1097	+0.3522	+67.5±1.7	0.2250
5.1406	−0.3586	−176.8±1.8	0.5520
5.1406	−0.3319	−103.1±1.6	0.4431
5.1406	−0.2986	−35.3±1.4	0.2500
5.1406	+0.2973	+38.0±1.4	0.2407
5.1406	+0.3201	+77.9±1.5	0.3832
5.1406	+0.3400	+124.4±1.7	0.4795
5.1663	−0.3563	−257.8±1.9	0.7885
5.1663	−0.3356	−188.6±1.7	0.7499
5.1663	−0.3004	−100.8±1.5	0.6584
5.1663	−0.2654	−44.2±1.4	0.5158
5.1663	−0.2355	−15.1±1.3	0.3225
5.1663	+0.2266	+12.6±1.3	0.2445
5.1663	+0.2561	+38.2±1.3	0.4651
5.1663	+0.2752	+61.8±1.4	0.5628
5.1663	+0.2965	+95.9±1.5	0.6457
5.1795	−0.2856	−98.0±1.4	0.8403
5.1795	−0.2519	−51.1±1.3	0.7728
5.1795	−0.2189	−23.1±1.3	0.6627
5.1795	−0.2019	−13.4±1.3	0.5764
5.1795	+0.1856	+9.5±1.2	0.4632
5.1795	+0.1955	+11.5±1.2	0.5366
5.1795	+0.2159	+24.1±1.3	0.6492
5.1795	+0.2315	+36.6±1.3	0.7116
5.1822	+0.1990	+17.5±1.3	0.6912
5.1822	+0.2162	+29.1±1.3	0.7554
5.1822	+0.2313	+41.1±1.3	0.7978
5.1835	−0.2022	−22.0±1.3	0.7656
5.1835	−0.1805	−11.9±1.2	0.6777
5.1862	+0.1887	+18.7±1.2	0.8692
5.1862	+0.2110	+32.9±1.3	0.9044
5.1862	+0.2355	+54.5±1.3	0.9298
5.1869	−0.1970	−21.8±1.3	0.9193
5.1869	−0.1753	−11.7±1.2	0.8880
5.1929	−0.3567	−340.4±2.0	1.042
5.1929	−0.3163	−203.8±1.6	1.059
5.1929	−0.2794	−120.1±1.4	1.083
5.1929	−0.2392	−61.5±1.3	1.128
5.1929	−0.2038	−31.4±1.3	1.202

TABLE 12. Reduced equation of state data for He^4.—Continued

T, K	$\Delta\rho^{*\,a}$	$10^4 \cdot \Delta\mu^{*\,a,b}$	$\frac{x+x_0}{x_0}^{a,c}$
5.1929	−0.1639	−13.4±1.2	1.372
5.1929	+0.1361	+8.5±1.2	1.628
5.1929	+0.1771	+21.1±1.2	1.299
5.1929	+0.2118	+41.8±1.3	1.181
5.1929	+0.2499	+79.4±1.4	1.114
5.1929	+0.2823	+129.9±1.5	1.081
5.1929	+0.3110	+190.5±1.6	1.061
5.1929	+0.3456	+291.3±1.9	1.046
5.2011	−0.3494	−340.7±1.9	1.127
5.2011	−0.3088	−210.2±1.6	1.179
5.2011	−0.2691	−124.2±1.4	1.264
5.2011	−0.2325	−74.2±1.3	1.399
5.2011	−0.1977	−42.0±1.3	1.629
5.2011	−0.1534	−19.9±1.2	2.284
5.2011	−0.1198	−9.8±1.2	3.575
5.2011	+0.1286	+11.1±1.2	3.109
5.2011	+0.1737	+26.4±1.2	1.905
5.2011	+0.2111	+51.4±1.3	1.523
5.2011	+0.2534	+98.2±1.4	1.313
5.2011	+0.2906	+161.8±1.5	1.213
5.2011	+0.3299	+263.4±1.8	1.149
5.2205	−0.3019	−238.6±1.6	1.486
5.2205	−0.2504	−129.6±1.4	1.822
5.2205	−0.2007	−69.0±1.3	2.531
5.2205	−0.1405	−30.7±1.2	5.170
5.2205	−0.0851	−14.1±1.2	1.808×10
5.2205	+0.0801	+13.0±1.2	2.128×10
5.2205	+0.1094	+23.2±1.2	9.441
5.2205	+0.1658	+46.9±1.2	3.620
5.2205	+0.2144	+87.4±1.3	2.271
5.2205	+0.2563	+144.7±1.4	1.770
5.2205	+0.3009	+236.2±1.6	1.490
5.2637	−0.2599	−240.2±1.5	2.739
5.2637	−0.1996	−133.3±1.3	4.656
5.2637	−0.1453	−77.2±1.3	9.923
5.2637	−0.0879	−40.0±1.2	3.771×10
5.2637	−0.0367	−15.6±1.2	4.305×10^2
5.2637	+0.0154	+7.0±1.2	4.886×10^3
5.2637	+0.0719	+32.9±1.2	6.565×10
5.2637	+0.1284	+66.6±1.3	1.363×10
5.2637	+0.2006	+137.8±1.3	4.604
5.2637	+0.2772	+283.0±1.6	2.451
5.3142	−0.0986	−80.9±1.3	4.545×10
5.3142	−0.0452	−33.6±1.3	3.999×10^2
5.3142	+0.0595	+49.6±1.3	1.852×10^2
5.3142	+0.1107	+97.2±1.3	3.307×10

[a] $\rho_c = 69.3$ kg/m³.
[b] $P_c/\rho_c = 24.60$ Torr · m³/kg = 0.003279 MPa · m³/kg.
[c] $T_c = 5.1885$ K, $\beta = 0.35556$, $x_0 = 0.3687$.

5.3.f. Analysis of the He^4 Data in Terms of the NBS Equation

The fit of the NBS equation to the He^4 data was carried out by fixing $\rho_c = 69.3$ kg/m³, $x_0 = 0.3687$ and $\beta = 0.35556$, varying δ and T_c on a grid and adjusting E_1 and E_2 at each point on the grid by the method of least squares as described in section 4.7. For the abso-

lute weight assignment the experimental errors were estimated as

$$\sigma_{T^*}=0.5\times10^{-4}\ (0.25\ \text{mK}),\qquad \sigma_{\rho^*}=3.3\times10^{-4},$$

$$\sigma_{\mu^*}=1.2\times10^{-4} \qquad (5.7)$$

At each point on the grid we calculated the value of the reduced variance χ^2; part of the χ^2 surface is shown in table 13.

The optimum fit occurs at $\delta=4.36$ and $T_c=5.1885$ K, but the minimum χ^2 is considerably larger than unity. As can be seen from figure 10 to be presented in section 5.3.h, no data points deviate by more than four standard deviations. Hence, the high value of χ^2 is probably due to an underestimate of the experimental error in at least one variable. A 10 percent increase in χ^2 occurs when T_c deviates by about 1 mK from its optimum value or when δ deviates by about 0.04 from its optimum value.

TABLE 13. The values of χ^2 as a function of δ and T_c for He^4. NBS equation with $\beta=0.35556$ and $x_0=0.3687$.

	$\delta=4.32$	4.34	4.36	4.38	4.40	4.42	4.44
$T_c=5.1875$ K	3.69	3.28	2.96	2.75	2.62	2.56	2.59
5.1880 K	3.06	2.82	2.62	2.53	2.53	2.60	2.70
5.1885 K	2.72	2.59	2.52	2.56	2.65	2.79	3.02
5.1890 K	2.59	2.56	2.62	2.76	2.92		

5.3.g. Analysis of the He^4 Data in Terms of the Linear Model

The fit of the Linear Model to the He^4 data was carried out by again fixing ρ_c, x_0 and β, varying δ, T_c and b^2 on a grid and calculating the average value $\bar{a}$ of $a(\theta)$ at each point of the grid, as described in section 4.5. The absolute error assignment was again based on the estimated errors in ΔT^*, $\Delta\rho^*$ and $\Delta\mu^*$ given in (5.7). The best fits were obtained for values of b^2 near the value b^2_{SLH} corresponding to the restricted Linear Model. The χ^2 surface, obtained with this particular choice $b^2=b^2_{SLH}$, is shown in table 14.

TABLE 14. The values of χ^2 as a function of δ and T_c for He^4. Linear Model with $\beta=0.35556$, $x_0=0.3687$, $b^2=b^2_{SLH}$

	$\delta=4.30$	4.32	4.34	4.36	4.38	4.40	4.42
$T_c=5.1875$ K	3.22	2.98	2.83	2.76	2.76	2.85	3.00
5.1880 K	2.77	2.61	2.53	2.54	2.62	2.77	3.00
5.1885 K	2.53	2.44	2.44	2.52	2.67	2.90	3.20
5.1890 K	2.49	2.48	2.55	2.70	2.93	3.23	3.60

A minimum χ^2 is obtained at $\delta=4.34$ and $T_c=5.1885$ K. A 10 percent increase in χ^2 corresponds to approximately 1 mK in T_c or 0.04 in δ. Thus the optimum values of δ and T_c for the NBS equation ($4.36\pm.04$, $5.1885\pm.001$) and for the restricted Linear Model ($4.34\pm.04$, $5.1885\pm.001$) are in agreement.

For the Linear Model fit we calculated the variance-covariance matrix for simultaneous variation of all adjustable parameters, as described in section 4.6. This matrix is shown in table 15 with the diagonal elements normalized to unity.

TABLE 15. Correlation matrix of parameters. Linear Model fit for He^4

	T_c	ρ_c	x_0	β	δ	b
T_c	1					
ρ_c	+0.11	1				
x_0	−0.58	−0.15	1			
β	+0.73	+0.16	−0.98	1		
δ	−0.95	−0.17	+0.66	−0.79	1	
b	+0.09	−0.03	+0.70	−0.55	−0.07	1

5.3.h. Critical Region Parameters for He^4

The parameters for the best restricted Linear Model and the NBS equation, as deduced from the data of Roach [R1], are presented in table 16. We also list the corresponding values of the coefficients and exponents of the power laws defined in section 4.2.

The errors quoted for ρ_c, T_c, x_0, β, δ and b^2 are those corresponding to one standard deviation in the six-parameter linearized error calculation. The error quoted for a is the standard deviation of the mean of $a(\theta)$ in the Linear Model fit.

In figure 8 we show the normalized deviations of $a(\theta)$ from the average value $\bar{a}$ for the Linear Model fit. Plots of the normalized deviations of the experimental chemical potential data are presented in figures 9 and 10 for the Linear Model and the NBS equation, respectively.

In table 17 we present critical region parameters for He^4 deduced from the $(\partial P/\partial T)_\rho$ data of Kierstead. The Linear Model parameters, presented in the first column of table 17, are those obtained by Kierstead himself [K1]. It should be remembered, however, that Kierstead's data do not conform to the Linear Model to within their accuracy. The Linear Model parameters from Kierstead's data are in good agreement with the Linear Model parameters deduced by us from the data of Roach. The agreement confirms the absence of any large systematic deviations between the measurements of Roach and the values calculated on the basis of Kierstead's Linear Model parameters [K1]. Since the data of Kierstead exhibit less scatter than those of Roach, Kierstead's Linear Model parameters should be used preferably.

In table 17 we also present the parameters for the NBS equation equivalent with Kierstead's parameters for the Linear Model. These parameters were not determined by fitting Kierstead's experimental data directly, but were deduced from the Linear Model parameters using the relations (5.3) and (5.4).

TABLE 16. Critical region parameters for He^4 from data of Roach

Linear Model		NBS equation	
P_c	0.22726 MPa (1704.6 Torr)	P_c	0.22726 MPa
ρ_c	(69.3 ± 0.02) kg/m³	ρ_c	69.3 kg/m³
T_c	(5.1885 ± 0.001) K (T_{58})	T_c	5.1885 K (T_{58})
x_0	0.3687 ± 0.02	x_0	0.3687
β	0.35556 ± 0.006	β	0.35556
δ	4.34 ± 0.06	δ	4.34
a	6.413 ± 0.1	E_1	2.6522
b^2_{SLH}	1.3888 ± 0.006	E_2	0.31763
χ	1.56	χ	1.61
α	0.101	α	0.101
γ	1.188	γ	1.188
B	1.426	B	1.426
D	2.863	D	2.852
Γ	0.1589	Γ	0.1560
Γ'	0.03985	Γ'	0.04099
Γ/Γ'	3.99	Γ/Γ'	3.81
A^+	0.524		
A_I^-	0.0220		
A_{II}^-	1.13		

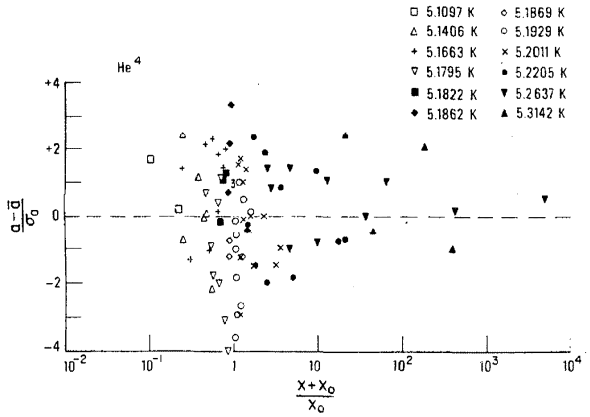

FIGURE 8. Plot of normalized deviations $(a-\bar{a})/\sigma_a$ as a function of $(x+x_0)/x_0$ for the optimum Linear Model fit to the He^4 data.

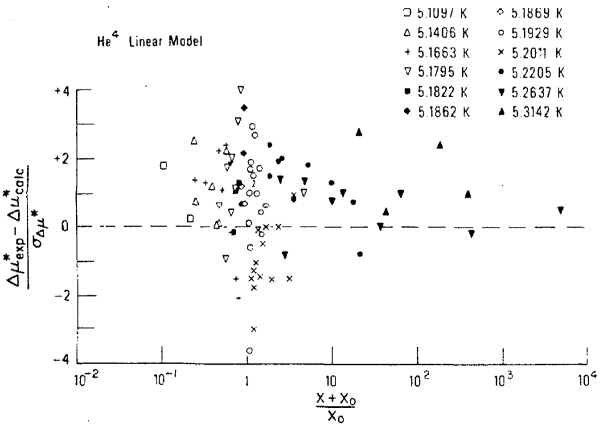

FIGURE 9. Plot of normalized deviations $(\Delta\mu^*_{exp}-\Delta\mu^*_{calc})/\sigma_{\Delta\mu^*}$ as a function of $(x+x_0)/x_0$ for He^4, when the data are represented by the Linear Model.

TABLE 17. Critical region parameters for He^4 from data of Kierstead

Linear Model		Equivalent NBS equation	
P_c	0.22746 MPa (1706.12 Torr)	P_c	0.22746 MPa
ρ_c	(69.58 ± 0.20) kg/m³	ρ_c	69.58 kg/m³
T_c	(5.18992 ± 0.00010) K (T_{58})	T_c	5.18992
x_0	0.392 ± 0.013	x_0	0.392
β	0.3554 ± 0.0028	β	0.3554
γ	1.1743 ± 0.0005	γ	1.1743
a	6.053 ± 0.016	E_1	2.8461
b^2_{SLH}	1.3649	E_2	0.27156
χ	1.5		
α	0.115	α	0.115
δ	4.304	δ	4.304
B	1.395	B	1.395
D	3.019	D	3.019
Γ	0.1611	Γ	0.1611
Γ'	0.04089	Γ'	0.04158
Γ/Γ'	3.94	Γ/Γ'	3.87
A^+	0.442		
A_I^-	0.0194		
A_{II}^-	1.08		

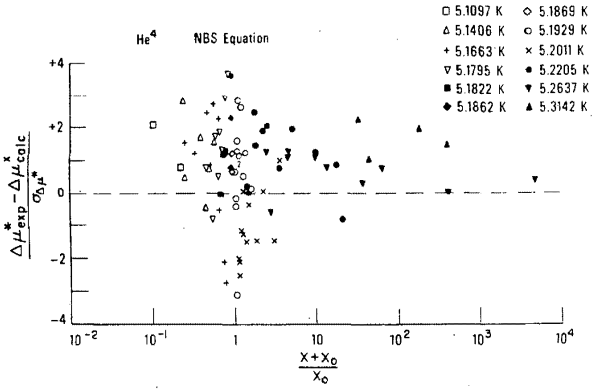

FIGURE 10. Plot of normalized deviations $(\Delta\mu^*_{exp}-\Delta\mu^*_{calc})/\sigma_{\Delta\mu^*}$ as a function of $(x+x_0)/x_0$ for He^4, when the data are represented by the NBS Equation.

5.4. Helium 3

5.4.a. Data Sources for He^3

In contrast to the study of the critical region of He^4, the work on He^3 spans no more than a decade or two. Only by the late fifties had enough He^3 been collected as a fission product in reactors for its bulk properties to be determined. Sydoriak, Grilly and Hammel at Los Alamos [G3, S7] determined the critical parameters of He^3 in 1949; the year before these parameters had been predicted by De Boer and Lunbeck on the basis of quantum-mechanical corresponding states [D1]. The Los Alamos group then proceeded to explore the *PVT* surface of He^3, first in the liquid phase [S8] and then along a great number of isochores from supercritical temperatures down to the coexistence curve [S9, S10, S11].

Concurrently with the Los Alamos *PVT* work, Moldover measured the specific heat C_v of He^3 and demonstrated that it was weakly divergent at the critical point [M8].

A systematic study of the equation of state in the critical region of He^3 was undertaken by Chase and Zimmerman in the mid-sixties [C5]. The dielectric constant was determined as a function of pressure and temperature. The coexistence curve and a large number of isotherms were measured and analyzed for the critical exponents β, γ, and δ. A full report on the results of these measurements was published only recently. In the meantime, a large body of thermodynamic data for He^3 in the critical region originated from Meyer's group at Duke University. The equation of state was determined by Wallace and Meyer [W1]; using the same sample of He^3, the specific heat C_v was subsequently measured by Brown and Meyer [B2].

The *PVT* data were obtained by measuring the dielectric constant of a sample of He^3 as a function of pressure and temperature in a cell with an effective height of less than 1.5 mm. The hydrostatic gas head was kept small by bringing the fill capillary out horizontally and heating it well above the critical temperature before it bent upwards. The pressure was measured on a quartz Bourdon gauge with a resolution of 4×10^{-5} atm. and an accuracy of 3×10^{-4} atm. Temperatures were measured with a germanium resistor calibrated with respect to the vapor pressure of He^4. The thermometer had a sensitivity of 5 μK and a stability of 20 μK.

A limited number of data points were obtained for a sample of He^3 with 10 ppm He^4 impurity. The main body of data, to be considered in this analysis, was obtained for a sample with 250 ppm He^4 impurity.

The experimental data cover a range of $|\Delta\rho^*| \leq 0.5$ in density and $-0.1 < \Delta T^* < 0.05$ in temperature. Wallace and Meyer have also integrated the *PVT* data to obtain tables of $\Delta\mu^*$ as a function of density and temperature; they have these tabulated data available on request [W4]. In view of the large amount of data it is not practical to reproduce the tabulated values in this paper.

Wallace and Meyer made an analysis of their equation of state data in terms of the NBS equation [W1]. In this paper we present a new analysis of the data with both the NBS equation and the Linear Model. For this purpose we consider the chemical potential data in the range $|\Delta\rho^*| \leq 0.25$ and at temperatures $3.27981\ \text{K} \leq T \leq 3.36699$ K. This range is comparable to the range in which scaling laws were found to describe the data for other gases.

5.4.b. The Coexistence Curve of He^3

Wallace and Meyer report the following values for the coexistence curve parameters of He^3 [W1].

$$T_c = (3.3105 \pm 0.0002)\ \text{K} \qquad \rho_c = (41.45 \pm 0.2)\ \text{kg/m}^3$$
$$\beta = 0.361 \pm 0.005 \qquad B = 1.31 \tag{5.8}$$

We have repeated the coexistence curve analysis principally because the value 0.361 for β is substantially higher than for other fluids. Our results can be summarized as follows. If all points are included in the fit, a minimum standard deviation of order unity occurs for $T_c = 3.3099$ K and $\beta = 0.3583$. However, if the furthest point is omitted, a substantially better fit, with standard deviation 0.6, is obtained with $T_c = 3.3103$ K and $\beta = 0.3648$. We have conducted power law fits with several pairs of T_c and β and found the fits to be very insensitive to the choice. We have ultimately settled on the value $\beta = 0.3583$ for the following reasons: the trend in β values from Xe to He^4 does not lead one to expect any strong increase in β for He^3; and the lower β of 0.358 corresponds with a T_c value below 3.31 K for which there is independent evidence in the specific heat experiment on the same sample by Brown and Meyer [B2].

5.4.c. Critical Region Parameters for He^3

The fit of the NBS equation to the He^3 data was carried out by fixing $\rho_c = 41.45$ kg/m^3, $x_0 = 0.48043$ and $\beta = 0.35831$, varying δ and T_c on a grid and adjusting E_1 and E_2 at each point on the grid by the method of least squares as described in section 4.7. The fit of the Linear Model to the He^3 data was carried out by again fixing ρ_c, x_0 and β, varying δ, T_c and b^2 on a grid and calculating the average value $\bar{a}$ of $a(\theta)$ at each point of the grid, as described in section 4.5. For the absolute weight assignment the experimental errors were estimated as

$$\sigma_{T^*} = 0.9\times10^{-4}\ (0.3\ \text{mK}), \qquad \sigma_{\rho^*} = 5\times10^{-4}, \qquad \sigma_{\mu^*} = 1.2\times10^{-4}. \tag{5.9}$$

The Linear Model fit was quite insensitive to the choice of b^2 which, therefore, was identified with b^2_{SLH}.

Both the NBS equation and the Linear Model yielded values of χ^2 between 0.8 and 0.9 which varied only slowly with δ and T_c. Hence, these parameters are not well defined from the data. In table 18 we present the parameters for the Linear Model and the NBS equation that correspond to $\delta = 4.26$ and $T_c = 3.3099$ K as determined from the optimum restricted Linear Model fit. We also list the corresponding values of the coefficients and exponents of the power laws defined in section 4.2.

The errors quoted for ρ_c, T_c, x_0, β, δ and b^2 are those corresponding to one standard deviation in the six-parameter linearized error calculation. The error estimate thus obtained for ρ_c is certainly too small. Wallace and Meyer quote an error of ± 0.02 kg/m^3 from their analysis of the coexistence curve. The error quoted for a is the standard deviation of the mean of $a(\theta)$ in the Linear Model fit.

TABLE 18. Critical region parameters for He^3 from data of Wallace and Meyer

Linear Model		NBS equation	
P_c	0.11678 MPa (859.6 Torr)	P_c	0.11678 MPa (859.6 Torr)
ρ_c	(41.45 ± 0.004) kg/m^3	ρ_c	41.45 kg/m^3
T_c	(3.3099 ± 0.003) K (T_{58})	T_c	3.3099 K (T_{58})
x_0	0.48043 ± 0.02	x_0	0.48043
β	0.35831 ± 0.005	β	0.35831
δ	4.26 ± 0.04	δ	4.26
a	4.1559 ± 0.1	E_1	2.6532
b^2_{SLH}	1.3639 ± 0.003	E_2	0.25773
χ	0.90	χ	0.89
α	0.115	α	0.115
γ	1.168	γ	1.168
B	1.300	B	1.300
D	2.810	D	2.800
Γ	0.2178	Γ	0.2200
Γ'	0.05638	Γ'	0.05736
Γ/Γ'	3.86	Γ/Γ'	3.84
A^+	0.271		
A_Γ	0.01		
$A_{\bar{\Pi}}$	0.685		

For the Linear Model fit we also calculated the variance-covariance matrix for simultaneous variation of all adjustable parameters, as described in section 4.6. This matrix is shown in table 19 with the diagonal elements normalized to unity.

TABLE 19. Correlation matrix of parameters. Linear Model fit for He^3

	T_c	ρ_c	x_0	β	δ	b
T_c	1					
ρ_c	−0.06	1				
x_0	−0.73	+0.05	1			
β	+0.81	−0.05	−0.99	1		
δ	−0.93	+0.07	+0.89	−0.93	1	
b	−0.24	−0.01	+0.78	−0.72	+0.41	1

In figure 11 we show the normalized deviations of $a(\theta)$ from the average value $\bar{a}$ for the Linear Model fit at a number of representative temperatures. However, the deviations are not random: for $\Delta\rho^* < 0$ the experimental a values are systematically higher than the average value and for $\Delta\rho^* > 0$ the experimental a values are systematically lower than the average value. This behavior indicates a lack of perfect antisymmetry in the chemical potential data in contrast to a claim of Wallace and Meyer [W1]. The lack of antisymmetry is more apparent in figures 12 and 13, where we have plotted the normalized deviations of the chemical potential itself for the Linear Model and the NBS equation, respectively. These results do not necessarily imply that the original *PVT* data of Wallace and Meyer are not consistent with our scaled equations. It is possible that systematic deviations were introduced by the numerical procedure followed by Wallace and Meyer in converting the pressure data into chemical potential data. We hope to resolve this issue in the future by fitting the Linear Model to the original *PVT* data directly, using a technique recently developed by Murphy and the authors [M2, M3].

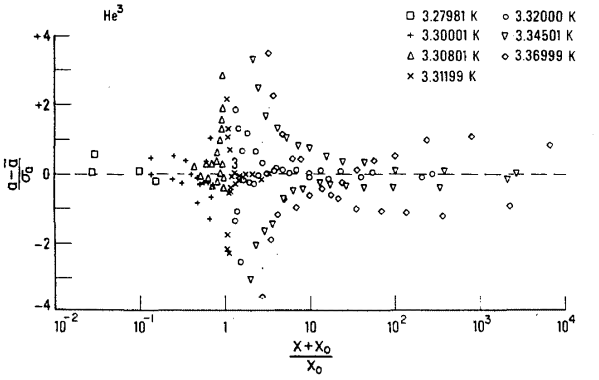

FIGURE 11. Plot of normalized deviations $(a-\bar{a})/\sigma_a$ as a function of $(x+x_0)/x_0$ for the optimum Linear Model fit to the He^3 data.

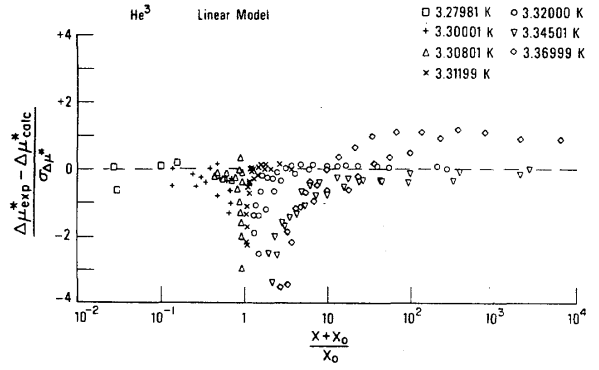

FIGURE 12. Plot of normalized deviations $(\Delta\mu^*_{exp}-\Delta\mu^*_{calc})/\sigma_{\Delta\mu^*}$ as a function of $(x+x_0)/x_0$ for He^3, when the data are represented by the Linear Model.

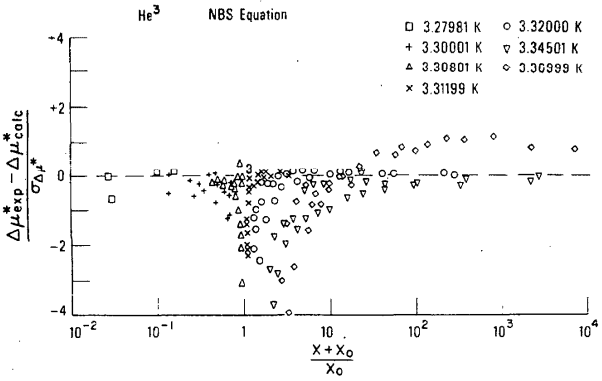

FIGURE 13. Plot of normalized deviations $(\Delta\mu^*_{exp}-\Delta\mu^*_{calc})/\sigma_{\Delta\mu^*}$ as a function of $(x+x_0)/x_0$ for He^3, when the data are represented by the NBS Equation.

Wallace and Meyer deduced the following parameters for the NBS equation

$$T_c = 3.3105\ \text{K} \qquad \beta = 0.361 \qquad E_1 = 2.53$$
$$x_0 = 0.475 \qquad \delta = 4.23 \qquad E_2 = 0.44 \qquad (5.10)$$

There are no substantial differences between their fit and ours, except for the value of the critical temperature, T_c. In our opinion, a lower value of T_c is definitely indicated. Our best value, $T_c = (3.3099 \pm 0.003)$ K, removes the discrepancy between Wallace and Meyer's value, $T_c = (3.3105 \pm 0.0002)$ K, based on the equation of state [W1] and Brown and Meyer's value, $T_c = (3.3092 \pm 0.0006)$ K, based on specific heat data for the same sample of He^3 [B2].

Chase and Zimmerman [C5] obtained $T_c = (3.30930 \pm 0.005)$ K, which agrees with our and Brown and Meyer's values within combined error. The critical exponents reported by Chase and Zimmerman, $\beta = 0.3653 \pm 0.005$, $\delta = 4.12 \pm 0.15$, and $\gamma = 1.19 \pm 0.03$ do not differ significantly from the values we have derived from Wallace and Meyer's data (table 18).

Huang and Ho have determined a set of Linear Model parameters for He^3 by accepting the values reported by Wallace and Meyer for T_c, β and δ and then determining optimum values for a and k with the result $a = 4.17$ and $k (= a\Gamma) = 0.909$ [H5]. Again, except for T_c, their parameters are quite close to the parameters obtained by us.

5.5. Carbon Dioxide

5.5.a. Data Sources for Carbon Dioxide

Since the original discovery of the critical point by Andrews in 1869 [A1] and the equation of state work conducted by Amagat around 1890 [A2], carbon dioxide has continued to be the object of many studies. The principal reason for this interest is probably the convenient location of its critical temperature (31 °C). The information concerning the thermodynamic behavior of CO_2 has been very important in the context of the development of equations of state, beginning with that of van der Waals [V2], and in relation to the understanding of critical phenomena. Recently, a supercritical thermodynamic power cycle has been proposed which would make an accurate formulation of the critical thermodynamic behavior of CO_2 an eminently practical enterprise [F2].

Work of high accuracy on the equation of state in the critical region started with the measurements of Meyers and Van Dusen at the National Bureau of Standards in 1933 [M10]. Though this work is of outstanding quality, its scope is too limited for data correlation. The largest single body of *PVT* data for CO_2 is that provided by the classical work of Michels and coworkers in the thirties [M1, M11]. Whereas data outside the critical region were taken by the piezometer method refined by Michels, the data in the critical region, spanning temperatures from 2 °C to 40 °C, and densities from 0.2 ρ_c to 1.7 ρ_c, were taken in a glass cell, in which a fixed amount of gas was confined by means of mercury transferred from a weighing bomb. The density determination was believed to be correct to at least 1:3000, while the pressure was measured to ± 0.001 atm. The temperature was measured to within 5 millidegrees. There are, however, some problems with the temperature scale to be discussed in section 5.5.c. Wentorf measured a few *PV* isotherms of CO_2 in 1956, but the data were confined to a narrow temperature range within 0.1 °C from the critical temperature [W9].

Concerning the more modern work on CO_2, we mention the refractive index versus height measurements conducted by Lorentzen [L8] and the subsequent more detailed studies of the coexistence curve and the density profiles by Schmidt and Straub [S12, S13]. The intensity of light scattered by CO_2 near the critical point has been studied by White and Maccabee [W10] and by Lunacek and Cannell [L9]; these measurements have yielded values for the exponents γ and γ'. Levelt Sengers and Chen have recently determined the vapor pressure curve and the P–T relation along the critical isochore in some detail and with an accuracy of 0.001 bar and 1 millidegree in pressure and temperature, respectively [L10]. The critical density and temperature were recently redetermined under well-controlled conditions by Moldover [M12]. The specific heat of CO_2 was measured in a ramping experiment by Lipa, Edwards and Buckingham [L11] superseding the earlier work of Michels and Strijland [M13]. The data were corrected for gravity effects by Hohenberg and Barmatz [H4] and by Schmidt [S3]. The low frequency sound velocity of CO_2 in the vicinity of the critical point was studied by Carome and coworkers [F3, F4].

For the purpose of a scaled analysis, the primary source is still the set of data of Michels, et al., because of their extent and accuracy. The other experiments can be used for several purposes. The coexistence curve data of Schmidt and Straub supplement the coexistence curve data of Michels which become rather scant and inaccurate very close to T_c. The vapor pressure curve of Levelt Sengers and Chen serves as a check on Michels' temperature scale. Moldover's redetermination of the critical point corrects Michels' estimate for T_c and corroborates his choice for the critical density. The light scattering data give additional insight in the value of the exponent γ for the compressibility.

5.5.b. The Coexistence Curve of Carbon Dioxide

A reanalysis of the coexistence curve data for CO_2 was recently published by Levelt Sengers, Straub and Vicentini-Missoni [L7]. The principal conclusions of interest are that the exponent β is between 0.347 and 0.351, T_c to be associated with Michels' experiment is somewhat below the value 31.04 °C favored by Michels, and the values of T_c for the two samples studied by

Schmidt and Straub are 30.99 °C and 31.03 °C, respectively, on the T_{48} scale.

For our analysis we shall use $\beta = 0.3486$ together with $x_0 = 0.14185$ and a critical density $\rho_c = 23^{\prime}$ amagat $= 467.8$ kg/m^3. The value of the critical temperature T_c will be adjusted to optimize the fit.

The critical temperature and density were recently redetermined by Moldover by visual observation of meniscus disappearance [M12]. We refer to his paper for a critical evaluation of about a dozen of the more reliable determinations of the critical parameters for CO_2. According to Moldover the most probable value of the critical parameters for CO_2 are

$$T_c = (304.127 \pm 0.004)\ \text{K}\ (T_{68}) = (30.977 \pm 0.004)\ ^\circ\text{C}\ \ (T_{68})$$

$$\rho_c = (468 \pm 2)\ \text{kg/m}^3 \qquad (5.11)$$

$$P_c = (72.789 \pm 0.007)\ \text{atm} = (7.3753 \pm 0.0007)\ \text{MPa}.$$

The value of the critical pressure was obtained by him from the vapor pressure measurements of Levelt Sengers and Chen [L10], given his own value for the critical temperature.

5.5.c. On the Temperature Scale of Michels' Data

In Michels' experiments, the temperature of the thermostat was read on mercury thermometers divided to 0.01 °C and calibrated at P.T.R. in Berlin. In the course of the experiment, the vapor pressure was determined at nine subcritical temperatures. These vapor pressures differ systematically from those of Meyers and Van Dusen in 1933 [M10] and those of Levelt Sengers and Chen in 1971 [L10]. While the latter two sets of data agree to the equivalent of 0.01 °C, the disagreement with Michels' data is the equivalent of 0.08 °C at 25 °C and 0.02 °C at a temperature 0.03 °C below the critical temperature. A similar systematic difference is noticeable at lower temperatures between

TABLE 20. Apparent differences between the T_{48} scale and the temperatures reported by Michels et al. [L10]

T_M, Michels [M1, M11] °C	$T_M - T_{48}$ °C	T_M, Michels [M1, M11] °C	$T_M - T_{48}$ °C
2.853	0.070	28.052	0.035
10.822	0.069	29.929	0.029
19.874	0.068	30.409	0.032
25.070	0.085	31.013	0.022
25.298	0.085		

Michels' data and a set of vapor pressure data obtained in the same laboratory at a later date [M14]. Since we have reasons to believe that Michels' sample purity was very high and that his pressure scale was correct to at least 1 part in 5000, we prefer to explain the observed differences in terms of the temperature scales used. Since both Meyers and Van Dusen's data and the Levelt Sengers and Chen data were obtained on the T_{48} scale, we can use the observed differences in vapor pressure to infer the relationship between Michels' temperature scale and the T_{48} scale. The results are summarized in table 20.

At this point, we can try to infer the consequences of this scale correction on the values of T_c as obtained from Michels' data. We reach our conclusion in three steps: a) as we shall see, a scaled analysis of Michels' *PVT* data leads to values for T_c between 30.99 °C and 31.03 °C on Michels scale; b) applying a correction of −0.03 °C, in accordance with table 20, brings T_c into the range 30.96 °C to 31.00 °C on T_{48}; c) a further correction of −0.01 °C [R6] brings T_c into the range 30.95 °C to 30.99 °C on T_{68}. This result is in satisfactory agreement with the value 30.977 °C as determined by Moldover on the T_{68} scale.

It is more difficult to decide how much the temperature scales differ at temperatures above the critical temperature, since the pressure differences will depend on how accurately the critical density was realized in the experiment of Levelt Sengers and Chen. For the purpose of this correlation, which is concerned with a temperature range from 1 °C below T_c to 10 °C above T_c, it was not considered urgent to correct Michels' temperature scale. It should, however, be kept in mind that an offset in scale of 0.07° at 25 °C and 0.01° at 31 °C would affect first temperature derivatives by as much as 1 percent and should be taken into account when C_v values, predicted on the basis of an equation of state deduced from Michels' data, are compared with experimental C_v data obtained on the international temperature scale.

5.5.d. The Equation of State Data for Carbon Dioxide

The experimental *PVT* data of Michels et al. [M1] were converted into chemical potential data by numerical integration as discussed in section 5.1. The resulting values for the reduced chemical potential $\Delta\mu^*$ are tabulated in table 21 as a function of temperature T and density $\Delta\rho^*$. The value used for reducing the chemical potential data is $\mu_c = P_c/\rho_c = 0.3083$ atm/amagat $= 0.01577$ MPa m^3/kg. The table is a slightly revised version of a table presented in an earlier paper [V1].

TABLE 21. Reduced equation of state data for carbon dioxide

T, K	$\Delta\rho^*$ [a]	$10^4 \cdot \Delta\mu^*$ [a,b]	$\frac{x + x_0}{x_0}$ [a,c]
303.079	+0.2834	+8.2±0.8	6.726×10^{-2}
303.559	−0.2422	−7.7±0.8	1.862×10^{-1}
303.559	+0.2382	+6.0±0.7	1.464×10^{-1}
304.163	−0.2179	−27.3±0.7	1.006
304.163	−0.1859	−13.9±0.7	1.009
304.163	−0.1550	−6.1±0.7	1.015
304.163	−0.1288	−2.8±0.7	1.025
304.163	+0.1302	+3.1±0.7	1.024

TABLE 21. Reduced equation of state data for carbon dioxide — Continued

T, K	$\Delta\rho^{*}$ [a]	$10^4 \cdot \Delta\mu^{*}$ [a,b]	$\frac{x+x_0}{x_0}$ [a,c]
304.163	+0.1520	+6.1±0.7	1.015
304.163	+0.2121	+24.2±0.7	1.006
304.163	+0.2714	+70.6±0.9	1.003
304.335	−0.2100	−31.0±0.7	1.357
304.335	−0.1518	−10.5±0.7	1.905
304.335	−0.1057	−4.3±0.7	3.557
304.335	−0.0699	−2.5±0.7	9.380
304.335	−0.0373	−0.9±0.7	5.190×10
304.335	+0.0476	+1.3±0.7	2.625×10
304.335	+0.0948	+3.5±0.7	4.498
304.335	+0.1503	+10.8±0.7	1.932
304.335	+0.2091	+31.0±0.7	1.361
304.470	−0.2097	−37.8±0.7	1.634
304.470	−0.1523	−15.1±0.7	2.590
304.470	−0.1058	−6.8±0.7	5.513
304.470	−0.0693	−3.6±0.7	1.621×10
304.470	−0.0372	−1.7±0.7	9.144×10
304.470	+0.0473	+1.7±0.7	4.652×10
304.470	+0.0961	+5.2±0.7	6.949
304.470	+0.1513	+14.9±0.7	2.619
304.470	+0.2096	+37.6±0.6	1.636
304.673	−0.2645	−101.2±0.9	1.539
304.673	−0.2117	−49.2±0.8	2.021
304.673	−0.1502	−20.1±0.7	3.736
304.673	−0.0860	−7.6±0.7	1.454×10
304.673	+0.0950	+8.3±0.7	1.117×10
304.673	+0.1467	+19.1±0.7	3.925
304.673	+0.2027	+42.8±0.7	2.157
305.204	−0.2921	−187.3±1.0	1.826
305.204	−0.2465	−114.4±0.9	2.345
305.204	−0.1905	−61.2±0.7	3.813
305.204	−0.1193	−26.2±0.7	1.177×10
305.204	−0.0511	−8.6±0.7	1.239×10²
305.204	+0.0386	+6.3±0.7	2.751×10²
305.204	+0.1398	+34.1±0.7	7.834
305.204	+0.2232	+87.6±0.8	2.786
307.871	−0.2737	−362.8±1.3	4.538
307.871	−0.1995	−206.3±1.0	9.771
307.871	−0.1094	−93.2±0.8	5.009×10
307.871	+0.0976	+83.0±0.8	6.916×10
307.871	+0.2141	+236.8±1.0	8.161
313.237	−0.0698	−160.8±1.4	4.372×10²
313.237	+0.0095	+21.4±1.3	1.329×10⁵
313.237	+0.1134	+271.6±1.4	1.095×10²

[a] $\rho_c = 236.7$ amagat $= 467.8$ kg/m³.
[b] $P_c/\rho_c = 0.3075$ atm/amagat $= 0.01577$ MPa · m³/kg.
[c] $T_c = 304.16$ K, $\beta = 0.3486$, $x_0 = 0.14185$.

5.5.e. Analysis of the CO_2 Data in Terms of the NBS Equation

The fit of the NBS equation to the CO_2 data was carried out by fixing $\rho_c = 236.7$ amagat $= 467.8$ kg/m³, $x_0 = 0.14185$ and $\beta = 0.3486$, varying δ and T_c on a grid adjusting E_1 and E_2 at each point on the grid by the method of least squares as described in section 4.7. For the absolute weight assignment the experimental errors were estimated as

$$\sigma_{T^*} = 0.2 \times 10^{-4}\ (0.006\ \text{K}), \quad \sigma_{\rho^*} = 3.3 \times 10^{-4}, \quad \sigma_{\mu^*} = 0.65 \times 10^{-4} \qquad (5.12)$$

At each point on the grid we calculated the value of the reduced variance χ^2; part of the χ^2 surface is shown in table 22.

TABLE 22. The values of χ^2 as a function of δ and T_c for CO_2. NBS equation with $\beta = 0.3486$ and $x_0 = 0.14185$.

	$\delta = 4.41$	4.44	4.47	4.50
$T_c = 30.98$ °C	2.41	1.71	1.37	1.37
30.99 °C	1.69	1.27	1.14	1.32
30.00 °C	1.28	1.06	1.14	1.49
31.01 °C	1.08	1.06	1.32	1.85
31.02 °C	1.08	1.27	1.85	2.34

The minimum values of χ^2 are obtained for $T_c = 31.00$ °C and 31.01 °C and $\delta = 4.44$. The χ^2 increases by about 10 percent when T_c is changed by 0.01 °C and δ by 0.03 from their optimum values. The variations of T_c and δ, however, are strongly coupled and lower values of T_c correspond to high values of δ. This explains why in an earlier fit [V1], where a coarse grid and a slightly different β was used, a minimum was found at $T_c = 30.96$ °C and $\delta = 4.6$. We now believe that the higher value of T_c around 31.01 °C, is a better choice. The value is corroborated by the most recent determination of the critical temperature of CO_2 as discussed in section 5.5.c.

5.5.f. Analysis of the CO_2 Data in Terms of the Linear Model

The fit of the Linear Model to the CO_2 data was carried out by again fixing ρ_c, x_0 and β, varying δ and T_c and b^2 on a grid and calculating the average value $\bar{a}$ of $a(\theta)$ at each point of the grid, as described in section 4.5. The absolute error assignment was again based on the estimated error in ΔT^*, $\Delta\rho^*$ and $\Delta\mu^*$ given in (5.12). Among all gases studied in this paper, CO_2 was the only case in which the optimum value of the Linear Model parameter b^2 differed from the restricted Linear Model value b^2_{SLH}. The optimum Linear Model fit was obtained for $b^2 = 1.80$; for this value of b^2 we show part of the χ^2 surface in table 23. We note that χ^2 attains

TABLE 23. The values of χ^2 as a function of δ and T_c for CO_2. Linear Model with $\beta = 0.3486$, $x_0 = 0.14185$, $b^2 = 1.80$.

	$\delta = 4.40$	4.42	4.44	4.46	4.48
$T_c = 30.99$ °C	2.59	1.95	1.53	1.32	1.31
31.00 °C	1.84	1.40	1.18	1.17	1.36
31.01 °C	1.37	1.14	1.11	1.29	1.68
31.02 °C	1.17	1.13	1.30	1.67	2.24

a minimum value of 1.11 at the same parameter values $T_c = 31.01$ °C and $\delta = 4.44$ as those corresponding to the optimum fit of the NBS equation. When b^2 was restricted to b^2_{SLH}, χ^2 attained the minimum value 1.70 which is substantially higher than that obtained with the

unrestricted Linear Model; the location of the minimum, however, occurs at the same value of δ.

For the Linear Model fit we calculated the variance-covariance matrix for simultaneous variation of all adjustable parameters, as described in section 4.6. This matrix is shown in table 24 with the diagonal elements normalized to unity.

TABLE 24. Correlation matrix of parameters. Linear Model fit for CO_2.

	T_c	ρ_c	x_0	β	δ	b
T_c	1					
ρ_c	+0.12	1				
x_0	−0.66	−0.33	1			
β	+0.78	+0.31	−0.97	1		
δ	−0.88	−0.24	+0.91	−0.95	1	
b	−0.03	−0.31	+0.60	−0.54	+0.26	1

5.5.g. Critical Region Parameters for CO_2

The parameters for the best fit of the Linear Model and the NBS equation to the data of Michels et al. [M1] are presented in table 25. We also list the corresponding values of the coefficients and exponents of the power laws defined in section 4.2.

TABLE 25. Critical region parameters for CO_2 from data of Michels et al. for the optimum Linear Model and NBS equation

Linear Model		NBS equation	
P_c	7.3755 MPa	P_c	7.3755 MPa
ρ_c	(467.8 ± 0.07) kg/m³	ρ_c	467.8 kg/m³
T_c	(304.16 ± 0.01) K	T_c	304.16 K
x_0	0.14185 ± 0.005	x_0	0.14185
β	0.3486 ± 0.004	β	0.3486
δ	4.44 ± 0.05	δ	4.44
a	28.021 ± 0.3	E_1	2.1779
b^2	1.800 ± 0.005	E_2	0.25344
χ	1.05	χ	1.03
α	0.104	α	0.104
γ	1.199	γ	1.199
B	1.975	B	1.975
D	2.353	D	2.323
Γ	0.06522	Γ	0.06533
Γ'	0.01419	Γ'	0.01539
Γ/Γ'	4.60	Γ/Γ'	4.25
A^+	2.20		
A_I^-	0.0148		
A_{II}^-	5.13		

The errors quoted for ρ_c, T_c, x_0, β, δ and b^2 are those corresponding to one standard deviation in the six-parameter linearized error calculation. The error quoted for a is the standard deviation of the mean of $a(\theta)$ in the Linear Model fit.

In figure 14 we show the normalized deviations of $a(\theta)$ from the average value $\bar{a}$ for the Linear Model fit. Plots of the normalized deviations of the experimental chemical potential data are presented in figures 15 and 16 for the Linear Model and the NBS equation, respectively.

In table 26 we present the parameters for the restricted Linear Model ($b^2 = b^2_{SLH}$) and the equivalent NBS equation.

In collaboration with Murphy we have developed a method for fitting the Linear Model to the experimental pressures directly. Linear Model parameters recently obtained by this new technique are shown in table 27 [M2]. The direct fit to the pressures confirms our conclusion that for Michels' data the optimum Linear Model fit has a b^2 that differs from the value of b^2_{SLH} corresponding to the restricted Linear Model.

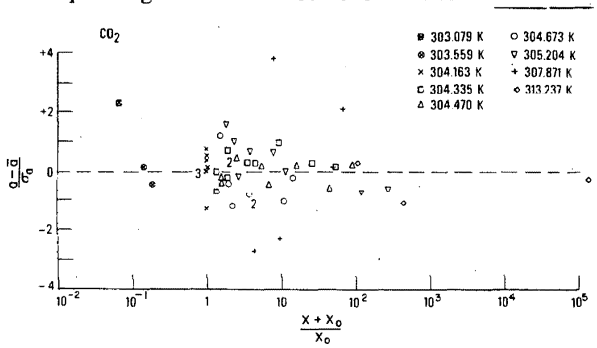

FIGURE 14. Plot of normalized deviations $(a-\bar{a})/\sigma_a$ as a function of $(x+x_0)/x_0$ for the optimum Linear Model fit to the CO_2 data.

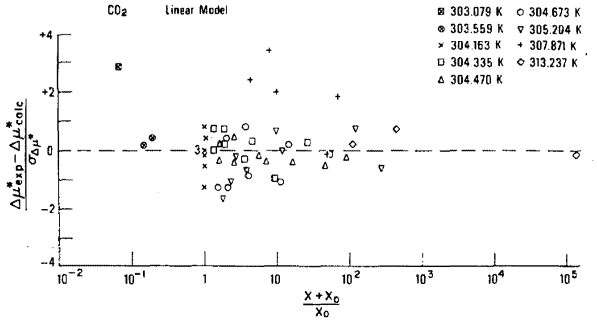

FIGURE 15. Plot of normalized deviations $(\Delta\mu^*_{exp}-\Delta\mu^*_{calc})/\sigma_{\Delta\mu^*}$ as a function of $(x+x_0)/x_0$ for CO_2, when the data are represented by the Linear Model.

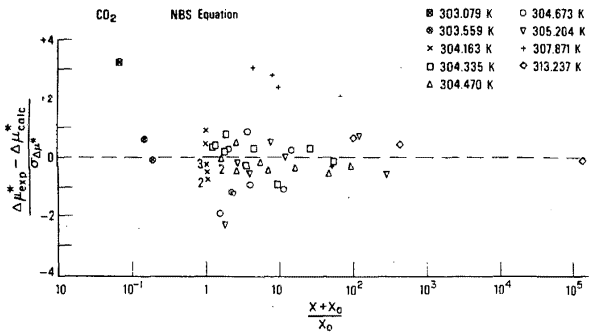

FIGURE 16. Plot of normalized deviations $(\Delta\mu^*_{exp}-\Delta\mu^*_{calc})/\sigma_{\Delta\mu^*}$ as a function of $(x+x_0)/x_0$ for CO_2, when the data are represented by the NBS Equation.

TABLE 26. Critical region parameters for CO_2 from data of Michels et al. for the restricted Linear Model and the equivalent NBS equation

Restricted Linear Model		Equivalent NBS equation	
P_c	7.3722 MPa	P_c	7.3722MPa
ρ_c	467.8 kg/m³	ρ_c	467.8 kg/m³
T_c	304.14 K	T_c	304.14 K
x_0	0.14185	x_0	0.14185
β	0.3486	β	0.3486
δ	4.44	δ	4.44
a	21.835	E_1	2.1379
b^2_{SLH}	1.3824	E_2	0.27170
χ	1.30	χ	1.12
α	0.104	α	0.104
γ	1.199	γ	1.199
B	1.975	B	1.975
D	2.271	D	2.290
Γ	0.06472	Γ	0.06525
Γ'	0.01553	Γ'	0.01568
Γ/Γ'	4.17	Γ/Γ'	4.16
A^+	2.67		
A_I^-	0.093		
A_{II}^-	5.58		

TABLE 27. Linear Model parameters for CO_2 obtained from a direct pressure fit [M2]

Linear Model		Restricted Linear Model	
ρ_c	467.8 kg/m³	ρ_c	467.8 kg/m³
T_c	304.18 K	T_c	304.16 K
x_0	0.141856	x_0	0.14185
β	0.3486	β	0.3486
δ	4.37	δ	4.38
a	24.48	a	19.56
b^2	1.70	b^2_{SLH}	1.3484

5.5.h. Comparison with Results of Other Authors

In table 28 we present a survey of the values reported for the critical exponent γ of CO_2. The value 1.26, initially reported from an analysis of the CO_2 data in terms of the NBS equation [V1], was too high for the reasons given in section 5.5.e.

White and Maccabee [W10] and Lunacek and Cannell [L9] measured the intensity of scattered light on the critical isochore and analyzed the data in terms of a power law. White and Maccabee found a low value $\gamma \approx 1.17$ when a power law was fitted to the data in a large range of temperatures above T_c. Lunacek and Cannell report a larger value $\gamma \approx 1.22$, although the two sets of light scattering data do agree in their range of overlap. Lunacek and Cannell, however, put more emphasis on the data very close to T_c, a region where the corrections in White and Maccabee's experiment become very large. All factors considered, our present value $\gamma = 1.20$ for CO_2 seems very reasonable.

There is, nevertheless, definitely room for improvement of our knowledge of the value for the exponent γ of CO_2. That the reported values of γ for such a carefully studied substance spans a range from 1.17 to 1.22 is unsatisfactory.

White and Maccabee have recently made an attempt to describe the chemical potential data, the light scattering data and the C_V data of CO_2 simultaneously in terms of the Linear Model. In this analysis they have revised their value for γ upwards to $\gamma = 1.217$ [W11].

Several authors have proposed Linear Model parameters for CO_2 [C6, H4] but these proposals are not based on a detailed independent examination of the experimental data.

The specific heat C_v of CO_2 was measured by Lipa, Edwards and Buckingham using a sample with a height of 1 mm [L11]. Hohenberg and Barmatz calculated the gravity corrections for a cell of this height and found them to be less than 1 percent in the entire experimental range [H4]. Buckingham and coworkers represented their data by a power law of the form

$$\frac{C_v}{R} = A^+ |\Delta T^*|^{-\alpha} + B^+ \quad (T > T_c),$$
$$\frac{C_v}{R} = A_{II}^- |\Delta T^*|^{-\alpha} + B^- \quad (T < T_c), \tag{5.13}$$

with the parameters $\alpha = 0.125$, $A^+ = 5.583$, $B^+ = -3.457$ and $A_{II}^- = 10.473$, $B^- = -0.024$. Our fit to the chemical potential data yields $\alpha = 0.10$, while a direct fit to the pressure data yields $\alpha = 0.13$. It thus seems possible to reconcile the Michels' data with the value $\alpha = 0.125$ reported by the Australian workers, but the asymptotic scaling laws cannot accommodate background terms B^+ and B^- that differ above and below T_c.

TABLE 28. Values reported for the exponent γ of CO_2

Experimenters	Ref.	Data analyzed by	Ref.	Method of analysis	Range of ΔT	Value of γ
Michels et al.	[M1]	Missoni et al.	[V1]	NBS eqn.	$-0.003 < \Delta T < 0.03$	1.26 ± 0.03
		this paper		NBS eqn.	$0.003 < \Delta T < 0.03$	1.20 ± 0.03
		this paper		Linear Model	$0.003 < \Delta T < 0.03$	
		Murphy et al.	[M2]	Linear Model for pressure	$0.003 < \Delta T < 0.03$	1.17
White and Maccabee	[W10]	White and Maccabee	[W10]	power law	$0.0001 < \Delta T < 0.3$	1.17 ± 0.02
Lunacek and Cannell	[L9]	Lunacek and Cannell	[L9]	power law	$0.0001 < \Delta T < 0.03$	1.22 ± 0.01

5.6. Steam

5.6.a. Introductory Comments

The practical importance of steam has prompted the experimental study of this substance over a pressure and a temperature range and with an accuracy exceeding that of any other fluid, notwithstanding the serious experimental difficulties resulting from the highly corrosive character of steam. Since steam engines and steam turbines were the objects of trade between many countries, the need for agreement on design and performance led to an international cooperation with the aim of obtaining a set of tables of the thermophysical properties of steam. This effort led to the adoption of the so called International Skeleton Tables in 1963 [M15, S14].

After these tables and their tolerances had been agreed upon, the need was felt for an analytic formulation that could be used to compute the properties of steam at any desired pressure and temperature including those used in the Skeleton Tables. An international formulating committee, established for this purpose, recommended a representation of the properties of steam for industrial use (IFC '67) which has been adopted internationally [M15, S14]. It also considered a representation for general and scientific use (IFC '68) [V5]. Both formulations used different equations in different ranges of pressure and temperature, while care was taken that derivatives vary smoothly across boundaries. In the critical region the IFC '68 was based on a master formulation completed by Jůza in 1966 [J2]. This formulation used polynomials in density and inverse temperature of degrees as high as 200; as mentioned by Jůza, the large number of parameters was needed to accomodate the steep rise of the constant volume heat capacity as determined by Amirkhanov. The most recent formulation of the thermodynamic properties of steam, namely that of Keenan, Keyes, Hill and Moore [K8], uses an analytic equation for the Helmholtz free energy as a function of volume and temperature containing a modest number of adjustable parameters. As a consequence, it has more trouble reproducing the experimentally observed divergence of the specific heat.

According to our current insight, analytic equations are fundamentally unsuitable for describing the thermodynamic behavior of fluids near the critical point. Steam is no exception and its critical anomalies are closely analogous to those of other fluids as was pointed out by one of us at the Seventh International Conference on the Properties of Steam [L4].

A reanalysis of the critical properties of steam cannot be based on the Skeleton Tables. First, the delicate nature of a critical anomaly can be masked by the process of averaging data of different origin. Secondly, some important experimental results have become available after the formulation of the Skeleton Tables. In particular, we refer here to Blank's redetermination of the critical parameters of steam [B6] and to the accurate and extensive set of experimental *PVT* data reported by Rivkin and coworkers [R2, R3, R4].

An analysis of the critical region anomalies of steam, an assessment of the critical parameters and a scaled analysis of Rivkin's *PVT* data in terms of the NBS equation was recently published by Levelt Sengers and S. C. Greer [L4]. In the present paper we present an analysis in terms of both the NBS equation and the Linear Model.

5.6.b. Data Sources for Steam

In our assessment, the most significant data sources concerning the thermodynamic behavior of steam in the critical region are the coexistence curve data obtained by Eck [E8], the vapor pressure data and the heat of vaporization data obtained by Osborne, Stimson and Ginnings [O1], the *PVT* data obtained by Rivkin and coworkers [R2, R3, R4], the constant volume heat capacity data obtained by Amirkhanov and coworkers [A3] and the constant pressure heat capacity data obtained by Sirota [S15].

The coexistence curve data of Eck are probably affected by the presence of dissolved quartz. However, since small amounts of impurities do not affect the value of the critical exponents [L7], Eck's data can be used to obtain a value for the exponent β.

The data of Osborne, Stimson and Ginnings are of outstanding quality. Their heat of vaporization data can also be used to obtain information concerning the shape of the coexistence curve. Their vapor pressure data confirm the nonanalytic behavior of the vapor pressure curve implied by the scaling laws [L4].

The data of Amirkhanov et al. can be used to demonstrate the divergence of C_v and the approximate validity of the scaling procedure [L4]. So far, we have not considered the C_p data of Sirota et al. in our analysis. However, they will function as important test data in future thermodynamic calculations that we are planning for steam.

This paper is primarily concerned with an analysis of a detailed set of *PV*-isotherms at temperatures between 360 °C and 420 °C obtained by Rivkin and coworkers [R2, R3, R4]. The data are generally of good quality. The only serious drawback is that no measurements of the coexistence curve or the vapor pressure were reported. This leaves considerable uncertainty concerning the location of the two-phase region.

For the purpose of this analysis the *PVT* data of Rivkin et al. were converted to chemical potential data as a function of density and temperature. However, the total body of available *PVT* data was so large as to preclude the use of the tedious process of graphical integration for the evaluation of the chemical potential. Instead, we used a numerical procedure based on Lagrangian interpolation in combination with the trapezoidal integration rule. Chemical potential values obtained with both 4- and 5-point interpolation were

compared. In those cases where significant differences were found, it was decided that the original data were too widely spaced for safe interpolation and the corresponding chemical potential values were rejected. In principle, the numerical integration method can introduce spurious oscillations. For this reason, we have decided not to publish tables of these chemical potential data. We expect to obtain more reliable results in the future by fitting the Linear Model directly to the original pressure data [M3].

5.6.c. Critical Parameters for Steam

The 6th International Conference on the Properties of Steam adopted along with the Skeleton Tables, the values $T_c = 374.15$ °C on the T_{48} scale, $\rho_c = 315$ kg/m^3, $P_c = 221.20$ bar [M15, S14]. The value 374.15 °C for the critical temperature was based on an analysis conducted by Osborne, Stimson and Ginnings of their accurate heat of vaporization data. The accuracy of this value was questioned by Bridgeman and Aldrich [B7] who basically performed a power law analysis of the data of Osborne et al. and showed that T_c could be as low as 374.02 °C. A reanalysis of these data by Levelt Sengers and Greer, omitting the datum point at 374 °C because of possibly large gravity effects, gave an optimum fit for $T_c = 373.85$ °C [L4].

Blank [B6] recently redetermined the critical temperature of steam as $T_c = 373.91$ °C by visual observation of meniscus disappearance. Our analysis of the *PVT* data, to be presented in the subsequent section, also leads to T_c values below 374 °C. We, therefore, conclude that the critical temperature is close to 373.9 °C.

The value for the critical pressure P_c can be determined from the vapor pressure data of Osborne, Stimson and Ginnings, once the value of T_c is chosen. Our scaled fit to these vapor pressure data yields $P_c = 220.60$ bar at 373.9 °C, while Blank finds 220.45 bar at 373.91 °C.

Values for the critical density, used in formulations of the properties of steam, vary from 305 kg/m^3 to 318 kg/m^3 with 315 kg/m^3 being accepted internationally. A power law analysis of the coexistence curve data of Eck leads to a value 324 kg/m^3 or 325 kg/m^3 for ρ_c [L4]. The $\mu(\rho)$ isotherms deduced from Rivkin's *PVT* data are antisymmetric around the value $\rho_c = 322$ kg/m^3. A direct fit of the Linear Model to the experimental pressures, yields $\rho_c = 324$ kg/m^3 [M3]. From the heat of vaporization data of Osborne et al. we calculate the limiting value $(\rho_g + \rho_l)\,(TdP/dT)^{-1} = 3.70$ kg/m^3 bar at 373.9 °C. Using the value $TdP/dT = 1724.3$ bar from a scaled fit to the vapor pressure data, we then find $\rho_c = 319$ kg/m^3. Thus, although the precise value of ρ_c is somewhat in doubt, all indications lead to a value of ρ_c substantially higher than the internationally accepted value.

In conclusion, the most probable values for the critical parameters of steam are

$$\begin{aligned} T_c &= 373.9\ ^\circ\text{C}, \\ P_c &= 22.06\ \text{MPa} = 220.6\ \text{bar}, \\ \rho_c &= 319\ \text{kg/m}^3 - 324\ \text{kg/m}^3, \\ (TdP/dT)_c &= 172.43\ \text{MPa} = 1724.3\ \text{bar}. \end{aligned} \tag{5.14}$$

5.6.d. Critical Region Parameters for Steam

In analyzing the steam data we adopted the value $\rho_c = 322.2$ kg/m^3 as the point of antisymmetry of the chemical potential isotherms. For the coexistence parameters we used $x_0 = 0.100$ and $\beta = 0.35$, which is one of the possible parameter sets recommended by Levelt Sengers and Greer on the basis of the data of Eck [L4].

The fit of the NBS equation to the steam data was carried out by fixing ρ_c, x_0 and β at the values mentioned above, varying δ and T_c on a grid and adjusting E_1 and E_2 at each point on the grid by the method of least squares as described in section 4.7. The fit of the

TABLE 29. Critical region parameters for H_2O from data of Rivkin et al.

Linear Model		NBS equation	
P_c	22.06 MPa	P_c	22.06 MPa
ρ_c	(322.2 ± 0.03) kg/m^3	ρ_c	322.2 kg/m^3
T_c	(647.05 ± 0.05) K (T_{48})	T_c	647.05 K (T_{48})
x_0	0.100 ± 0.010	x_0	0.100
β	0.350 ± 0.013	β	0.350
δ	4.50 ± 0.13	δ	4.50
a	24.473 ± 0.3	E_1	1.2154
b^2_{SLH}	1.4286 ± 0.0035	E_2	0.37155
χ	1.94	χ	1.37
α	0.075	α	0.075
γ	1.225	γ	1.225
B	2.239	B	2.239
D	1.380	D	1.345
Γ	0.06825	Γ	0.06737
Γ'	0.01611	Γ'	0.01715
Γ/Γ'	4.24	Γ/Γ'	3.93
A^+	3.93		
$A_{\bar{1}}$	0.128		
$A_{\bar{11}}$	6.55		

TABLE 30. Correlation matrix of parameters. Linear Model fit for steam

	T_c	ρ_c	x_0	β	δ	b
T_c	1					
ρ_c	+0.10	1				
x_0	−0.55	+0.06	1			
β	+0.72	−0.02	−0.96	1		
δ	−0.74	−0.002	+0.95	−0.99	1	
b	−0.53	+0.12	+0.98	−0.96	+0.95	1

Linear Model to the steam data was carried out by again fixing ρ_c, x_0 and β, varying δ, T_c and b^2 on a grid and calculating the average value $\bar{a}$ of $a(\theta)$ at each point of the grid, as described in section 4.5. For the absolute weight assignment the experimental errors were estimated as

$$\sigma_{T^*} = 0.15 \times 10^{-4}\,(0.01\ \text{K}), \qquad \sigma_{\rho^*} = 5 \times 10^{-4},$$

$$\sigma_{\mu^*} = 1.0 \times 10^{-4}. \qquad (5.15)$$

Near the minimum value of χ^2 the Linear Model fit was quite insensitive to the choice of b^2 which, therefore, was identified with b^2_{SLH}.

The χ^2 surface showed a minimum in the neighborhood of $T_c = 373.90$ °C and $\delta = 4.50$. In table 29 we present the corresponding parameters for the Linear Model and the NBS equation. The errors quoted for ρ_c, T_c, x_0, β, δ and b^2 for the Linear Model are those corresponding to one standard deviation in the six-parameter linearized error calculation. In table 29 we list also the values of the coefficients and exponents of the power laws defined in section 4.2.

For the Linear Model fit we also calculated the variance-covariance matrix for simultaneous variation of all adjustable parameters as described in section 4.6. This matrix is shown in table 30 with the diagonal elements normalized to unity.

In figure 17 we show the normalized deviations of $a(\theta)$ from the average value $\bar{a}$ for the optimum Linear Model fit. Plots of the normalized deviations of the chemical potential data are presented in figures 18 and 19 for the Linear Model and the NBS equation, respectively.

In view of the large body of data for steam we performed the error estimates of the individual points for only one choice of critical parameters, rather than repeating the estimate for each point of the grid in parameter space. As a consequence, the value $\chi^2 = 1.88$ corresponding to the NBS equation is not quite

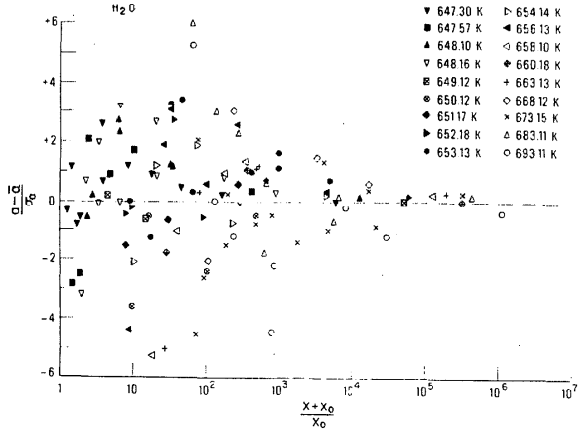

FIGURE 17. Plot for normalized deviations $(a-\bar{a})/\sigma_a$ as a function of $(x+x_0)/x_0$ for the optimum Linear Model fit to the H_2O data.

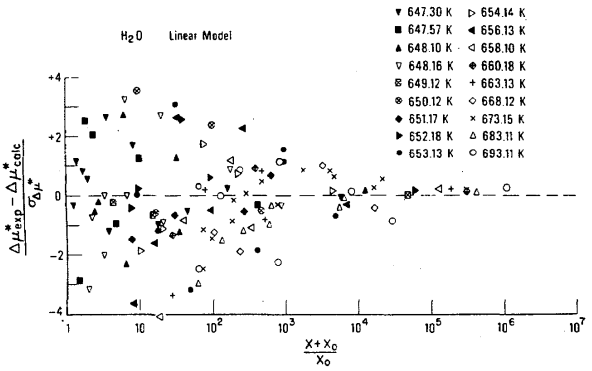

FIGURE 18. Plot of normalized deviations $(\Delta\mu^*_{\text{exp}} - \Delta\mu^*_{\text{calc}})/\sigma_{\Delta\mu^*}$ as a function of $(x+x_0)/x_0$ for H_2O, when the data are represented by the Linear Model.

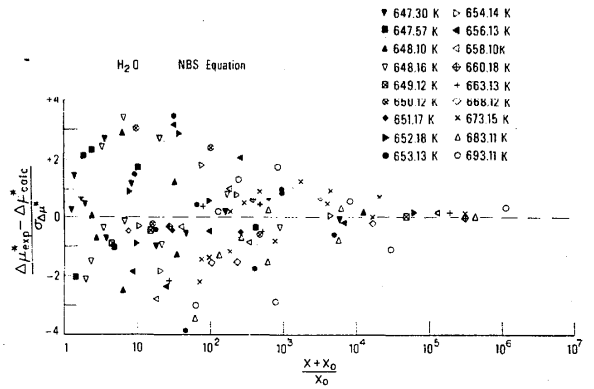

FIGURE 19. Plot of normalized deviations $(\Delta\mu^*_{\text{exp}} - \Delta\mu^*_{\text{calc}})/\sigma_{\Delta\mu^*}$ as a function of $(x+x_0)/x_0$ for H_2O, when the data are represented by the NBS Equation.

reliable. No such approximations were used in fitting the Linear Model. On comparing figures 18 and 19 it is evident that the Linear Model and the NBS equation yield representations of the chemical potential data of similar quality. We suspect that the value $\chi^2 = 3.75$ corresponding to the Linear Model fit is larger than unity in part as a result of spurious errors introduced by integrating the *PVT* data numerically. Direct fits to the pressure data, which we have performed recently, lead to parameter values similar to those obtained here from the chemical potential, but reduce χ^2 to 1.4 [M3].

5.7. Oxygen

5.7.a. Data Sources for Oxygen

There exists only a limited number of reliable data sources concerning the thermodynamic behavior of oxygen in the critical region. The vapor pressure of oxygen was measured very carefully by Hoge in 1950 [H8]. Sound velocity measurements have been reported by Van Itterbeek and coworkers [V6, V7], but the data are generally limited to the dense liquid.

Fortunately, an accurate, extensive and comprehensive set of data for the properties of oxygen has been obtained by Weber. He determined the equation

of state at temperatures between 56 K and 300 K and at pressures from 0.5 bar to 360 bar using an isochoric method developed at the Boulder Laboratories of the National Bureau of Standards [W12]. The pressure measurements were accurate up to a few millibar, the temperature was controlled at the millidegree level and the density was determined to better than 0.1 percent. With Goodwin he also measured the specific heat C_v along isochores and near the coexistence boundary [G4].

Near the critical point Weber's *PVT* data lacked detail and accuracy; in particular, the accuracy was limited due to the effects of unknown hydrostatic heads. Therefore, Weber decided to build a cell in which the gravity effect could be studied directly using the variation of the dielectric constant with height as an indication of the density profile in the field of gravity [W2]. In this experiment five capacitors, with a 0.1 mm spacing between their plates, were stacked at intervals of 2.5 cm along the height of the cell. The capacitors were calibrated by filling the cell at a temperature away from the critical temperature where the density was distributed uniformly through the cell and could be calculated from Weber's earlier equation of state data. Near the critical point the capacitors would indicate the presence of a density gradient in the field of gravity. At each temperature the experimentally observed density as a function of height can be interpreted as density as a function of chemical potential. In total about 200 $\mu(\rho)$ data were thus obtained for oxygen. In the same apparatus Weber also measured the coexisting vapor and liquid densities of oxygen in a temperature span of 5° below the critical temperature. The temperature was controlled to better than 1 mK. Weber attributes a precision of 0.05 percent to the density measurements, taking into account possible calibration errors and small hysteresis effects in the capacitors. The positions of the capacitors were measured to 0.003 cm.

Weber analyzed his coexistence curve data with the result

$$T_c = 154.576\ \text{K} \qquad \rho_c = 436.2\ \text{kg/m}^3$$
$$\beta = 0.3530 \pm 0.005 \qquad B = 1.819 \pm 0.005 \tag{5.15}$$

He analyzed the compressibility data by taking the observed values of $\Delta\rho/\Delta h$ and applying, when necessary, a curvature correction to obtain the limiting value $(\partial\rho/\partial h)_T \propto (\partial\rho/\partial\mu)_T$ at the critical density and at the coexistence boundary as a function of temperature. He deduced

$$\gamma = 1.247 \pm 0.013 \qquad \gamma' = 1.241 \pm 0.018$$
$$\Gamma = 0.0526 \pm 0.0050 \qquad \Gamma' = 0.0118 \pm 0.0018 \tag{5.16}$$

Similarly, from the compressibilities along the critical isotherm the exponent δ was determined as

$$\delta = 4.59 \pm 0.06. \tag{5.17}$$

In this paper we present the results of a statistical analysis of all of Weber's density profile data in terms of the Linear Model. The data are ideally suited for such an analysis since they provide the chemical potential directly. A preliminary account of this work was presented at the 1973 Cryogenic Engineering Conference [L12].

5.7.b. The Coexistence Curve of Oxygen

For the coexistence curve of oxygen we have on the one hand Weber's coexistence data between 150 K and T_c [W2] and on the other hand coexisting densities derived from his *PVT* data at temperatures below 150 K [W12]. Because of the detail, accuracy and completeness of the data, they permit us to answer a number of questions which are of current interest [L3, L13], but perhaps somewhat outside the scope of this paper.

From the combined set of capacitance and *PVT* data for the coexistence curve, Weber showed that the coexistence curve diameter is a straight line to within the accuracy of the data [W2]. If a power law is fitted to the $\rho_l - \rho_g$ data from the capacitance experiment only, the standard deviation goes through a minimum at $T_c = (154.576 \pm 0.001)$ K on the T_{48} scale; the value of the exponent β varies from 0.355 to 0.353 when the temperature range is shrunk from $|\Delta T^*| \leq 0.03$ to $|\Delta T^*| \leq 0.004$. If the exponent β is calculated from data in the range $|\Delta T^*| \leq 0.1$ by including *PVT* data points, then the value 0.356 is obtained. Thus the exponent β seems to be virtually independent of the range of the power law fit.

In our analysis of Weber's density profile data we have assumed

$$T_c = (154.576 \pm 0.001)\ \text{K}\ (T_{48}) \qquad \beta = 0.353$$
$$\rho_c = 436.2\ \text{kg/m}^3 \qquad B = 1.8185$$
$$(x_0 = 0.183624) \tag{5.16}$$

in accordance with Weber's analysis of his coexistence curve and as confirmed by our own reevaluation of this curve.

5.7.c. Analysis of Density Profile Data in Terms of the Linear Model

Consider two capacitors at heights h_i and h_j, respectively. Since the sum of the chemical potential μ and the gravitational potential gh is a constant throughout the fluid at equilibrium, we have, in reduced units,

$$\Delta\mu^*(h_j) - \Delta\mu^*(h_i) = \frac{\rho_c g}{P_c}(h_i - h_j), \tag{5.17}$$

where g is the gravitation constant. It is convenient to define a dimensionless height h^* as

$$h^* = \frac{\rho_c g}{P_c} h. \tag{5.18}$$

Thus the chemical potential difference is equal but opposite to the reduced height difference.

Once a choice is made for T_c, ρ_c, and b^2, and using the observed densities and temperature, we can calculate the values x_i and x_j of the scaling variable x and, hence, the values θ_i and θ_j of the Linear Model parameter θ corresponding to the levels h_i and h_j. From each pair of data points corresponding to the subscripts i, j we then calculate a value of the adjustable parameter a which we shall designate as a_{ij}.

$$a_{ij} = (h_j^* - h_i^*)|\Delta T^*|^{-\beta\delta}\left[\frac{\theta_j(1-\theta_j^2)}{|1-b^2\theta_j^2|^{\beta\delta}} - \frac{\theta_i(1-\theta_i^2)}{|1-b^2\theta_i^2|^{\beta\delta}}\right]. \tag{5.19}$$

The variance in a_{ij} is estimated from the errors in θ_i and θ_j and the estimated experimental errors in ΔT and the levels h_i and h_j. A weighted average $\bar{a}$ is then calculated from the complete set of a_{ij}'s. The process is repeated for other choices of T_c, δ and b^2. That set of values for T_c, δ and b^2 is considered optimum which minizes the standard deviation of $\bar{a}$. When this minimum is attained, a check is made of the distribution of the individual a_{ij} values around the average $\bar{a}$ to see whether deviations grossly exceeding the estimated error occur.

Since there are no more than five simultaneous density readings at any given temperature and average filling density, not all choices of (i, j) pairs are independent. From those sets of data for which five densities were recorded along the length of the cell, we have usually formed the (i, j) pairings (1, 3), (1, 4), (2, 5) and (3, 5). If fewer than five densities were reported, we formed fewer pairs chosen in as symmetric a fashion as possible. We have generally avoided taking data pairs if the two readings corresponded to opposite sides of the coexistence curve, because a small error in B or β would then lead to large systematic errors. In addition to the data presented in reference [W2], we have also included four unpublished isotherms, kindly provided by Weber [W13]. In total we had almost 150 data pairs at our disposal.

In a first group of fits we estimated the errors to be 0.3 mK in temperature, 0.05 percent in density and 0.038 cm in height. The last number was arrived at as the maximum possible error due to 0.01 cm uncertainty in the location of the center of each capacitor and to the fact that the height differences under consideration usually involved three or four capacitors. We shall refer to the weights based on these error estimates as weight assignment I. Using these error estimates we obtained minimum χ^2 values of about 2.4. The minimum was obtained at $T_c = 154.576$ K or 154.577 K (T_{48}) and for δ values near 4.30. Upon inspection it was found that the data near the critical isochore exhibited large and systematic deviations. Several fits were made in which some of the data sets were removed, until it was found that removal of the run at 154.609 K resulted in a reduction of χ^2 by about 20 percent to 1.9. Removal of the unpublished data resulted in a further reduction of χ^2 to 1.7; however, we did not consider this reduction sufficiently convincing to reject the unpublished data.

We thus proceeded with all data except those at 154.609 K. When b^2 was restricted to b^2_{SLH}, a minimum χ^2 of 1.91 was obtained at $\delta = 4.33$ and $T_c = 154.577$ K corresponding to $b^2_{SLH} = 1.37$. When b^2 was varied independently, a slightly lower χ^2 of 1.82 was obtained for $b^2 = 1.15$, the lowest value we tried. Again, we decided that the decrease was not enough to warrant deviating from the choice $b^2 = b^2_{SHL}$. On examining the details of the fit, we found that the data near the critical isochore again showed the largest deviations, albeit smaller than when the points at $T = 154.609$ K were included.

Finally, we tried a rather drastic change in the error estimates, since we might have overestimated the error in the height and underestimated the error in temperature. Therefore, we considered an alternate weight assignment, to be referred to as weight assignment II, for which the error in height was taken to be 0.02 cm and the error in temperature 0.6 mK, while the error in density was left unchanged at 0.05 percent. With these error estimates we again obtained minimum χ^2 values near 2. The minimum was obtained at $\delta = 4.33$ and

TABLE 31. Optional choices for the Linear Model parameters of oxygen [a]

Data	All	All except 154.609 K	All except 154.609 K
Weight assignment	I	I	II
T_c	154.577 K	154.577 K	154.577 K
δ	4.29	4.33	4.33
b^2_{SLH}	1.337	1.371	1.371
a	12.41 ± 0.52	13.94 ± 0.63	13.93 ± 0.61
χ^2	2.59	1.91	2.00
T_c	154.576 K	154.576 K	154.576 K
δ	4.30	4.37	4.37
b^2_{SLH}	1.340	1.395	1.395
a	12.55 ± 0.52	15.49 ± 0.69	15.48 ± 0.67
χ^2	2.66	2.02	2.12

[a] $P_c = 50.43$ bar, $\rho_c = 436.2$ kg/m^3, $\beta = 0.353$, $x_0 = 0.183624$.

$T_c = 154.477$ K and the larger deviations were again concentrated near the critical isochore.

The results of our analysis are summarized in table 31. The values obtained for the Linear Model parameters turn out to be very insensitive to the choice of weight assignment.

5.7.d. Critical Region Parameters for Oxygen

In table 32 we present the Linear Model parameters for oxygen together with the corresponding coefficients and exponents of the power laws. As explained in the previous section these parameter values are obtained from an analysis in which the experimental isotherm at $T = 154.609$ K is omitted. We selected the fits with weight assignment I since they lead to slightly lower χ^2 values. We preferred the fits for $T_c = 154.576$ K, since the same critical temperature is obtained from an analysis of the coexistence curve.

In table 32 we also present the parameters for the equivalent NBS equation. These parameters, however, were not obtained by fitting the NBS equation to the density profile data directly, but were deduced from the Linear Model parameters using the relations (5.3) and (5.4).

TABLE 32. Critical region parameters for O_2 from density profile data of Weber

Linear Model		Equivalent NBS equation	
P_c	5.043 MPa	P_c	5.043 MPa
ρ_c	436.2 kg/m^3	ρ_c	436.2 kg/m^3
T_c	154.576 K (T_{48})	T_c	154.576 K (T_{48})
x_0	0.183624	x_0	0.183624
β	0.353	β	0.353
δ	4.37	δ	4.37
a	15.485 ± 0.69	E_1	2.2278
b^2_{SLH}	1.3827	E_2	0.2855
χ	1.43		
α	0.104	α	0.104
γ	1.190	γ	1.190
B	1.819	B	1.819
D	2.383	D	2.383
Γ	0.08369	Γ	0.08369
Γ'	0.02070	Γ'	0.02110
Γ/Γ'	4.04	Γ/Γ'	3.97
A^+	1.64		
A^-_I	0.0647		
A^-_{II}	3.56		

5.7.e. Discussion

The results of our Linear Model fits to Weber's data yield optimum values for the critical exponents that are very much in line with those obtained for other fluids. However, we face the problem that our values $\delta = 4.37$ and $\gamma = 1.19$ are much lower than the values $\delta = 4.59$ and $\gamma = 1.25$ reported by Weber [W2]. This difference, we feel, arises from the fact that we have analyzed all data in terms of a scaled equation of state, while Weber's analysis was restricted to the data along the critical isochore and the critical isotherm.

We determined the value of χ^2 that we would obtain for Weber's choice of the exponent δ and found that it led to a substantial increase in χ^2. Specifically, the Linear Model parameters listed in table 32 with $\delta = 4.37$ give $\chi^2 = 2.02$, while Weber's value $\delta = 4.59$ leads to $\chi^2 = 2.93$. A 10 percent increase of χ^2 to the value 2.23 is obtained when δ is taken to be 4.47. Therefore, although the Linear Model fit does not define δ much better than to ± 0.1, the high value 4.59, subsequently used by Hohenberg and Barmatz in their evaluation of Linear Model parameters for oxygen [H4], seems excluded by our fits.

We have made some attempts to find an explanation for the large scatter of the data near the critical isochore. A recent study of the coexistence curve of SF_6 by Weiner, Langley and Ford [W14] indicates the possibility that a value of ρ_c, deduced by extrapolating the rectilinear diameter, may be too high by a few parts in 1000. However, if we decrease the value of ρ_c in our fits, we find that the value of χ^2 increases. It is possible that the Linear Model has the tendency of depressing the values for the exponents γ and δ. The only other alternative seems to be the presence of small temperature gradients. Even a gradient of a few tenths of a millidegree would affect the shape of the density profile close to the critical point drastically [W15].

In summary, we have obtained a moderately satisfactory Linear Model fit to Weber's density profile data with critical exponents that are fairly well defined and comparable to those obtained for other fluids. However, some of these exponents, namely γ and δ, differ substantially from those deduced by Weber from a power law analysis. The reason for this difference is not entirely clear.

6. "Universal" Critical Region Parameters for a Number of Fluids

6.1. The Principle of Universality of Critical Behavior

In addition to the one-component fluids which form the subject of this study, there are many other examples of experimental systems exhibiting critical behavior. Partially miscible binary liquids, superfluid liquid helium, ferromagnets and solids exhibiting order-disorder transitions all have critical points. In addition to these experimental systems, many model systems have critical points: thus, rigorous or approximate results are available for the critical behavior of the 2- and 3-dimensional Ising and Heisenberg models. The principle of universality groups these systems in so-called universality classes; within each class, the critical behavior is universal, so that a unified description can be given for all its members. The resulting economy of description is a great advantage; it can roughly be compared with the simplifying and predictive power of

he law of corresponding states, albeit limited to the critical region. Before attempting to decide how to catalog systems according to universality class, it is necessary to know what causes these classes to differ from each other. The differences between the systems listed must be contained in their Hamiltonians. Typical parameters entering the Hamiltonian are, for instance, the system's dimensionality, its spin dimensionality, its lattice structure (if any), the form and range of the interaction forces between its fundamental particles. From a study of model systems, it has become clear that the values of the critical exponents depend on only a few of these parameters in the Hamiltonian, while being totally independent of others. Physically, this arises from the fact that in the critical region large "clusters" or ordered regions are in interaction with each other, so that many of the fine details of interparticle interactions become screened.

The parameters in the Hamiltonian can be classified as "relevant" or "irrelevant" depending on whether they affect critical exponents or not. Careful study of model systems has shown that the system's dimensionality and its spin dimensionality or symmetry are "relevant" parameters. Thus, the critical exponents of the 2-dimensional Ising model are much further removed from the classical values than are those of the 3-dimensional Ising model. Also, the critical exponents of the Ising model, for which only one spin component enters into the Hamiltonian, are different from those of the Heisenberg model with three spin components. The range of the interparticle forces is only relevant in a very crude sense: finite-range forces lead to nonclassical critical behavior, whereas in the limit of infinite-range forces the "mean-field" or classical behavior obtains. Critical behavior in these model systems does not depend on details of the interparticle interaction, such as the size of the spin. It is also expected that critical exponents do not change if interactions extend beyond nearest neighbors, as long as their range remains finite. It must be remarked, though, that the available "experimental" evidence on this point from model calculations is not entirely conclusive [D2, F5]. Irrelevant is also the lattice symmetry, so that f.c.c., b.c.c. and simple cubic Ising models all have the same critical exponents.

Our insight into the critical behavior of model systems thus leads us to expect that systems exhibiting critical behavior can be grouped into a number of universality classes. Within each class, the relevant parameters are the same, but the irrelevant ones may differ from system to system. The principle of universality implies that the critical exponents are the same for all systems within one universality class. The exponents change abruptly when a relevant parameter is changed, which results in a new universality class. The principle of universality implies, in addition, that the reduced scaled equation of state is the same for all systems within one universality class, except for two nonuniversal constants. Thus the function $h(x)$ which characterizes the scaled equation (cf (2.12)) may be written as

$$h(x) = Dh^*(x/x_0), \tag{6.1}$$

where h^* is the same function of x/x_0 for all systems within the universality class, while D and x_0 are characteristic of the individual systems.

These ideas about universality have been corroborated for model systems by the recently developed renormalization group approach towards the calculation of critical exponents [W16, W17]. The relevant parameters are those that persist in the renormalization procedures, while the irrelevant ones disappear.

For fluids, no realistic models or rigorous results are available. The so-called lattice gas, a version of the Ising model, is often used as a (highly artificial) model for the liquid-vapor phase transition. This would lead to the expectation that fluids should have the same critical exponents as the Ising model. The experimental evidence, however, argues against this assumption [L13]. Thus, the exponent β characteristic of fluids is near 0.35, a full 10 percent higher than the Ising value of 0.3125. We may, however, use the experience gathered with the renormalization group approach, especially with respect to the "relevance" or "irrelevance" of parameters in the Hamiltonian, to speculate about the validity of universality in fluids. Universality may then certainly be expected to hold within the class of nonionized fluids. For such fluids the intermolecular forces are sufficiently short-ranged, so that their details can be expected to be irrelevant. The presence of dipolar interactions might be thought to present some complications, since these forces are long-ranged, and lead to many subtle effects in the solid systems, where they have been studied by the renormalization group approach [A4]. These results, however, have probably no analogy in the fluid case where the ordering is spatial rather than orientational, and where the dipolar forces average out to a potential that is effectively short-ranged [S16].

In the absence of a workable renormalization group procedure for fluids, however, the question of the universality of critical behavior in fluids must be considered open from a theoretical point of view. In the absence of a theoretical framework, it seems therefore important to investigate the experimental material, gathered in this paper, to see whether it supports or disproves the hypothesis of universality of critical behavior in fluids.

6.2. Universality of Fluid Critical Behavior

The universality hypothesis has two parts to it: (a) within a universality class the critical exponents are the same and (b) within such a class the scaled function $h^*(x/x_0)$ is the same. In order to see the implications of the latter statement for fluid critical behavior, it may be useful to compare it with the well-known principle of corresponding states, as formulated originally by

van der Waals. The latter requires that the equation of state, if expressed in units of P_c, V_c and T_c, be independent of the substance. This principle is known to have only limited validity. For instance, no close correspondence exists between the equations of state of heavy noble gases and air constituents on the one hand, and such substances as CO_2 (cigar-shaped molecules) or steam (large dipole moment) or helium (large quantum effects), even if one limits the comparison to the critical region only. While corresponding states implies that the function $h(x)$ in (6.1) should be the same for all fluids, it is in fact not. Attempts have been made to generalize the corresponding states principle by adding one additional parameter. The principle of universality, while allowing more latitude than does the principle of corresponding states, asserts that to determine the equation of state in the critical region of nonionized fluids in addition to the critical parameters one never needs more than only two substance-dependent parameters, namely D and x_0.

Our test of the two parts of the universality hypothesis will be carried out in two steps. First, we will investigate the experimental results for the critical exponents of the six fluids that we have studied, to see whether these exponents are the same within experimental error. Then, we will test the universality of the scaled function $h^*(x/x_0)$ by comparing this function for four fluids that very distinctly violate the principle of corresponding states.

Turning to the first part of the program, involving the critical exponents, we summarize, in table 33, the critical parameters from our "best" restricted Linear Model fits, together with the error estimates as obtained from a simultaneous 6-parameter variation as described in section 4.6.

It is seen that the exponents in table 33 have the "universal" value $\beta=0.355$ in common within one standard deviation, and the "universal" value $\delta=4.35$ within two standard deviations. The values $\beta=0.355\pm0.007$ and $\delta=4.35\pm0.10$ agree within combined error with all experimental values reported in table 33. Using the exponent equalities (2.5) and (2.6), the universal values $\gamma=1.19\pm0.03$ and $\alpha=0.10\pm0.04$ are obtained. The parameter set

$$\begin{aligned}\beta&=0.355\pm0.007,\\ \delta&=4.35_2\pm0.10\\ \gamma&=1.19\pm0.03,\\ \alpha&=0.10\pm0.04,\end{aligned}\qquad(6.2)$$

is also in quite good agreement with many other values of α, β, γ and δ reported in the literature. A review of the values reported in the literature for β and γ was presented in [L13]. The spread in the γ values presented in table 33 is no larger than is the "natural spread" in γ for a single substance, if different model functions, different ranges or data from different sources are used in the analysis [L3, L13]. Any such spread in that table is therefore not necessarily indicative of a violation of universality. The exponent β is generally more accurately known and less range-dependent than γ. The noble gases have β values between 0.355 and 0.362, a spread too small to be significant. For several polyatomic fluids, such as CO_2, N_2O, $CClF_3$ [L7] and, in particular, SF_6 [B8] β seems to fall slightly below 0.35. Although the possibility that this difference between monatomic and polyatomic fluids might be real cannot be excluded, it is nevertheless marginal at best and will need more convincing experimental corroboration before a firm conclusion can be reached. Thus, the hypothesis of universality of the critical exponents of gases is confirmed by the experimental evidence investigated in this paper and elsewhere.

The second half of the hypothesis, universality of the scaled function $h^*(x/x_0)$, has been implicitly demonstrated by the observation that a two-parameter scaled equation is capable of representing critical-region data of many fluids to within experimental accuracy. A more direct test can be performed by plotting the experimental values of $\Delta\mu^*/(\Delta\rho^*)|\Delta\rho^*)|^{\delta-1}$ as a function of the experimental values of x/x_0 for a number of fluids,

TABLE 33. Linear Model parameters from statistical fit, $b^2=b^2_{SLH}$

	He^3	He^4	Xe	CO_2	H_2O	O_2
x_0	0.480 ± 0.02	0.369 ± 0.02	0.186 ± 0.1	0.142 ± 0.006	0.100 ± 0.01	0.184
a	4.16 ± 0.1	6.4 ± 0.1	17.7 ± 0.5	21.8 ± 0.4	24.5 ± 0.3	15.5 ± 0.7
b^2_{SLH}	1.364 ± 0.003	1.389 ± 0.006	1.407 ± 0.04	1.382 ± 0.006	1.429 ± 0.004	1.383
β	0.358 ± 0.005	0.356 ± 0.006	0.350 ± 0.04	0.349 ± 0.005	0.350 ± 0.013	0.353
δ	4.26 ± 0.04	4.34 ± 0.06	4.46 ± 0.3	4.44 ± 0.06	4.50 ± 0.13	4.37
$\alpha=2-\beta(\delta+1)$	0.115	0.101	0.089	0.104	0.075	0.104
$\gamma=\beta(\delta-1)$	1.168	1.188	1.211	1.199	1.225	1.190

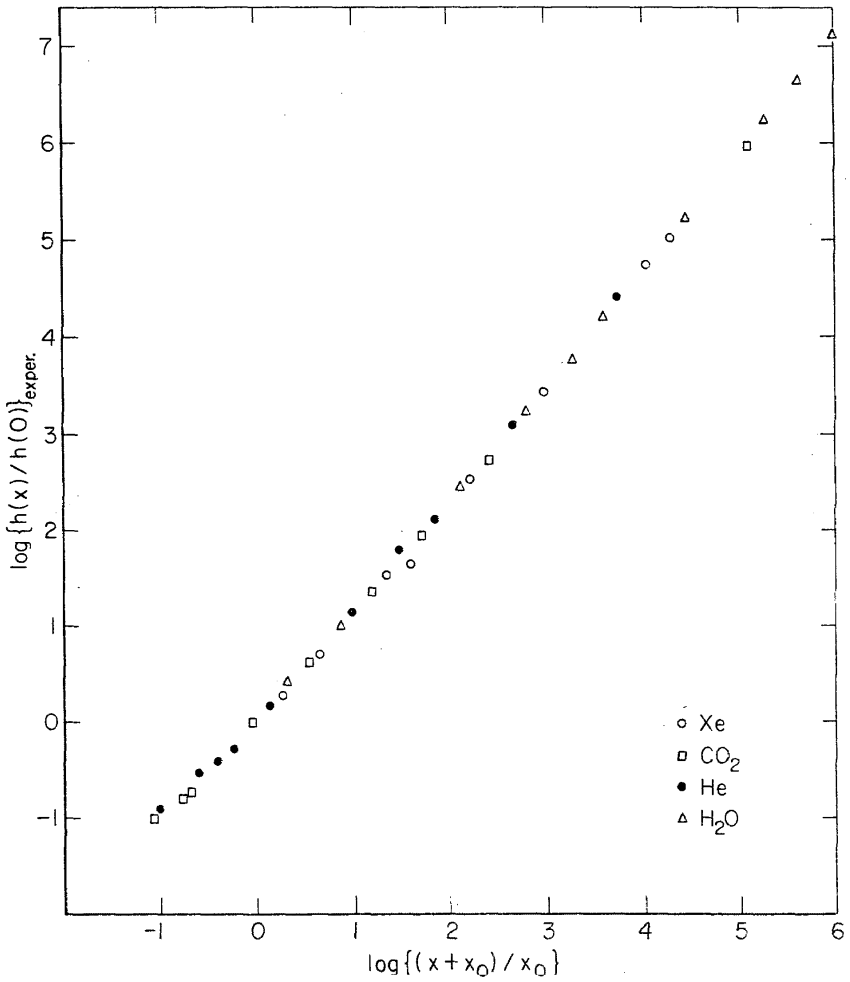

FIGURE 20. Test of universality for Xe, CO_2, H_2O and He^4.

to see whether these curves can be made to coincide by adjusting the vertical scales by a factor. Such a test was performed in [L3], using "universal" critical exponent values only slightly different from the ones we prefer here. The result is displayed in figure 20 which is taken from [L13]. It is seen that the scaled functions $h^*(x/x_0)$ of the noble gas Xe, the nonspherical molecule CO_2, the polar fluid H_2O and the quantum fluid He^4 coincide within error. Thus the hypothesis of universality of the scaled function $h^*(x/x_0)$ is confirmed by the experimental data.

6.3. Critical Region Parameters for Gases in Terms of a Universal Equation

In view of the corroboration of the principle of universality by the experimental data for the six fluids studied, it seems useful to produce for as many gases as possible a table of parameters in terms of one universal scaled equation. The "universal" form of the Linear Model was assumed to be that for which $\beta=0.355$, $\delta=4.35_2$ and $b^2=b^2_{\mathrm{SLH}}$. By (5.2), this implies a universal value, $E_9=0.287$, for the constant E_2 in the NBS equation. We then need, in addition, estimates of two nonuniversal constants for each gas considered. For the six fluids that we studied in the preceding chapter, we determined E_1 by fitting the NBS equation to the experimental $\Delta\mu^*-\Delta\rho^*-T$ data while E_2 was fixed at the universal value 0.287. For some other gases, scaled equations were available in the literature; usually, small shifts had to be made in the coefficients B (or x_0), Γ or D, in order to have them correspond with the universal values adopted here for the critical exponents β, γ or δ. We made these shifts using the "rule of thumb" $B_0|\Delta T^*_{\max}|^{\beta_0}=B|\Delta T^*_{\max}|^{0.355}$, or equivalently for the other exponents; the subscript max denotes the maximum temperature range over which the data were fitted. From two of the three coefficients the two constants in the scaled equation were calculated, whereas the third one was used as a check. For other gases, we had to obtain two of the coefficients B, Γ or D from whatever data were available in the literature. Estimates of B were obtained by fitting coexistence curve data using $\beta=0.355$, while estimates for Γ were made from the slope of supercritical isotherms or from data on the intensity

of scattered light using $\gamma = 1.19$. In a few cases, it was possible to estimate D as well, so that a check on the procedure was possible. The results of this work are summarized in table 34, in which the critical parameters and the parameters for the universal scaled equation, in terms of the Linear Model and the NBS equation are listed for 15 fluids.

Our choice of critical parameters was not based solely on the particular data fitted. In most cases, additional experimental material was available that, if considered reliable, contributed to the final values listed in table 34. The values of the critical temperature are given on the T_{68} temperature scale wherever applicable; those for He^3 and He^4 are on the T_{58} scale. Details on the calculation of the parameters in table 34 for those gases not studied in the previous sections are given below.

TABLE 34. Critical region parameters for 15 fluids based on "universal" exponents.

	Critical point parameters			Critical region parameters		
	P_c MPa	ρ_c kg/m³	T_c K	x_0	a	E_1
He^3	0.11678	41.45	3.3099	0.489	4.58	2.96
He^4	0.22742	69.6	5.1895	0.369	6.40	2.67
Ar	4.865	535	150.725	0.183	16.1	2.27
Kr	5.4931	908	209.286	0.183	16.1	2.27
Xe	5.8400	1110	289.734	0.183	16.1	2.27
O_2	5.043	436.2	154.580	0.183	15.6	2.21
N_2[a]	3.398	313.9	126.24	0.164	18.2	2.17
CH_4	4.595	162.7	190.555	0.164	17.0	2.03
C_2H_4	5.0390	215	282.344	0.168	17.5	2.17
p-H_2[a]	1.285	31.39	32.935	0.260	9.6	2.34
CO_2	7.3753	467.8	304.127	0.141	21.3	2.01
SF_6[a]	3.7605	730	318.687	0.172	22.2	2.86
NH_3[a]	11.303	235	405.4	0.109	21.4	1.37
H_2O	22.06	322.2	647.13	0.100	21.6	1.20
D_2O	21.66	357	643.89	0.100	21.6	1.20

$\beta = 0.355$ $\delta = 4.352$ $b^a_{SLH} = 1.3909$
$\gamma = 1.190$ $\alpha = 0.100$ $E_2 = 0.287$

[a] Estimated parameters of limited reliability; see discussion in this section.

(1) *Argon.* Use was made of unpublished *PVT* data kindly provided to us by Wu and Pings [W6]. Their fit to the NBS equation was used and the coefficients B_0, Γ_0 and D_0 transformed to correspond to the universal exponents by the "rule of thumb" mentioned. The shifts were quite small, the largest one, occurring in, Γ, being only 3 percent. Values of a were calculated from Γ_1 and D_1 and were 15.2 and 16.7, respectively, leading to the average values $a = 16.0$ and $E_1 = 2.26$. Values of x_0 of 0.183 to 0.184 were obtained. We considered the parameter $x_0 = 0.183$, that we used for xenon adequately representative of argon.

(2) *Krypton.* Unpublished *PVT* data were kindly provided to us by Gulari and Pings [G2], and, in addition, their fits to the NBS equation for the derived μ, ρ, T data. The *PVT* data were fitted directly by Murphy and Gulari [M16] to a Linear Model pressure equation. The resulting values of B_0, Γ_0, D_0 were transformed to correspond to "universal" exponents, the largest shift being one of 6 percent in Γ. From Γ and D, two a values resulted, of 16.2 and 16.6, respectively. We also calculated a from the NBS equation parameters of Gulari and Pings, finding $a = 16.1$ and 16.5, respectively. For x_0, 0.182 was found. The fit to the xenon data using the universal exponents gave $a = 15.8$. The small differences between xenon, argon, and krypton were not considered significant and we attributed to all three gases $x_0 = 0.183$ and $a = 16.1$.

(3) *Nitrogen.* The correlation by Jacobson [J3] was used as a guide. The coexistence curve data of Mathias et al. [M17], of 1914, were used to estimate x_0. Using T, $\Delta\rho$ data points at various temperatures, x_0 values between 0.171 and 0.142 were found. The parameter Γ was estimated from the slopes of the three isotherms reported in [K9]. We found Γ values from 0.065 to 0.084, the higher values being more accurate. Γ was similarly estimated from near-critical *PVT* data in [W18] which yielded values of 0.062 to 0.073 in approximately the same temperature range as that of [K9]. The available data were too scarce to permit a calculation of D.

(4) *Methane.* Several scaled fits are available in the literature, all obtained by the Louvain group of Verbeke and coworkers, and based on their own *PVT* data [J4, J5, G6]. From the parameters of the scaled fit presented in [G6], we calculated the coefficients B and D and made the small adjustments needed for correspondence with the universal parameters. The coefficient Γ was calculated directly from the pressure differences, at the same temperature, between two isochores, 3 percent above and 1 percent below the critical density, respectively. From the values $B = 1.90$ and $\Gamma = 0.080$, we calculated the parameters reported in table 34. They lead to a predicted value of $D = 2.19$, to be compared with the value of 2.18 derived from the scaled fit in [G6].

(5) *Ethylene.* The coexistence curve of ethylene was measured in Leiden in 1927 [M18]. From four ρ_l, ρ_g data points between +6.5 and −11 °C, we calculated x_0 values ranging from 0.169 to 0.157, the former being more precise. The coefficient Γ could be accurately calculated from four supercritical isochores, with densities within a percent from the critical density, recently determined by Hastings and Levelt Sengers [H9]. The densities of the four isochores were calculated from the pressures at 30 °C, making use of unpublished *PVT* data at this temperature, kindly provided to us by Trappeniers and Wassenaar [T2]. From isothermal pressure differences at several temperatures we found Γ to equal 0.077 to within about 2 percent. The parameters in table 33 were calculated from $B = 1.885$, $\Gamma = 0.077$, while the critical parameters are those recently determined by Moldover [M12].

(6) p-*Hydrogen.* The data for hydrogen stem from the NBS Boulder group [G7, R7]. From a reanalysis of the coexistence curve of hydrogen the values $\beta=0.3619$, $B=1.639$, $T_c=32.955$ K resulted. The B value was shifted to 1.613, to correspond with $\beta=0.355$. From a number of slightly supercritical isotherms, values for Γ ranging from 0.09 to 0.13 were obtained. A value of 0.12 was accepted. It was also found that a slightly lower value of T_c, $T_c=32.935$ K, was more compatible with the compressibility data and a γ value of 1.19, than the value of 32.955 obtained from the coexistence curve analysis. From B and Γ the parameters listed in table 33 were calculated. The predicted value of D was 2.5 at one end of the range of values (2.5 to 4.4) obtained by analyzing several slightly supercritical isotherms. The critical pressure reported in table 34 has been adjusted from the published value [C7] so as to correspond with the lowered value of T_c.

(7) *Sulfur Hexafluoride.* Coexistence curve data on SF_6 were recently reported by Balzarini and Ohrn [B8] and by Rathjen and Straub [R8], while prepublication results were kindly provided to us by Weiner, Langley, and Ford [W14]. In [B8], β is reported to have the value 0.346 in the range $7\times10^{-3}<|\Delta T^*|<10^{-1}$ and 0.339 in the range $5\times10^{-6}<|\Delta T^*|<5\times10^{-3}$. Low values for β in the close-in range were also found by Hocken [H7]. In [R8], the value 0.3422 is reported in the range $10^{-3}<|\Delta T^*|<10^{-1}$. Thus there seems to be a number of indications that SF_6 may depart from universality, which should be borne in mind when using our table 34. The B value reported in that table was obtained by shifting it from the value reported in [B8] to correspond with $\beta=0.355$. Using the PVT data of MacCormack and Schneider [M19], the coefficient D was calculated from several points on the critical isotherm; D values ranging from 3.3 to 4.4, with an average of 3.5 considered most likely, were obtained. Values for the compressibility derived from [M19] agree splendidly with those reported by Benedek and coworkers [F6] using light scattering and lead to a Γ value of 0.060. The B and Γ parameters in table 34 lead to a predicted value $D=3.06$, to be compared with the experimental value of 3.5.

(8) *Ammonia.* The critical point parameters of NH_3 were taken from a recent correlation by Haar [H10]. x_0 was taken from a fit by Haar [*H*10] to the (scanty) coexistence curve data. The critical region parameters were determined using a fit of the pressure version of the Linear Model [M20] to the experimental data of Date [D3]. Some Linear Model fits with exponents close to the "universal" ones were chosen, B, Γ and D calculated and shifted to correspond to "universal" exponents.

(9) *D_2O.* For the critical point parameters, we have made use of a compilation of properties of heavy water [J6], which was kindly provided to us by R. Mareš prior to publication. Mareš et al. [J6] have also demonstrated that the thermodynamic behavior of *D_2O* is very similar to that of H_2O in terms of corresponding states. For this reason we have assumed that the critical region parameters of D_2O are the same as those for H_2O.

6.4. Validity of "Hyperscaling" Relations between Critical Exponents

The thermodynamic exponents α, β, γ, δ that we have obtained using the scaling laws fulfill the exponent relations (2.5) and (2.6) automatically. There are however, other critical exponents that are related to the thermodynamic ones by inequalities or conjectured equalities. These exponents describe the asymptotic behavior of the pair correlation function. Near the critical point, correlations extend over ranges much larger than the interaction range. Their size is indicated by the correlation length ξ. The critical exponent ν indicates how the correlation length diverges when the critical point is approached along the critical isochore

$$\xi\sim|\Delta T^*|^{-\nu}. \tag{6.3}$$

At the critical point, the correlation length would decay, in d dimensions, as $1/r^{d-2}$ if the Ornstein-Zernike theory were valid. The small exponent η denotes the deviations from the Ornstein-Zernike theory. It is defined by assuming the form

$$G(r)\sim 1/r^{d-2+\eta}, \tag{6.4}$$

for the behavior of the pair correlation function at the critical point for large values of r [F7]. Scaling considerations [W3, S17] lead to the following relations between the correlation function exponents ν, η, the dimensionality and the thermodynamic exponents:

$$d\nu=2-\alpha, \tag{6.5}$$

$$(2-\eta)/d=(\delta-1)/(\delta+1). \tag{6.6}$$

These relations are known as hyperscaling relations. They are satisfied by the 2-dimensional Ising model and the 3-dimensional spherical model for which cases the exponents are known exactly. There is some uncertainty about the validity of these relations for the 3-dimensional Ising model [H2]. With the values we have obtained for the thermodynamic critical exponents, we can now test the validity of these hyperscaling relations.

The experimental values of the exponent ν have been reviewed by Chu [C7]. The best value is $\nu=0.63\pm0.02$. With our most probable value $\alpha=0.10\pm0.04$, we predict, from the hyperscaling relation (6.5): $\nu=0.63\pm0.015$. From neutron scattering data in neon, an accurate value for the exponent η was recently reported by Warkulwiz, Mozer and Green [*W*20], namely $\eta=0.11\pm0.03$; this value is supported by Lin and Schmidt's results from X-ray scattering in argon [L14]. Our most probable value $\delta=4.35\pm0.10$ leads, with the hyperscaling rela-

tion (6.6) to $\eta=0.12\pm0.02$. The conclusion is that the hyperscaling relations are obeyed by fluids to within the present state of experimental accuracy.

6.5. Conclusions

We have tested the principle of universality and found it to apply for the six fluids studied. The universal values of the critical exponents have been shown to fulfill other, conjectured equalities involving the dimensionality and the correlation function exponents. Using these universal values, we have predicted critical region parameters for several other gases. These predicted values should be considered as informed estimates, based on sometimes scanty or inaccurate experimental data. They should be useful for predicting fluid compressibilities in the critical region.

In extending their use to the prediction of other properties care should be taken. The capability of the scaled equation of state to predict the specific heat C_v is still to be demonstrated. Work on simultaneous fits of scaled equations to coexistence curve, PVT and specific heat data is currently in progress [M20].

The principle of universality very definitely needs further testing as well. A decisive experiment would be one by which coexistence curves or compressibilities would be measured in the same apparatus for a variety of fluids of quite different molecular structure, and in which all data would be analyzed by the same fitting function in the same range. This would eliminate many of the sources of parameter variability presently clouding the issue of universality.

Acknowledgements

The research was supported by the Office of Standard Reference Data, by the National Aeronautics and Space Administration Grant NGR-21-002-344 and by the Center of Materials Research of the University of Maryland. Part of the computer time was provided by the Computer Science Center of the University of Maryland.

T. A. Murphy provided us with valuable information on comparing the Linear Model with experimental data, F. W. Balfour assisted us in calculating chemical potential data for CO_2, F. J. Cook made some valuable comments concerning the thermodynamic properties of CO_2, E. Gulari and C. J. Pings informed us about their work on krypton and argon prior to publication and L. Haar provided us with critically evaluated data for NH_3. G. W. Mulholland and M. Klein carefully read the manuscript and made several valuable suggestions.

Appendix

Derivatives of the variable θ with respect to the adjustable parameters

$$\frac{\partial\theta}{\partial x}=\left(\frac{\partial\theta}{\partial x}\right)_{\beta,x_0,b}=-\frac{1}{x}\frac{\beta\theta(1-b^2\theta^2)}{\{1-b^2\theta^2(1-2\beta)\}} \quad (A.1)$$

$$\left(\frac{\partial\theta}{\partial\rho_c}\right)_{T_c,\beta,x_0,b}=+\frac{x}{\beta\Delta\rho^*}\frac{\partial\theta}{\partial x}\frac{\rho}{\rho_c^2} \quad (A.2)$$

$$\left(\frac{\partial\theta}{\partial T_c}\right)_{\rho_c,\beta,x_0,b}=-\frac{x}{\Delta T^*}\frac{\partial\theta}{\partial x}\frac{T}{T_c^2} \quad (A.3)$$

$$\left(\frac{\partial\theta}{\partial\beta}\right)_{\rho_c,T_c,x_0,b}=+\frac{x}{\beta^2}\frac{\partial\theta}{\partial x}[\ln|\Delta\rho^*|-\ln|\theta|] \quad (A.4)$$

$$\left(\frac{\partial\theta}{\partial x_0}\right)_{\rho_c,T_c,\beta,b}=-\frac{x}{x_0}\frac{\partial\theta}{\partial x} \quad (A.5)$$

$$\left(\frac{\partial\theta}{\partial b}\right)_{\rho_c,T,\beta,x_0}=+\frac{2bx}{1-b^2\theta^2}\frac{\partial\theta}{\partial x}\left[\frac{x}{x_0}|\theta|^{1/\beta}+\theta^2\right] \quad (A.6)$$

Derivatives of the quantity a with respect to the adjustable parameters

$$a=\left\{\left(\frac{b^2-1}{x_0}\right)^{\beta}\frac{|\theta|}{\Delta\rho^*}\right\}^{\delta}\frac{\Delta\mu^*}{\theta(1-\theta^2)} \quad (A.7)$$

$$\frac{\partial a}{\partial\theta}=\left(\frac{\partial a}{\partial\theta}\right)_{\rho_c,\beta,\delta,x_0,b}=a\frac{\delta-1-\theta^2(\delta-3)}{\theta(1-\theta^2)} \quad (A.8)$$

$$\left(\frac{\partial a}{\partial\rho_c}\right)_{T_c,\beta,\delta,x_0,b}=\frac{a\delta}{\Delta\rho^*}\frac{\rho}{\rho_c^2}+\frac{\partial a}{\partial\theta}\frac{\partial\theta}{\partial\rho_c} \quad (A.9)$$

$$\left(\frac{\partial a}{\partial T_c}\right)_{\rho_c,\beta,\delta,x_0,b}=\frac{\partial a}{\partial\theta}\frac{\partial\theta}{\partial T_c} \quad (A.10)$$

$$\left(\frac{\partial a}{\partial\beta}\right)_{\rho_c,T_c,\delta,x_0,b}=a\delta\ln\left(\frac{b^2-1}{x_0}\right)+\frac{\partial a}{\partial\theta}\frac{\partial\theta}{\partial\beta} \quad (A.11)$$

$$\left(\frac{\partial a}{\partial\delta}\right)_{\rho_c,T_c,\beta,x_0,b}=a\beta\ln\left(\frac{1-b^2\theta^2}{\Delta T^*}\right) \quad (A.12)$$

$$\left(\frac{\partial a}{\partial x_0}\right)_{\rho_c,T_c,\beta,\delta,b}=-\frac{a\beta\delta}{x_0}+\frac{\partial a}{\partial\theta}\frac{\partial\theta}{\partial x_0} \quad (A.13)$$

$$\left(\frac{\partial a}{\partial b}\right)_{\rho_c,T_c,\beta,\delta,x_0}=\frac{2ab\beta\delta}{b^2-1}+\frac{\partial a}{\partial\theta}\frac{\partial\theta}{\partial b} \quad (A.14)$$

References

[A1] Andrews, T., Philos. Trans. R. Soc. Lond. **159**, 575 (1869).
[A2] Amagat, E. H., C. R. Acad. Sci. (Paris) **114**, 1093 (1892).
[A3] Amirkhanov, Kh. I., Stepanov, G. V. and Alibekov, B. G., "Isochoric Heat Capacity of Water and Steam" (Amerind Publ. Co., New Delhi, 1974; available from U.S. Dept. Commerce National Technical Information Service, Springfield, Va.).
[A4] Aharony, A. and Fisher, M. E., Phys. Rev. **B8**, 3323, (1973). Aharony, A. Phys. Rev. **B8**, 3342, 3349, 3358, 3363, 4314, 4270, (1973).
[B1] Bevington, P. R., "Data Reduction and Error Analysis for the Physical Sciences" (McGraw-Hill, New York, 1969).
[B2] Brown, G. R. and Meyer, H., Phys. Rev. **A6**, 364 (1972).
[B3] Beattie, J. A., Barriault, R. J. and Brierley, J. S., J. Chem. Phys. **19**, 1219 (1951).

[B4] Brickwedde, F. G., Van Dijk, H., Durieux, M., Clement, J. R. and Logan, J. K., J. Res. Natl. Bur. Stand. (U.S.) **64A**, 1 (1960).
[B5] Bagatskii, M. I., Voronel, A.V. and Gusak, V. G.. Soviet Phys.–JETP **16**, 517 (1963).
[B6] Blank, G., Wärme-und Stoffübertragung **2**, 53 (1969).
[B7] Bridgeman, O. C., and Aldrich, E. W., J. Heat Transfer **87C**, 266 (1965).
[B8] Balzarini, D. and Ohrn, K., Phys. Rev. Lett. **29**, 840 (1972).
[C1] Cook, F. J. Private Communication.
[C2] Cook, F. J., "Theoretical Study and Data Analysis of Thermodynamic Properties in the Neighborhood of the Critical Point", Ph. D. Thesis (Department of Physics, Temple Univ., Philadelphia, 1972).
[C3] Cornfeld, A. B. and Carr, H. Y., Phys. Rev. Lett. **29**, 28 (1972); Carr, H. Y., Private Communication.
[C4] Cetas, C. T. and Swenson, C. A., Metrologia **8**, 46 (1972).
[C5] Chase, C. E., and Zimmerman, G. O., Phys. Rev. Lett. **15**, 483 (1965), **19**, 15 (1967); J. Low Temp. Phys. **11**, 551 (1973).
[C6] Chapela. G. A. and Rowlinson. J. S., J. Chem. Soc. Faraday Trans. I **70**, 584 (1974).
[C7] Chu, B., Ber. Bunsenges. Phys. Chem. **76**, 202 (1972).
[D1] De Boer, J. and Lunbeck, R. J., Physica **14**, 510 (1948).
[D2] Dalton, N. W. and Wood, D. W., J. Math. Phys. **10**, 1271 (1969).
[D3] Date, K., Rev. Phys. Chem., Japan **43**, 17 (1973).
[E1] Estler, W. T., "Interferometric Determination of the Equation of State of Xenon Near the Critical Point", Ph. D. Thesis (Department of Physics, State Univ., New York, Stonybrook, 1972); Estler, W. T., Hocken, R., Charlton, T., and Wilcox, L. R., Phys. Rev. **A12**, 2118 (1975).
[E2] Edwards, C., Lipa, J. A. and Buckingham, M. J., Phys. Rev. Lett. **20**, 496 (1968).
[E3] Edwards, M. H., Can. J. Phys. **36**, 884 (1958).
[E4] Edwards, M. H. and Woodbury, W. C., Phys. Rev. **129**, 1911 (1963).
[E5] Edwards, M. H., in "Critical Phenomena", NBS Miscell. Publ. 273, M. S. Green and J. V. Sengers, eds. (U.S. Gov't. Printing Office, Washington, D.C., 1966), p. 82.
[E6] Edwards, M. H., Proc. 11th International Conference on Low Temperature Physics, Vol. 1, J. F. Allen, P. M. Finlayson and D. M. McCall, eds. (Univ. St. Andrews, St. Andrews, Scotland, 1968), p. 231.
[E7] El Hadi, Z. E. H. A. and Durieux, M., Physica **41**, 305 (1969).
[E8] Eck. H.. Physik. Z. **40**, 3 (1939).
[F1] Fisher, M. E., in "Critical Phenomena", Proc. Intern. School of Physics "Enrico Fermi", Course LI, M. S. Green, ed. (Academic Press, New York, 1971), p. 1.
[F2] Feher, E. G., Energy Conversion **8**, 85 (1968).
[F3] Feke, G. T., Fritsch, K. and Carome, E. F., Phys. Rev. Lett. **23**, 1282 (1969).
[F4] Fritsch, K. and Carome, E. F. "Behavior of Fluids in the Vicinity of the Critical Point," NASA CR–1670 (National Aeronautics and Space Administration, Washington, D.C., 1970).
[F5] Farrell, R. A. and Meijer, P. H. E., Phys. Rev. **B5**, 3747 (1972).
[F6] Feke, G. T., Hawkins, G. A., Lastovka, J. B. and Benedek, G. B., Phys. Rev. Lett. **27**, 1780 (1971).
[F7] Fisher, M. E., J. Math. Phys. **5**, 944 (1964).
[G1] Griffiths, R. B., Phys. Rev. **158**, 176 (1967).
[G2] Gulari, E. C., "A Study of Critical Phenomena in Krypton", Ph. D. Thesis (California Institute of Technology, Pasadena, 1973); C. J. Pings, Private Communication.
[G3] Grilly, E. R., Hammel, E. F. and Sydoriak, S. G., Phys. Rev. **75**, 1103 (1949).
[G4] Goodwin, R. D. and Weber, L. A., J. Res. Natl. Bur. Stand. (U.S.) **73A**, 1, 15 (1969).
[G5] Griffiths, R. B., Phys. Rev. Lett. **24**, 1479 (1970).
[G6] Gielen, H., Jansoone, V. and Verbeke, O. B., J. Chem. Phys. **59**, 5763 (1973).
[G7] Goodwin, R. D., Diller, D. E., Roder, H. M. and Weber, L. A., J. Res. Natl. Bur. Stand. (U.S.) **67A**, 173 (1963).
[H1] Habgood, H. W. and Schneider, W. G., Can. J. Chem. **32**, 98 (1954).
[H2] Hankey, A. and Stanley, H. E., Phys. Rev. **B6**, 3515 (1972).
[H3] Ho, J. T. and Litster, J. D., Phys. Rev. Lett. **22**, 603 (1969).
[H4] Hohenberg, P. C. and Barmatz, M., Phys. Rev. **A6**, 289 (1972).
[H5] Huang, C. C. and Ho, J. T., Phys. Rev. **A7**, 1304 (1973).
[H6] Ho, J. T. and Litster, J. D., Phys. Rev. **B2**, 4523 (1970).
[H7] Hocken, R. J., private communication.
[H8] Hoge, H. J., J. Res. Natl. Bur. Stand. (U.S.) **44**, 321 (1950).
[H9] Hastings, J. R. and Levelt Sengers, J. M. H., prepublication data, 1974.
[H10] Haar, L., to be published.
[J1] Josephson, B. D., J. Phys. C **2**. 1113 (1969).
[J2] Jůza, J., Rozpravy Ceskoslovenska Academie Ved., Rada Technickych Ved. **76** (1) (1966).
[J3] Jacobsen, R. T., "The Thermodynamic Properties of Nitrogen from 65 K to 2000 K with Pressures to 10,000 Atms.", thesis (Washington State University. Pullman, 1972).
[J4] Jansoone, V., "Experimentele Bijdrage tot het Onderzoek van het Kritisch Gedrag van Fluida en Molekulaire Dynamika als Test voor Enkele Intermolekulaire Potentiaalmodellen", thesis (Univ. Leuven, Belgium, 1971).
[J5] Jansoone, V., Gielen, H., De Boelpaap, J. and Verbeke, O. B., Physica **46**, 213 (1970).
[J6] Jůza, J., Mareš, R. and Šifner, O., Proc. 8th. Int. Conf. Prop. Steam, to be published.
[K1] Kierstead, H. A., Phys. Rev. **A7**, 242 (1972).
[K2] Kierstead, H. A., Phys. Rev. **A3**, 329 (1971).
[K3] Kadanoff, L. P., Physics **2**, 263 (1966).
[K4] Kamerlingh Onnes, H., Communications Physical Laboratory, Univ. Leiden, No. **102a** (1907).
[K5] Kamerlingh Onnes, H., Communications Physical Laboratory, Univ. Leiden, No. **108** (1908).
[K6] Kamerlingh Onnes, H., Communications Physical Laboratory, Univ. Leiden, No. **124b** (1911).
[K7] Keesom, W. H., "Helium" (Elsevier Publ. Comp., Amsterdam, 1942).
[K8] Keenan, J. H., Keyes, F. G., Hill, P. G. and Moore, J. G. "Steam Tables" (John Wiley, New York, 1969).
[K9] Kamerlingh Onnes, H. and Van Urk, Th., Communications Physical Laboratory, Univ. Leiden, No. **169d** (1924).
[L1] Levelt Sengers, J. M. H., Ind. Eng. Chem. Fundam. **9**, 470 (1970).
[L2] Levelt Sengers, J. M. H., in Experimental Thermodynamics, Vol. II, B. Vodar and B. Le Neindre, eds. Ch. XV (Butterworth, London, 1975), p. 657.
[L3] Levelt Sengers, J. M. H., Physica **73**, 73 (1974).
[L4] Levelt Sengers, J. M. H. and Greer, S. C., Int. J. Heat Mass Transfer **15**, 1865 (1972).
[L5] Lentini, E. and Vicentini-Missoni, M., J. Chem. Phys. **58**, 91 (1973).
[L6] Levelt Sengers, J. M. H., "The Statistical Analysis of *PVT* Data and Derived Properties", unpublished report (1966).
[L7] Levelt Sengers, J. M. H., Straub, J. and Vicentini-Missoni, M., J. Chem. Phys. **54**, 5034 (1971).
[L8] Lorentzen, H. L., Acta Chem. Scand. **7**, 1335 (1956).
[L9] Lunacek, J. H. and Cannell, D. S., Phys. Rev. Lett. **27**, 841 (1971).
[L10] Levelt Sengers, J. M. H. and Chen, W. T., J. Chem. Phys. **56**, 595 (1972).
[L11] Lipa, J. A., Edwards, C. and Buckingham, M. J., Phys. Rev. Lett. **25**, 1086 (1970).
[L12] Levelt Sengers, J. M. H., Greer, W. L. and Sengers, J. V., Advances in Cryogenic Engineering, **19**, K. D. Timmerhaus, ed. (Plenum Press, New York, 1974), p. 358.
[L13] Levelt Sengers, J. M. H., in "Renormalization Group in Critical Phenomena and Quantum Field Theory: Proceedings of a

Conference", J. D. Gunton and M. S. Green, eds. (Department of Physics, Temple Univ., Philadelphia, 1973), p. 112.
[L14] Lin, J. S. and Schmidt, P. W., Phys. Lett. **48A,** 75 (1974); Phys. Rev. **A10,** 2290 (1974).
[M1] Michels, A., Blaisse, B. and Michels, C., Proc. R. Soc. Lond. **160A,** 358 (1937).
[M2] Murphy, T. A., Sengers, J. V. and Levelt Sengers, J. M. H., Proc. 6th Symposium on Thermophysical Properties, P. E. Liley, ed. (American Society of Mechanical Engineers, New York, 1973), p. 180.
[M3] Murphy, T. A., Sengers, J. V. and Levelt Sengers, J. M. H., Proc. 8th International Conference on the Properties of Steam (in press).
[M4] Moldover, M. R., Phys. Rev. **182,** 342 (1969).
[M5] Michels, A. and Wassenaar, T., Physica **16,** 253 (1950).
[M6] McCarty, R. D., J. Phys. Chem. Ref. Data **2,** 923 (1973).
[M7] Moldover, M. R. and Little, W. A., Proc. 9th International Conference on Low Temperature Physics, J. G. Daunt, D. O. Edwards, F. J. Milford and M. Yaqub, eds. (Plenum Press, New York, 1965), p. 653.
[M8] Moldover, M. R. and Little, W. A., Phys. Rev. Lett. **15,** 54 (1965); in "Critical Phenomena", NBS Miscell. Publ. 273, M. S. Green and J. V. Sengers, eds. (U.S. Gov't. Printing Office, Washington, D.C., 1966), p. 79.
[M9] Mathias, E., Crommelin, C. A. Kamerlingh Onnes, H. and Swallow, J. C., Communications Physical Laboratory Univ. Leiden, No. **172b** (1925).
[M10] Meyers, C. H. and Van Dusen, M. S., J. Res. Natl. Bur. Stand. (U.S.) **10,** 381 (1933).
[M11] Michels, A. and Michels, C., Proc. R. Soc. Lond. **A153,** 201 (1935).
[M12] Moldover, M. R., J. Chem. Phys. **61,** 1766 (1974).
[M13] Michels, A. and Strijland, J. C., Physica **18,** 613 (1952).
[M14] Michels, A., Wassenaar, T., Zwietering, Th. N. and Smits, P., J. Appl. Phys. **16,** 501 (1950).
[M15] Meyer, C. A., McClintock, R. B., Silvestri, G. J. and Spencer, R. C., "ASME Steam Tables" (American Society of Mechanical Engineers, New York, 1967).
[M16] Murphy, T. A. and Gulari, E., private communication.
[M17] Mathias, E., Kamerlingh Onnes, H. and Crommelin, C. A., Communications Physical Laboratory, Univ. Leiden, No. **145C** (1914).
[M18] Mathias, E., Crommelin, C. A. and Garfit Watts, H., Communications Physical Laboratory, Univ. Leiden, No. **189** (1927).
[M19] Mac Cormack, K. E. and Schneider, W. G., Can. J. Chem. **29,** 699 (1951).
[M20] Murphy, T. A., private communication.
[N1] Natrella, M. G., "Experimental Statistics", NBS Handbook 91 (U.S. Gov't. Printing Office, Washington, D.C., 1963).
[O1] Osborne, N. S., Stimson, H. F. and Ginnings, D. G., J. Res. Natl. Bur. Stand. (U.S.) **18,** 389 (1937).
[P1] Patterson, H., Crips, R. and Whytlaw-Gray, R., Proc. R. Soc. Lond. **A86,** 579 (1912).
[P2] Plumb, H. and Cataland, G., Metrologia **2,** 127 (1966).
[R1] Roach, P. R., Phys. Rev. **170,** 213 (1968).
[R2] Rivkin, S. L. and Akhundov, T. S., Teploenergetika **9** (1), 57 (1962); **10** (9), 66 (1963).
[R3] Rivkin, S. L. and Troianovskaia, G. V., Teploenergetika **11** (10), 72 (1964).
[R4] Rivkin, S. L., Akhundov, T. S., Kremnevskaia, E. K. and Assadulaieva, N. N., Teploenergetika **13** (4), 59 (1966).
[R5] Roach, P. R. and Douglass, D. H., Phys. Rev. Lett. **19,** 287 (1967).
[R6] Riddle, J. L., Furukawa, G. T. and Plumb, H. H., "Platinum Resistance Thermometry", NBS Monograph 126 (U.S. Gov't. Printing Office, Washington, D.C., 1972).
[R7] Roder, H. M., Weber, L. A. and Goodwin, R. D., NBS Monograph 94 (U.S. Gov't. Printing Office, Washington, D.C., 1965).
[R8] Rathjen, W., and Straub, J., Kältetechnik I.I.F.-I.I.R. Zürich (1973/74) p. 129.
[S1] Schofield, P., Phys. Rev. Lett. **22,** 606 (1969).
[S2] Schofield, P., Litster, J. D. and Ho, J. T., Phys. Rev. Lett. **23,** 1098 (1969).
[S3] Schmidt, H. H., J. Chem. Phys. **54,** 3610 (1971).
[S4] Scheffé, H. "The Analysis of Variance", (John Wiley, New York, 1959).
[S5] Stacey, L. M., Pass, B. and Carr, H. Y., Phys. Rev. Lett. **23,** 1424 (1969).
[S6] Smith, I. W., Giglio, M. and Benedek, G. B., Phys. Rev. Lett. **27,** 1556 (1971).
[S7] Sydoriak, S. G., Grilly, E. R. and Hammel, E. F., Phys. Rev. **75,** 303 (1949).
[S8] Sherman, R. H. and Edeskuty, F. J., Annals Physics **9,** 522 (1960).
[S9] Sydoriak, S. G. and Sherman, R. H., J. Res. Natl. Bur. Stand. (U.S.) **68A,** 547 (1964).
[S10] Sherman, R. H., Sydoriak, S. G. and Roberts, T. R., J. Res. Natl. Bur. Stand. (U.S.) **68A,** 579 (1964).
[S11] Sherman, R. H., in "Critical Phenomena", NBS Miscell. Publ. 273, M. S. Green and J. V. Sengers, eds. (U.S. Gov't. Printing Office, Washington, D.C., 1966), p. 7.
[S12] Schmidt, E. H. W., in "Critical Phenomena", NBS Miscell. Publ. 273, M. S. Green and J. V. Sengers, eds. (U.S. Gov't. Printing Office, Washington, D.C., 1966), p. 13.
[S13] Straub, J., Chem.-Eng.-Tech. **39,** 291 (1967).
[S14] Schmidt, E. "Properties of Water and Steam in SI–Units", (Springer-Verlag, New York, 1969).
[S15] Sirota, A. M., Belyakova, P. E. and Shrago, Z. Kh., Teploenergetika **13,** (11), 112 (1966).
[S16] Stell, G., Phys. Rev. Lett. **32,** 286 (1974).
[S17] Stell, G., Phys. Rev. Lett. **24,** 1343 (1970).
[T1] Thoen, J. and Garland, C. W., Phys. Rev. **A10,** 1311 (1974).
[T2] Trappeniers, N. J. and Wassenaar, T., Private Communication.
[V1] Vicentini-Missoni, M., Levelt Sengers, J. M. H. and Green, M. S., J. Res. Natl. Bur. Stand. (U.S.) **73A,** 563 (1969).
[V2] Van der Waals, J. D., Verh. Kon. Akad. Wetensch. Amsterdam **1** (1893), nr.8.
[V3] Van Dijk, H. and Durieux, M., Physica **24,** 920 (1958).
[V4] Voronel, A. V., to be published.
[V5] Vukalovich, M. P., Vargaftik, N. B., Rivkin, S. L. and Aleksandrov, A. A., Teploenergetika **14,** (1) 91 (1967).
[V6] Van Itterbeek, A. and Van Dael, W., Physica **28,** 861 (1962).
[V7] Van Dael, W., Van Itterbeek, A., Cops, A. and Thoen, J., Physica **32,** 611 (1966).
[W1] Wallace, B. and Meyer, H., Phys. Rev. **A2,** 1563, 1610 (1970).
[W2] Weber, L. A., Phys. Rev. **A2,** 2379 (1970).
[W3] Widom, B., J. Chem. Phys. **43,** 3898 (1965).
[W4] Wallace, B. and Meyer, H., "Tabulation of the Original Pressure–Volume–Temperature Data for He^3–He^4 Mixtures and for He^3", Technical Report (Dept. Physics, Duke Univ., Durham, N.C., 1971).
[W5] Weinberger, M. A. and Schneider, W. G., Can. J. Chem. **30,** 422 (1952).
[W6] Wu, S. Y. "Study of *Equilibrium Critical Phenomena in* Fluid Argon", Ph. D. Thesis (California Institute of Technology, Pasadena, 1972); C. J. Pings, Private Communication.
[W7] Whiteway, S. G. and Mason, S. G., Can. J. Chem. **31,** 569 (1953).
[W8] Wilcox, L. and Estler, W. T., J. Phys. (Paris) **32** (C5a) 175 (1971).
[W9] Wentorf, R. H., J. Chem. Phys. **24,** 607 (1956).
[W10] White, J. A. and Maccabee, B. S., Phys. Rev. Lett. **26,** 1468 (1971).
[W11] White, J. A. and Maccabee, B. S., Phys. Rev. **A11,** 1706 (1975).
[W12] Weber, L. A., J. Res. Natl. Bur. Stand. (U.S.) **74A,** 93 (1970).
[W13] Weber, L. A., Private Communication.
[W14] Weiner, J., Langley, K. H. and Ford, N. C., Phys. Rev. Lett. **32,** 879 (1974).

[W15] White, J. A., Private Communication.
[W16] Wilson, K. G., Phys. Rev. **B4**, 3174, 3184 (1971).
[W17] Wilson, K. G. and Fisher, M. E., Phys. Rev. Lett. **28**, 240 (1972).
[W18] Weber, L. A., J. Chem. Thermod. **2**, 839 (1970).
[W19] White, D., Friedman, A. S. and Johnston, H. L., J. Am. Chem. Soc. **73**, 5713 (1951).
[W20] Warkulwiz, V. P., Mozer, B. and Green, M. S., Phys. Rev. Lett. **32**, 1410 (1974).
[Y1] Young, S., Trans. Chem. Soc. **59**, 39 (1891).